The Study of Culture Redox Potential's Effect On Glycosylation and Production of Monoclonal Antibodies In Mammalian Cell Cultures

by

Benjamin Dionne

**A Thesis submitted to the Faculty of Graduate Studies of
The University of Manitoba
in partial fulfillment of the requirements for the degree of**

Doctor of Philosophy

**Department of Microbiology
University of Manitoba
Winnipeg, Canada**

Thesis Abstract

The glycosylation patterns of monoclonal antibodies (Mabs) have become very important in determining therapeutic abilities of many drugs. The thesis studied 3 cell lines producing humanized Mabs in the presence of variable concentrations of the reducing agent dithiothreitol (DTT) to artificially lower the CRP and affect glycan patterns. A new high-throughput hydrophilic interaction chromatography (HILIC) method was developed and used to show a decrease in the Galactosylation Index (GI) of NS0 IgG1 by as much as 50% in cultures with CRP values lower than -100 mV. The shift in GI was unique to NS0 cultures; CHO DP-12 indicated no significant change in GI but did have a 7% increase in fucosylated species in cultures with higher [DTT]. Furthermore no DTT related shifts were observed in any of the CHO EG2-hFc glycans. EG2-hFc did however have an exceptionally high GI of 0.625 compared to GIs of 0.245 in DP-12 and 0.314 in NSO. Another component of the trials determined, using S^{35} radiolabeling, that the assembly pathway of IgG1 progressed via $HC \rightarrow HC_2 \rightarrow HC_2LC \rightarrow HC_2LC_2$ and that the ratio of heavy chain dimer to heavy chain monomer increased greatly over time for cultures with higher DTT concentrations. The increase in heavy chain dimers and lower GI appear to be correlated, possibly due to disruption of the disulfide bonds between LC and HC within the Golgi. This disruption in disulfide bonds affecting galactosyltransferase (GalT) activity is supported by the findings

that the partially reduced fragments of IgG1; HC and HC_2, are less galactosylated than the HC_2LC and whole IgG1 when treated with GalT. When native and agalactosylated EG2-hFc and IgG1 were treated with GalT *in vitro,* EG2-hFc exhibited an almost 10 fold higher activity level. The cause for the higher activity may be due to overall size difference or point mutations in the Fc region of EG2-hFc. Through the manipulation of CRP, glycan patterns can be influenced however the effect is not universal and must be determined on a per cell line basis. Furthermore, EG2-hFc's higher GI value may translate into better *in vivo* activity as a therapeutic and determination of reasons for the high GI may lead to better means for future glycoengineering.

Acknowledgements

I would like to thank my PhD advisor Dr. Michael Butler for his continued support and patience with my efforts over the past few years. He has been a great mentor and extremely valuable when facing dilemmas relating to both research and personal matters. I would also like to thank my committee members Dr. Deborah Court and Dr. Hélène Perreault for their guidance throughout these PhD studies.

A great big thank you goes out to the members of the Butler lab, past and present; Vince Jung, Sarah Chan, Katrin Braasch, Carina Villacres, Bo Liu, Natalie Krahn, Neha Mishra, Dr. Venkata Tayi and a special thanks to Dr. Maureen Spearman. Thank you for your encouragement and camaraderie.

For financial support I am very appreciative to the Manitoba Health Research Council, Natural Science and Engineering Council of Canada, MabNet and PhD Scholarship for Aboriginal Scholars. Special thanks also goes out to my colleagues at Abbvie who provided the NS0 cell line and media for this thesis.

And finally thank you to my family and friends who supported me emotionally and financially over the course of this research.

Thank you Rose, Danielle, Luc, Isabelle, Kaitlyn and Ethan for everything I have.

Dedication

To Bernie and Ken

"The scientist is not a person who gives the right answers, he's one who asks the right questions."

— *Claude Lévi-Strauss*

"Do or do not, there is no try"   —*Yoda*

Table of Contents

List of Tables

List of Figures

List of Acronyms

%RSD	% relative standard deviation
2-AB	2-aminobenzamide
AB	Assay Blank
AC	Assay Control
ACN	Acetonitrile
Asn-297	Asparagine-297
ATCC	American Type Culture Collection
CD	Chemically Defined
C_H	Constant heavy region
CHO	Chinese Hamster Ovary
CMP	Cytidine MonoPhosphate
CPC	Coupling Phosphatase Control
CV	Column Volume
Cys/Met	Cysteine/Methionine
Da	Dalton
DIH2O	Deionized water
DMEM	Dulbecco's Modified Eagle's Medium
DMSO	Dimethyl sulfoxide
DTT	Dithiothreitol
EGF	Epidermal Growth Factor
ELISA	Enzyme-Linked Immunosorbent Assay
Ems	Emission
EUFS	Energy Units Full Scale
Exc	Excitation
Fab	Fragment, antigen binding
FBS	Fetal Bovine Serum
Fc	Fragment, crystallizable
GalT	β1,4-Galactosyltransferase
GD	Gradient Duration
GI	Galactosylation Index
GU	Glucose Units
H2O	Water
HC	Heavy Chain

HC$_2$	Heavy Chain dimer
HILIC	Hydrophilic Interaction Liquid Chromatography
HT	Hypoxanthine, Thymidine
IAM	Iodoacetamide
IgG	Immunoglobulin G
IL-8	Interleukin-8
IVCD	Integral of Viable Cell Concentration
kDa	KiloDaltons
LC	Light Chain
Mab	Monoclonal antibody
MeOH	Methanol
MTX	Methotrexate
MWCO	Molecular Weight Cut Off
NAC	Negative Assay Control
NeuAc	N-acetylneuraminic acid
NeuGc	N-glycolylneuraminic acid
NIBRT	National Institute for Bioprocessing Research and Training
NP-HPLC	Normal Phase-High Pressure Liquid Chromatography
ORP	Oxido Reduction Potential
PBS	Phosphate Buffered Saline
PFBM	Protein Free Basal Media
PNGaseF	Peptide -N-Glycosidase F
RIPA	RadioImmunoPrecipitation Assay buffer
SD	Standard Deviation
SDS	Sodium Dodecyl Sulfate
PAGE	Polyacrylamide Gel Electrophoresis
TCD	Total Cell Density
tPa	Tissue Plasminogen Activator
VCD	Viable Cell Density
V$_H$	Variable heavy region
V$_L$	Variable light region

Chapter 1 - - Introduction

In recent years monoclonal antibodies (Mabs) have become the largest sector of therapeutic proteins in clinical and preclinical development with US sales exceeding $25 billion in 2012 (Aggarwal 2014). Monoclonal antibodies are glycoproteins and work in a number of ways depending on the illness/disease targeted. They have been engineered meticulously at the amino acid level with respect to antigen binding, effector function and immunogenicity. They are highly specific for targeted proteins or antigens and have the ability to recruit cells to elicit an immune response or to simply bind an antagonist antigen and remove its effects on the patient. The eliciting of an immune response occurs via the binding of the constant region (Fc) of an antibody to effector cells and a large contributor to the binding efficiency is played by the N-glycans, at Asn297, linked to this constant region of the Mab. Specific glycosylation forms have the ability to increase or decrease the activation of antibody dependent cell-mediated cytotoxicity (ADCC) or cell-dependent cytotoxicity (CDC) (Raju 2008). Other attributes include longer/shorter half-lives, induction of anti-inflammatory responses and solubility in final formulation (Jefferis 2012; Anthony et al. 2010; Sinclair et al. 2005). In recent years regulatory agencies like Health Canada and the US FDA have been pushing for a Quality by Design (QbD) approach where critical

parameters and quality attributes are set-out at the beginning of a project instead of defining them as the process evolves. This is a means of understanding the process as it is built rather than as reacting to it after the fact. Of increased importance is also the entrance of biosimilars and biobetters to the marketplace which must demonstrate comparable glycan profiles to the brand name drugs. Having the ability to manipulate glycans during production would ease the introduction of these new products thus decreasing timelines and cost of drugs. To this end, the research here focused on examining mammalian cell culture conditions and determining which parameters had an influential effect on glycan profiles of Mabs. The future goal of being able to produce Mabs with a designed glycan structure in the Fc region would allow manufacturers the ability to produce therapeutics with higher efficacy rates and less risk for adverse side effects. They would also gain a better understanding of the process and thereby establish better quality control mechanisms.

1.1 Monoclonal antibodies

Monoclonal antibodies (Mabs) were first developed in the Nobel Prize winning work of Kohler and Milstein (Kohler et al., 1975). Originally conceived by fusing an immortal cell with a short-lived, antibody producing plasma cell, the resulting hybridoma cell lines had the capability to produce a specific antibody indefinitely. Over the past few

decades many improvements have been made and more cell lines have been developed for production purposes, each with their own advantages and disadvantages (Al-Rubeai 2011). The decision about what type of antibody to express is equally as important as cell line selection. Different types of Mabs include murine, chimeric, humanized and human with five different classes to choose from: IgG, IgA, IgE, IgD, and IgM. Depending on the antibody's intended target and mechanism of action, the selection of type and class is made to maximize efficacy and effectiveness. The human immune system is primed to fight off foreign pathogens and antigens, including non-human Mabs used as therapeutics. The rapid clearance of non-human Mabs has led to innovations with regard to genetic engineering for new types of Mabs as well as modifications of existing ones. Alternatively, some mechanisms of action require only antibody binding and quick clearance, a role suited well by murine and chimeric models (Liu et al. 2012) as well as Mab fragments (Miethe et al. 2014).

IgG is the most predominant class chosen for therapeutics however others have been explored due to their unique advantages like IgA's enhanced effect on neutrophil recruitment (Dechant et al. 2001; Dechant et al. 2007). The selection of type and class of Mab can be strongly associated with the many options for expression systems. Many host cell lines are available including the predominant mammalian cell lines, and

lesser used bacterial fungal and insect cell cultures. The selection of the optimal cell line for each antibody may depend on the Mabs desired characteristics such as long or short half-lives (Dall'Acqua et al. 2006), ADCC activity, glycosylation profiles (Werner et al. 2007) and patient safety.

There are five classes of antibodies: IgG, IgA, IgE, IgD, IgM. The most common for industrial purposes is IgG which can be subclassified into 4 groups: IgG1, IgG2, IgG3 and IgG4. The subclasses vary the greatest in their hinge regions makeup. Changes at the amino acid level lend to slightly shorter hinge regions and less flexibility in IgG2 and IgG4 compared to IgG1 while the IgG3 subclass has an extended hinge region with greater flexibility (Meulenbroek 2008). The change in flexibility may have an effect on antigen interactions. These differences in the hinge region may also contribute to unique glycosylation patterns (Wuhrer et al. 2007) between classes. These subclasses are not necessarily mandated for specific targets and it is possible for multiple subclasses to target the same antigen as seen with commercially available anti-EGFR Mabs cetuximab (IgG1) and panitumumab (IgG2) (Price et al. 2014). Most importantly the production trains of these molecules changes little for all 4 subclasses of IgG.

The common structure of IgG Mabs is a Y-shaped molecule consisting of light and heavy chains bound together with disulfide bonds

(**Figure 1.1**). The heavy chains of IgG1 are made up of 3 constant domains (C_H) and one variable domain (V_H). The light chains consist of 2 domains; one constant (C_L) and one variable (V_L). The Mab can be further characterized by its two segments: Fab and Fc. The Fab portion contains the antigen binding domains of the light and heavy chains while the Fc portion is comprised entirely of heavy chains and is the site that assists in effector function (Kubota et al. 2009). The two main components that influence effector function are the amino acid sequence and glycosylation of the Fc region. It has become routine to design Mabs with appropriate amino acid sequences however the goal of achieving optimal and consistent glycosylation patterns on Mabs has remained elusive.

The 2 inter-heavy chain disulfide bonds of IgG1 are located in the hinge region (a.a. 216-230) which lies in close proximity to the Asn-297 site of glycosylation. The location of these disulfide bonds lends to the flexibility of the molecule and differentiates it from the other IgG subclasses (Liu et al., 2012).

Figure 1.1 Composition of IgG1 monoclonal antibody
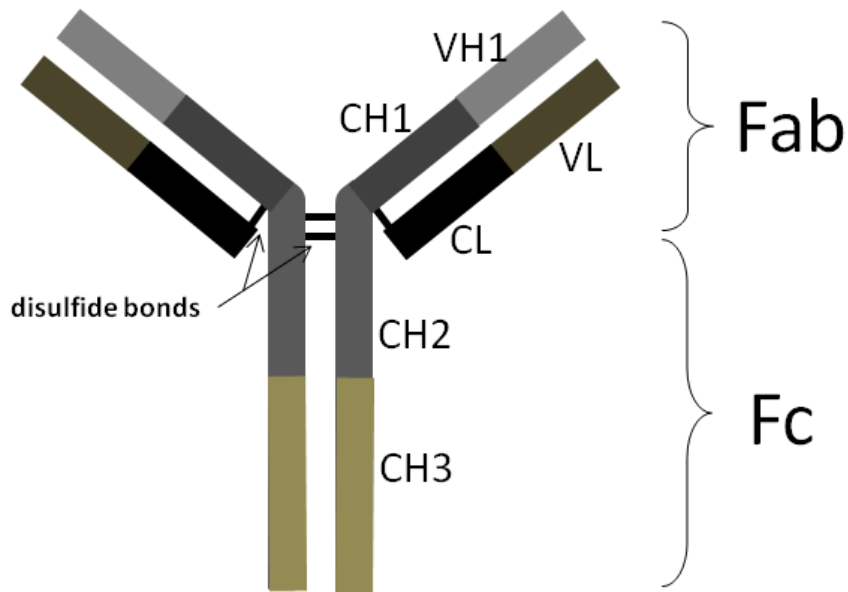
Beyond antibody class and subclass, different types of Mabs exist including murine, chimeric, humanized and fully human. The first clinically tested and approved Mabs were of the murine variety, including Orthoclone OKT3 for autoimmune and inflammatory disorders (AIID)(Goldstein 1987; Reichert 2013). Murine Mabs have demonstrated good antigen binding characteristics however several side effects and short half-life in serum have downplayed their importance as therapeutics (Brekke et al., 2003). More recently the focus has been on genetically engineering chimeric, humanized and fully human Mabs for less immunogenic therapeutics. A chimeric Mab consists of murine antigen binding regions (Fab) grafted with human Fc regions for an approximate total of 50% murine and 50% human. This human Fc region enables

effector function for ADCC activity. The largest concern with murine and chimeric Mabs is that they elicit immune responses resulting in human anti-mouse and anti-chimeric antibodies (HAMA and HACA respectively) which lead to quick clearance of the Mabs from the serum thus nullifying any long term effects. This does not negate the usefulness of all chimeric Mabs however due to the need for rapid clearance in techniques involving radioimmunotherapy (Stillebroer et al. 2013) and diagnostic imaging of tumors (Börjesson et al. 2006).

Humanized Mabs consist of <10% murine antibody, including the hypervariable region in the antigen binding domain. This diminished murine presence leads to increased half-lives, less immunogenicity and increased ADCC and CDC activity. The majority of top selling Mabs on the market are humanized (Maggon 2010; Buss et al. 2012) followed by chimeric and fully human. Humanized Mabs can be similarly expressed in all major mammalian cell lines with differences mainly observed in the N-glycosylation patterns.

Human Mabs, produced in either human or hybridoma cell lines, are 100% human in sequence and theoretically exhibits the least amount of side effects. In addition, depending on the host cell line, the glycosylation pattern may be the most human-like of all Mab types lending to greater effector function. The number of humanized and human Mabs in pipelines account for the majority of Mab research and will continue to

lead the way for the foreseeable future (Pavlou et al. 2005). The advances in genetic engineering that led to humanized and human Mabs has also resulted in manipulations to acquire less immunogenic traits as well as increased efficiency (Chames et al. 2009, Presta 2008). In this manner the engineered sequences become more relevant than the actual type of Mab being produced.

1.1.1 Single domain antibodies

Referred to sometimes as nanobodies, single domain antibodies are a group of novel immunoglobulins that generally consist of only a fragment of a traditional Mab, such as the Fc or Fab portion. The idea behind smaller Mabs, which has yet to be proven in clinical trials, is that better tissue penetration (Monnier et al. 2013) may be possible for use in targeting cancerous tumors. In the research presented here, a novel humanized camelid (**Figure 1.2)** antibody was produced which consisted of only 2 heavy chains and no light chains (Zhang et al. 2009). The other significant difference between an IgG1 Mab and this camelid is the lack of a CH1 domain. This is the domain which would normally bind to light chains. The Fc region of this camelid antibody is human, composed of the CH3 and CH2 domains, with one intact glycosylation sequon as in IgG. There have been very few published results with regard to glycosylation of these antibodies and therefore this area was a main focus of the research

performed here. Production techniques for these antibodies are identical
to IgG including cell culture and purification.

Figure 1.2 Composition of camelid single domain monoclonal antibody
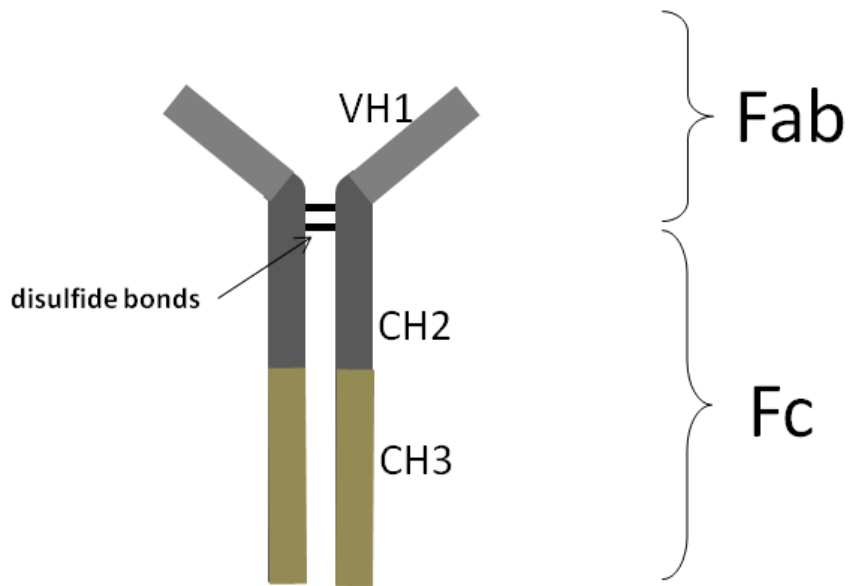
1.2 N-linked glycosylation

N-glycosylation events are traced to both the endoplasmic reticulum
and Golgi apparatus within mammalian cell cultures. Beginning in the
ER, nascent polypeptides are glycosylated with high mannose structures
containing 1-3 glucose end units via oligosaccharyltransferases (Stanley
et al. 2009). The site of N-glycosylation is specific to a Asn-X-Ser/Thr
sequon, where X can be any amino acid except proline. The presence of a

sequon does not guarantee glycosylation will take place; however within IgG Mabs the site at Asn297 is almost always occupied. In other molecules like tPA which has three such sequons, there can be variable glycosylation where two or three sites are occupied leading to a macroheterogeneous population. The terminal glucose residues are initially present on the high mannose structures to interact with the calnexin/calreticulin system for proper protein folding before being shuttled to the Golgi for further processing (Spearman et al. 2011).

Once the recombinant proteins enter the Golgi, more post-translational modifications are made to the glycans including the addition of N-acetylglucosamine (GlcNAc), Galactose (Gal), sialic acid and fucose by glycosyltransferases. These events occur in different parts of the Golgi (cis, medial or trans) depending on where the specific transferase is embedded in the membrane. In addition to the need for transferases, there must also be a supply of nucleotide sugars and cofactors like manganese present. The modifications made in the Golgi are not strict and multiple forms of glycans will be produced over an entire population leading to a high level of microheterogeneity. For therapeutic drug use in humans, the glycosylation should mimic what the host cell will recognize as "self" and not foreign in order to elicit the immune responses mentioned earlier and to reduce its own immunogenic profile. This is the reason why bacterial and yeast expression systems, although useful in the past for many of our

therapeutic drugs today like antibiotics, cannot be readily used. Yeast and bacterial systems do not have the same enzymes necessary to glycosylate proteins such that the human immune system would recognize them as "self" (Brooks 2004). Many methods have been established previously that can influence the glycan patterns on Mabs through cell culture or genetic engineering (Hossler 2011). The Butler lab in the Department of Microbiology has performed a great deal of work in this area as well, characterizing cell culture conditions that affect glycosylation of recombinant proteins and monoclonal antibodies. In particular the control of ammonia, dissolved oxygen and media additives have been found to be critical to the glycosylation profiles of the secreted glycoproteins (Yang et al. 2002; Kunkel et al. 1998; Liu et al. 2014). The hydrophilic interaction chromatography (HILIC) method used in the lab for glycan profiling is widely accepted and used in industry and academia alongside other methods like capillary electrophoresis and mass spectrometry (Hamm et al. 2013) however has the downside of being labour intensive with long preparation and run times. To further enhance the lab's capabilities a new method had to be devised to increase throughput, sample reproducibility and resolution that would work across multiple recombinant protein types. Higher resolutions offer greater isoform identification and the separation of overlapping peaks which may

be concealing glycans like high mannose structures which have variable effects on therapeutics (Yu et al. 2012).

1.3 Redox potential

Building on the work by Kunkel (1998), there was a possible link between redox state of the cell and glycan profiles. The internal redox of mammalian cells has been studied in the cytoplasm (Chen et al. 2000) and mitochondria (Robinson et al. 2006; Dickinson et al. 2008) through the use of redox sensitive dyes and direct measurement of glutathione and/or thioredoxin levels in oxidized/reduced forms. More work has been accomplished on the ER (Chakravarthi et al. 2006) where the mechanism of redox control assists in the formation of disulfide formation to get fully folded proteins and means have been developed to manipulate the redox control system for greater productivity (Mohan et al. 2010). More recent advancements have been accomplished through the use of roGFP constructs where an oxidative sensitive GFP is localized to the ER and direct values can be attained for redox potential (Birk et al. 2013). Unfortunately no dyes or roGFPs have been developed specific to Golgi localization and therefore the redox potential of this organelle is largely unknown. Means of determining extracellular redox potential are well established and those are employed in the current research.

Research performed here looked at the various components of the glycosylation pathway and how Mabs are produced. By following the post-translational modifications of different cell lines (NS0 and CHO) and different types of antibodies (IgG1 and camelid single domain antibodies) under similar conditions a better understanding would develop with regard to the parameter being universal for all mammalian cell lines and antibody types or very specific. The chief parameter being explored was culture redox potential (CRP), which can be influenced by dissolved oxygen concentrations, media components and cell growth. For these experiments a reducing agent, dithiothreitol (DTT), was used to drive the CRP to a decreased state. The supposed role redox may play in the glycan profiles of Mabs was outlined by Kunkel et al. (1998) where dissolved oxygen was limited and glycans became more agalactosylated. To this end, experiments were designed to test low redox states within the cell culture environment and monitor all glycan profiles, with a specific focus on the galactosylation index. The presence or absence of galactose residues can have multiple variable effects on therapeutics including but not limited to changes in aggregation and radius (Zheng et al. 2011), Mab conformation (Houde et al. 2010) and an anti-inflammatory role (Karsten et al. 2012).

In addition, radiolabeling studies were performed to monitor the intracellular process of antibody formation. The pulse-labelling experiments enable us to define the specific stages of translation from the

formation of the light and heavy chains to when they bind via interchain disulfide bonds. Depending on these disulfide bonds and how they are influenced under the pressure of a reducing agent, different glycosylation profiles may arise with multiple glycoforms on the Mab.

As a means to determining what may be occurring intracellularly in the Golgi, β-1,4 galactosyltransferase studies were performed on multiple candidates of different forms to determine their interaction with the enzyme. Glycosyltransferases' activity may be altered when changing redox conditions affect the disulfide bonds in close proximity to Asn-297 varying the glycan profiles *in vivo*. Understanding this interaction may lead to targets for modification.

The role of glycoforms in the activity of therapeutic monoclonal antibodies cannot be understated. By controlling this aspect of assembly, more reliable and efficacious drugs can be produced for the treatment of numerous diseases and ailments.

Chapter 2 - Materials and Methods

2.1. Cell culture

2.1.1. Cell lines and media

2.1.1.1.   *NS0 and PFBM-1*

A proprietary NS0 cell line (Hu1D10) was provided by Abbvie (Redwood City, CA, USA). This cell line had been adapted to be cholesterol independent and then transfected with a gene for recombinant humanized IgG1; displaying 90% human and 10% murine amino acid sequence. Due to its origin as a B-cell, it grows in suspension culture with very low aggregation rates. PFBM-1 is a proprietary chemically defined protein free basal medium from Abbvie. This media has 15 g/L glucose, starting pH of 7.2 ±0.1 and osmolality of 300 mOsm/kg H_2O. This cell line is considered a high producer of IgG1 with titres greater than 500 µg/mL in batch culture over 7 days. Cell passaging for maintenance was performed every 3 days, seeded at 2.0 x 10^5 cells/mL in 75 cm^2 vented T-flasks with 30 mL of PFBM-1 (25 cm^2 and 150 cm^2 T-flasks were also used when needed).

For the dithiothreitol (DTT) experiments T-75 flasks were seeded at 2.5x10^5 cells/mL in 30 mL basal medium with viabilities >95% and incubated at 37°C and 10% CO_2. Dithiothreitol was added to experimental cultures prior to inoculation at the following concentrations: 0.25, 0.50, and 0.75 mM. The control cultures received no DTT. All cultures were

established in duplicate over multiple trials with samples removed daily for analysis. Cultures were harvested on day 4 when viabilities were $\geq$90%. The high viability at harvest minimized any protein degradation in the supernatant.

2.1.1.2. *Biogro medium*

Biogro medium is a proprietary serum free media developed in the Butler lab. This media, used for CHO DP-12 anti-IL-8 and EG2-hFc cultures, was supplemented with 0.5 g/L yeast extract, thereby being animal component free. It has a pH of 7.4 and osmolality of 285-300 Osm/kg.

2.1.1.3. *CHO EG2-hFc*

Provided through MabNet (Bell et al. 2010; Zhang et al. 2009), the CHO EG2-hFc cell line produces a chimeric single domain antibody (sdAb) with camelid variable region and human Fc region. Expected titres for a 4 day batch culture are <40 µg/mL. Maintenance of these cells was done by passaging every 3 days into 125 mL vented shake flasks at 2.5×10^5 cells/mL in 30 mL Biogro media and 0.5 g/L yeast extract. Shake flasks were rotated at 120 rpm. Cells would occasionally clump requiring forceful agitation prior to counting.

The reducing culture conditions applied to EG2-hFc included [DTT] of 0, 0.25, 0.50, 0.75, and 1.00 mM. DTT was added once prior to inoculation. The control cultures received no DTT. All cultures were established in duplicate over multiple trials with samples removed daily for analysis with supernatant frozen for future glycan processing. All flasks were incubated at 37°C and 10% CO_2 at 120 rpm. Harvest criteria were set on day 4 when viabilities $\geq$ 90%.

2.1.1.4.   *CHO DP-12 anti-IL-8*

Acquired from the ATCC (CRL-12445), these cells produce a human IgG1 and are capable of producing 250 μg/mL in batch culture. Maintenance of these suspension adapted cells was done by passaging every 2 days, seeding at 2.5 x 10^5 cells/mL in 125 mL vented shake flasks with 30 mL Biogro medium and 0.5 g/L yeast extract. The reducing culture conditions applied to DP-12 included [DTT] (concentrations of dithiothreitol) of 0, 0.25, 0.50, 0.75, and 1.00 mM. All other conditions remained consistent with EG2-hFc trials.

2.1.2.   Cell counting

Cells were counted using the Trypan-blue dye exclusion method. A 50 μL cell culture sample was mixed with 50 μL of 0.4% Trypan blue. This mix was then loaded onto a Cedex XS (Roche, Indianapolis, IN, USA) slide.

Images of samples were taken in duplicate and average values attained. The automated Cedex XS imager software delivered total cell density, viable cell density, viability, aggregation and cell size distribution. No adjustment in CEDEX counting parameters was needed between NS0 and CHO cells.

2.2. Redox potential and pH measurements

Redox potential was measured using a redox probe (9179BNMD Thermo Fisher, Waltham, MA, USA) and pH measurements with a low maintenance gel-filled pH probe (Thermo Fisher, Waltham, MA, USA). Both probes were plugged into an Orion 420A meter (Thermo Fisher, Waltham, MA, USA). The pH probe was calibrated with 4, 7 and 10 pH buffers. The redox probe was set up daily prior to sampling by immersing the probe for a period of 10-15 minutes in the appropriate preconditioned room temperature media; PFBM-1 for NS0 and Biogro for EG2-hFc and DP-12. This allowed for more accurate and stable redox values of samples (Pluschkell et al. 1995). A 3 mL sample was removed every 24 hours from each sample flask. The 3 mL sample was placed in a 15 mL conical tube for sequential redox potential and pH measurements. The assay requires samples to be agitated as little as possible so as to minimize gas exchange. The redox probe is placed in the conical tube and readings taken after the sample has stabilized; for best results the meter readings were allowed to

stabilize over a period of 1-3 minutes (Meneses et al. 2000). The pH probe was then immersed and values recorded. Samples were retained for titre determination.

2.3. Protein A purification

2.3.1. HiTrap columns

1 mL HiTrap Protein A HP columns (GE Healthcare, Pittsburgh, PA, USA) were prepared for use by flushing with 3 column volumes (CV) of elution buffer (0.1 M glycine pH 3.0) and equilibrated with 5 CV of washing buffer (PBS pH 7.0). Equilibration of the column took place prior to every sample. The sample was loaded by syringe and washed with 5 CV of PBS. The bound antibody was stripped with 3 CV of elution buffer and the eluant collected. All flow rates varied between 1.0 and 1.5 mL/minute. The eluant was neutralized to pH 6.5-7.5 with Tris buffer pH 9.0 so as to minimize sialic acid loss. The maximum binding capacity of the column (20 mg IgG/mL) was never reached.

2.3.2. Spin filters

Protein A HP SpinTrap filters (GE Healthcare, Pittsburgh, PA, USA) were prepared for use by placing filter in 1.5 mL microfuge tube, spinning out the storage solution and resuspending the protein A media in 600 µL of binding buffer (PBS pH 7.0). Binding buffer was spun out and up to 600 µL of sample were loaded. After gently mixing for 4 minutes to allow

antibody binding, the column was spun down and twice resuspended in 600 µL of binding buffer, spinning down each time. All filtrate was discarded. The bound antibody was then eluted with 2 rounds of elution buffer (0.1M glycine pH 3.0), each using 400 µL, into a new 1.5 mL microfuge tube. The eluant was neutralized to pH 6.5-7.5 with Tris buffer pH 9.0. All centrifugation steps were performed at 70 x g. SpinTrap columns were re-equilibrated prior to every sample and maximum binding capacity (>1 mg) was never reached.

Both purification methods were validated by running reduced SDS-PAGE gels and looking for only 25 kDa and 50 kDa bands for IgG1 and a lone 40 kDa band for EG2-hFc.

2.4. Titre determination

2.4.1. ELISA

All ELISA were performed according to MabNet SOP# MNSOP0009 using culture supernatant. Briefly, a sandwich ELISA was performed by coating a 96-well plate with a primary antibody of anti-human IgG (Fc specific). A serially diluted sample was added and incubated for an hour to allow for binding before washing off excess. A secondary antibody of anti-human IgG (Fc specific)-peroxidase was added and allowed to bind for one hour. TMB (tetramethylbenzidine) solution was then added which acted as a substrate for the peroxidase developing a blue color; this was

read at 650 nm. The peroxidase reaction was stopped by adding 2 M H_2SO_4 which changed the solution from blue to yellow; the samples was then read at 450 nm on a 96-well plate reader. All optical density results are converted to concentrations using a standard curve which is included on every plate.

2.4.2. Mab titre determination by A280 on Nanodrop

Purified antibody was measured at A280 nm on a Nanodrop 2000 (Thermo Fisher, Waltham, MA, USA) instrument. To begin, 1.5 μL of buffer was placed on the pedestal to get a blank measurement. After wiping off the buffer, 1.5 μL of sample was placed on the pedestal to get an absorbance. This was repeated to get an average of two readings. These absorbance values were then used to calculate the antibody concentrations based on their molar extinction coefficients and molecular weights:

$$concentration(mg/mL) = \left(\frac{absorbance}{molar\ ext.coeff.}\right) \times MW$$

Table 2.1 Identity and values for molecular weight, molar and percent extinction coefficients of Mabs used in the thesis

Mab	MW (kDa)	Molar extinction coefficient ($M^{-1}cm^{-1}$)	$\varepsilon_\%$
IgG1 (NS0, DP-12)	150	210,000	1.40
sdAb (EG2-hFc)	80	114,805	1.44

2.5. SDS-PAGE Electrophoresis

The Laemmli discontinuous buffer system (Laemmli 1970) was used for separation of proteins according to molecular weight in SDS-PAGE (sodium dodecyl sulfate polyacrylamide gel electrophoresis). Mini-Protean TGX precast gels (Bio-Rad, Mississauga, ON, Canada) of 4-12% acrylamide were used with a Tris/Glycine/SDS pH 8.3 running buffer. Samples run on reduced and denatured gels were mixed in 1:1 proportions with sample buffer containing bromophenol blue, 10% SDS and the reducing agent β-mercaptoethanol. Samples were heated for 4 minutes at 95^{0}C before loading in wells.

Non-reducing gels had samples mixed 1:1 with sample buffer containing bromophenol blue and SDS. Non-reduced samples were not subject to β-mercaptoethanol or heating.

Gels were placed in Bio-Rad Mini Protean 3 cell system and run at 25 mA/gel for approximately 1 hour using Bio-Rad power supply (Model 1000/500). In most cases a pre-stained protein marker of 10-250 kDa (Bio-Rad #161-0374) was used to determine the molecular weights of the sample proteins.

Gels intended for autoradiography were placed in Destain#1(50% MeOH, 7% acetic acid, 43% H_2O) for 5 minutes. This reduced the water content of the gel aiding in the drying process. All other gels were placed in Coomassie brilliant blue stain for >3 hours followed by destaining with

Destain#1 for 5 minutes and Destain#2 (5% MeOH, 7% acetic acid, 88% H_2O) for >4 hours to reveal the protein bands.

2.6. Glycan extraction, labelling and analysis

2.6.1. In-gel

In-gel glycan release was performed following a protocol devised by Royle et al. (Royle et al. 2007) beginning with a Coomassie stained SDS-PAGE gel. The band of interest was cut out of the gel and minced into 1 mm cubes. The gel was frozen for a period of at least 4 hours and then thawed for destaining. Destaining was done by four alternating washes with ACN and 20 mM sodium bicarbonate, each wash lasting for 30 minutes on a mixer. After a final wash with ACN, the gel was dried in a SpeedVac (Thermo, Waltham, MA, USA) centrifuge for 5 minutes. 3 μL of a 1000 U/mL stock of PNGaseF (Roche, Mannheim, Germany) was then added to the gel pieces and covered with 1-2 mm of 20 mM sodium bicarbonate. The gel was then placed in a 37^0C incubator for a minimum of 16 hours. During this time the PNGaseF cleaved the N-glycans from the protein backbone locked within the gel. The cleaved glycans were free within the gel and their small size allowed for extraction by sonicating the sample in a water bath. Several rounds of sonication were performed using water as the solvent followed by ACN. The resulting extract was 0.45 μm filtered and dried down in a SpeedVac. The samples were then 2-AB labelled or frozen at -20°C.

23

2.6.2.   In-solution

In-solution glycan release was performed by using ≈ 200 µg of pure Mab that had been buffer exchanged into 200 µL of 20 mM sodium bicarbonate using 10 kDa molecular weight cut-off (MWCO) filters (Millipore, Billerica, MA). 2 µL of a 1000 U/mL stock of PNGaseF (Roche, Mannheim, Germany) was then added to the solution and placed in a 37^{0}C incubator for a minimum of 4 hours. During this time the PNGaseF cleaved the N-glycans which were then isolated from the protein by performing a Protein A SpinTrap purification as outlined earlier. In this case however the glycan-containing filtrate was retained. The bound antibody was eluted separately and discarded. The glycans were then 0.45 µm filtered (Millipore, Billerica, MA) and dried down in a SpeedVac. Samples were then 2-AB labelled or frozen at -20°C.

2.6.3.   2-aminobenzamide (2-AB) labelling

Dried glycans, either bought or produced in-house, were fluorescently labelled with 2-AB. 2-AB labelling solution was made by mixing 100 µL of a 30% acetic acid/70% DMSO solution and 5 mg 2-AB until dissolved. 6 mg of sodium cyanoborohydride was then added and mixed until dissolved. 5 µL of this solution was added to the dried glycans and incubated at 65^{0}C for 2.5 hours. The sample was cleaned of excess

2-AB label with a Glycoclean S cartridge (Prozyme, Hayward, CA, USA); briefly the labelled sample was loaded onto the column, allowed to bind, and washed with 96% ACN. The bound glycan was eluted using 1.5 mL of water and collected. The released glycan was dried down to approximately 100 µL awaiting injection on the HPLC.

2.6.4. HILIC on Waters HPLC

NP-HPLC methods were originally performed with a 250 mm, 5 µm bead size TSKgel amide-80 column (TOSOH, King of Prussia, PA) heated to 30⁰C. The method was run on the following equipment: a Waters 717plus autosampler (Waters, Milford, MA), Waters 1525 pump and Waters 2475 multi λ fluorescent detector. The detector was set for excitation at 330 nm, emission at 420 nm, gain of 1 and EUFS at 1000. Samples were prepared by mixing 100 µL ACN with 25 µL of sample. 100 µL of this mix was injected onto the column under the conditions outlined in **Table 2.2**. Where A is 50 mM ammonium formate pH 4.4 and B is HPLC grade acetonitrile. A standard of partially hydrolyzed dextrose was run with every sample set to provide a means of determining the glucose unit values.

A new HILIC method was developed that provided better separation and higher throughput, see **Results Chapter 3**.

The new 3.5 μm column was run on same/similar equipment as was the previous method using the gradient profile in **Table 2.3**. Solvents remained the same as old method. Samples were prepared by mixing 24 μL ACN with 6 μL of sample. 25 μL of this mix was injected onto the column. Final HILIC running conditions for new 3.5 μm column can be found in **Table 2.4**.

Table 2.2 HILIC gradient conditions with 5 μm bead column run on

Waters HPLC. Solvent A: 50 mM ammonium formate Solvent B:

Acetonitrile

Time (minutes)	Flow rate mL/min	A	B
0	0.4	20	80
152	0.4	58	42
155	0.4	100	0
157	1.0	100	0
162	1.0	100	0
163	1.0	20	80
177	1.0	20	80
178.5	0.4	20	80
200	0.4	20	80
201	0.0	20	80

Table 2.3 HILIC gradient conditions with 3.5 µm bead column run on Waters HPLC. Solvent A: 50 mM ammonium formate Solvent B: Acetonitrile

Time (minutes)	Flow rate mL/min	A	B
0	0.86	20	80
48	0.86	50	50
49	0.86	100	0
53	0.86	100	0
55	0.86	20	80
63	0.86	20	80
64	0.86	20	80

Table 2.4 Finalized HILIC running conditions with 3.5 µm bead column run on Waters HPLC for 2-AB labelled glycan analysis

Feature	3.5 µm Waters
Flow rate	0.86 mL/min
Gradient Duration	48 minutes
Gradient buffer A% (50 mM Ammonium formate pH4.4)	20-50
Run time	64 minutes
Injection volume	25 µL
Column ID	4.5 mm
Column length	250 mm
Column temp	30ºC
Exc/Ems	330/420 nm

2.6.5. Glycan analysis

Data from HILIC HPLC runs were analysed to determine GU values. The standard dextran ladder was fit with a 5th order polynomial equation to render Glucose Unit (GU) values for the different peaks. The partially hydrolyzed peaks were labelled according to size of oligomer, i.e. GU 1 corresponding to monomer glucose, GU 2 referring to dimer glucose and so on. A minimum of 13 GU peaks were identified so that all possible glycan structures were accounted for. Retention times of samples were inserted into a 5th order polynomial equation to derive GU values corresponding to individual peaks (see **Figure 2.1**). Certain criteria were applied to the HPLC data such that only relevant peaks would be identified; these criteria included only peaks found in the GU 3-12 range and peaks that made up >2% of overall glycans. The determined GU values were cross-referenced with the NIBRT Glycobase database (Dublin, Ireland). In the case of GU values overlapping, an exoglycosidase digest was performed.

Figure 2.1 Example of 5th order polynomial fit to standard dextran ladder

data for use in determining GU values for samples
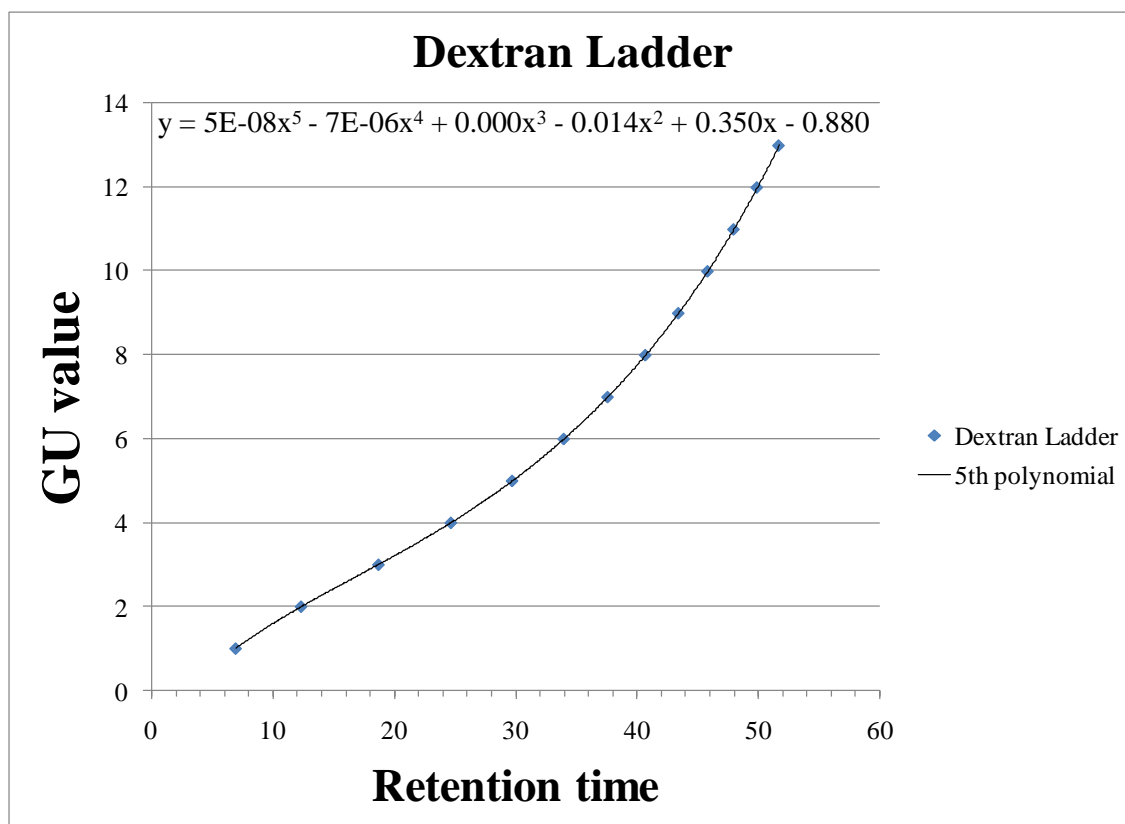
2.6.6.   Exoglycosidase digestion

Exoglycosidase digestions were performed to elucidate the glycan structures. Individual 2-AB labelled samples were portioned out into 5 or 6 tubes (depending on number of digests performed) and dried down in a SpeedVac (Thermo, Waltham, MA, USA) centrifuge. The samples were then reconstituted to a total of 10 μL using various exoglycosidases, buffers and water.   The proportions relied on the number of exoglycosidases being used per sample. An example of a digest array can be seen in the **Table 2.5**. The 5X buffer is specific for the exoglycosidase used. In cases where mixed exoglycosidases were present, the sialidase 5x buffer was used.

After preparing the array, tubes were incubated at 37^0C for a minimum 16 hours. Samples were spun down in 10,000 Da MWCO filters (Millipore, Billerica, MA) to separate the enzymes from the glycans. Glycan samples were injected onto the HPLC using the HILIC method. Data from the HPLC was analysed in the same manner as the original sample to obtain GU values. The difference in profiles among the exodigests can be related to the loss of individual monosaccharides as seen in shifts in their peaks.   These shifts can be extrapolated to determine the original structure.

Table 2.5 Exoglycosidase digestion array for already released and 2-AB labelled N-glycans

Exoglycosidase (Prozyme,Hayward,CA)	Tube 1	Tube 2	Tube 3	Tube 4	Tube 5	Tube 6
Glyko® Sialidase A™(GK80040)	1 µL	1 µL	1 µL	1 µL		
β(1-4,6)-Galactosidase (jack bean) (GKX-5012)		1 µL	1 µL	1 µL		
β-N-Acetylhexosaminidase (jack bean)/HEXase III (GKX-5003)			1 µL	1 µL		
α(1-2,3,4,6)Fucosidase (bovine kidney) (GKX-5006)				1 µL	1 µL	
α(1-2,3,6)-Mannosidase (jack bean) (GKX-5010)						1 µL
5x buffer	2 µL	2 µL	2 µL	2 µL	2 µL	2 µL
DIH$_2$O	7 µL	6 µL	5 µL	4 µL	7 µL	7 µL

2.6.7. Galactosylation Index

Galactosylation Index values were calculated using the raw data of peak areas using the following equation:

Equation (2.1)
$$GI = \frac{G2 + 0.5 \times G1}{G2 + G1 + G0}$$

All peaks with biantennary galactosylation, with or without sialic acid, were considered G2. All peaks with only one galactose residue on either antennae were considered G1. All peaks with a minimum base structure of GlcNAc2Man3 and no galactose residue were considered G0. All GI values are independent of fucosylation.

2.7. Radiolabelling IgG and analysis

2.7.1. Radiolabelling IgG with S^{35} cysteine/methionine

Healthy NS0 cell cultures were counted and 6 x 10^7 cells recovered. Cells were pelleted by centrifugation for 3 minutes at 1500 x g and supernatant discarded. Each pellet was washed with PBS and spun down and then washed a second time to ensure that all extracellular IgG was removed. Cells were resuspended at 6 x 10^6 cells/mL in 10 mL of Biogro medium sans cysteine/cystine/methionine in a 25 cm^2 T-flask. After incubation at 37^{0}C for 45 minutes, the flask was removed from the incubator and 90 µL (3.7MBq/mL) of EasyTag ExpreSS S^{35} Met/Cys (Perkin-Elmer, Waltham, MA, USA) added. Sample intervals included 1,

3, 6, 12, 30, 60, 120 minutes. At each time point a 1 mL sample was removed and the flask returned to the incubator until the next sample. The 1 mL samples were all treated identically. Initially spun down at 2000 x g for 1 minute, the supernatant was discarded and three rounds of washing with ice cold PBS were performed; with pelleting of the cells done in between washes and supernatant discarded. The final pellet had 1 mL of RIPA buffer containing 50 mM IAM and 10 µL protease inhibitor P-8340 (Sigma, St. Louis, MO) added. Samples were kept on ice for 10 minutes after RIPA addition whereupon 2 mL of PBS was added. Samples were then passed through a 0.22 µm filter prior to loading on the HiTrap Protein A HP column. Following the Protein A purification, as described earlier, the samples were concentrated in 10,000 Da MWCO filters (Millipore, Billerica, MA) from approximately 3 mL to 200 µL. This allowed for a sufficient amount of product to be loaded into the SDS-PAGE gel.

The same loads of concentrated samples were run in a non-reduced SDS-PAGE as described earlier. After being treated with Destain#1, the gels were placed in a Tut's tomb gel dryer (Idea Scientific, Minneapolis, MN) overnight with one side of the gel covered in cellophane. Once dry, the gel was exposed to an X-ray film with the gel side (uncovered) facing the film. X-ray film and gel were secured in autoradiography cassette in a dark room. The entire cassette was placed in -80^{0}C freezer for 15-30 days.

Duplicate gels were often run with varying exposure times to maximize band intensity.

The film was developed with Kodak (Toronto, ON) developer and fixer in the following manner: 4 minutes in developer, 30 second rinse in water, 8 minutes in fixer, and 12 minutes in water bath. The film was hung to dry prior to imaging.

2.7.2.   Gel and X-ray film imaging and densitometry

An Alphaimager (ProteinSimple, Santa Clara, CA) was used to capture images of gels and X-ray films. White light transillumination was used with no filters. After image capture, AlphaEaseFC software was used to label and perform densitometry measurements on bands. Densitometry measurements were done by manually selecting the bands of interest and purposefully including some background pixels. The automated background function was enabled so that an average of the 10 lightest pixels from the selected area was set as background and thereby subtracted from the band intensity. In the case of X-ray film bands, ratios of bands were compared simply by using the densitometry values.

2.8. Partial reduction of IgG1

NS0-IgG1 was partially reduced to a pool of fragments containing heavy chains by DTT. In a microfuge tube, 5 μL of a stock solution of 100 mM DTT was added to 95 μL of IgG1 (3.9 mg/mL buffer pH 7.2) to get the final [DTT] of 5 mM. After 10 minutes, alkylation was performed by adding 10 μL of a 100 mM iodoacetamide (IAM) solution. Each microfuge tube was placed in the dark for 30 minutes followed by a buffer exchange into 100 μL of GalT assay buffer from R&D systems (Minneapolis, MN) using 10-kDa MWCO filters. A 10 μL sample was removed from each sample to confirm by SDS-PAGE that 50, 100, 125, and 150 kDa species were present. The approximate concentration of IgG1 fragments was 3.4 mg/mL.

2.9. Degalactosylation

Purified Mabs were treated with β(1-3,4)-Galactosidase (bovine testis, Prozyme, Hayward, CA) to cleave off all galactose residues. Approximately 400 μL of EG2-hFc (1.6 μg/μL) and IgG1-NS0 (3.9 μg/μL) were buffer exchanged into 125 μL of galactosidase buffer using 10-kDa MWCO filters. 5 μL of galactosidase was added to each tube and left overnight at 37°C. After incubation, contents of each tube were buffer exchanged into phosphate buffer (pH 7.2) in preparation for Protein A clean up to remove the galactosidase. HiTrap protein A spin filters were

used as previously described; eluting with 0.1 M glycine (pH 3.0) and neutralizing eluant with 100 μL 1M Tris buffer pH 9.0. 30 μg of each Mab were used to confirm degalactosylation by in-solution HILIC glycan extraction and analysis.

2.10. β-1,4 galactosyltransferase (GalT) activity assays using Malachite Green detection method

GalT assays require three main components: donor, acceptor and the co-factor manganese. The donor in all assays was UDP-Galactose (EMD Millipore, Billerica, MA) and a stock solution of 100 mM Mn^{2+} was made up. The acceptor was either N-acetylglucosamine (GlcNAc) monomer or the Mabs IgG1 and EG2-hFc. GalT activity was monitored by colorimetry of Malachite Green reagents in the presence of free inorganic phosphates. Inorganic phosphates are released in the cleaving of UDP to UMP by a coupling phosphatase (R&D Systems, Minneapolis, MN). Only UDP, and not UDP-Gal, will be cleaved by the phosphatase indicating that GalT was active in the addition of a galactose residue.

2.10.1. Reagent Preparation

Assay Buffer (AB) was prepared using 150 μL Phosphatase Buffer 1 (R&D Systems, Minneapolis, MN), 150 μL 100 mM $MnCl_2$ and 1.2 mL DI water. Other reagents included: 10 mM UDP-Gal (Sigma, St.Louis, MO)

made up in DI water and diluted to 0.5 mM UDP-Gal in AB, 1 M GlcNAc (Sigma, St.Louis, MO) made up in DI water and diluted to 50 mM in AB, coupling phosphatase 1 (CP) (100 μg/mL, R&D Systems) diluted to 20 μg/mL in AB, GalT (10 μg/μL, G5507, Sigma, St.Louis, MO) diluted 20 fold to 0.5 μg/μL in AB, and 0.1 mM UDP (R&D Systems, Minneapolis, MN) made up in AB. Concentrations of IgG1 and EG2-hFc used were 4.42 μg/μL (29.5 μM) and 1.7 μg/μL (21.25 μM) in AB respectively.

2.10.2.　Phosphate standard curve

Using a R&D Systems EA001 glycosyltransferase kit, 40 μL of the 1 mM Phosphate Standard was added to 360 μL of assay buffer in a microcentrifuge tube and mixed well. Serial dilutions were performed to yield phosphate standards with a range of 0.078 to 5.0 nmol per well; 50 μL of each standard were placed in duplicate wells. Assay buffer alone was used as the zero standard. After incubation and detection (see section **2.10.5**), each standard`s duplicate readings were averaged and the blank's value subtracted. Standard curves and linear equations were generated by plotting phosphate input (pmol/well) vs. the corrected OD (**Figure 2.2**).

39

Figure 2.2 Example of phosphate standard curve as detected by Malachite Green at 630 nm

Phosphate stnd — Linear (Phosphate stnd)

$y = 3593x - 12.597$
$R^2 = 0.9995$

Phosphate Input (pmol/well)

Optical density (630 nm)
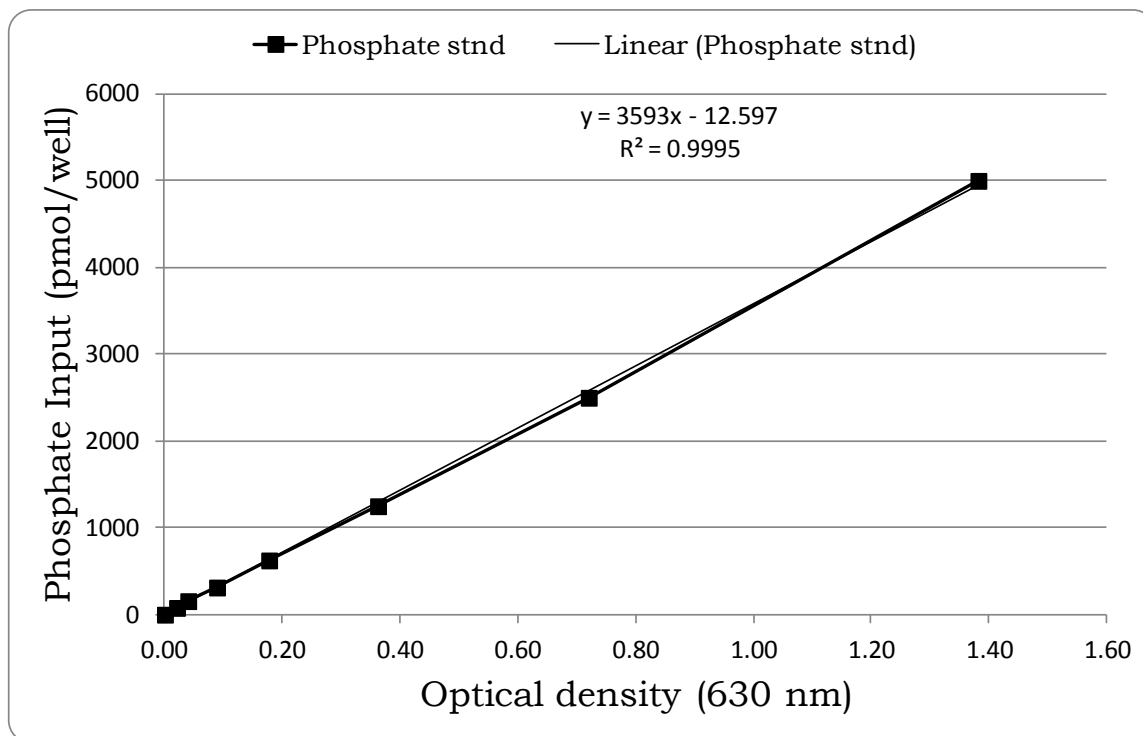
2.10.3. Plate Set-up for GalT in presence of dithiothreitol

Using a 96-well V-bottom plate, all trials were performed in duplicate with a 50 µL final volume. See **Table 2.6** for plate set-up. All wells received 10 µL of UDP-Gal donor, 10 µL of GlcNac and 5 µL of CP. The negative assay control (**NAC**) received 25 µL of assay buffer. The assay control (**AC**) received 20 µL assay buffer and 5 µL GalT. A stock solution of 10 mM DTT was prepared in DIH_2O and used to target the selected DTT concentrations seen in **Table 2.6**. Volumes of DTT ranged from 1.25 – 5.00 µL. All DTT wells were topped up to 45 µL with assay buffer followed by addition of 5 µL GalT. The assay blank (**AB)** received 50 µL assay buffer. The coupling phosphatase control (**CPC**) received 20 µL of assay buffer, 5 µL of CP and 25 µL of 0.1 mM UDP. The plate was covered with sealing-film and incubated at 37°C for 1 hour.

Table 2.6 Plate layout for GalT activity with GlcNAc as acceptor and UDP-gal as donor in presence of variable concentrations of DTT. All conditions were performed in duplicate

	1	2	3
A	CPC	NAC	NAC
B	AB	AC-1	AC-2
C		0 mM-1	0 mM-2
D		0.25 mM-1	0.25 mM-2
E		0.50 mM-1	0.50 mM-2
F		0.75 mM-1	0.75 mM-2
G		1.00 mM-1	1.00 mM-2

2.10.4.　　Plate Set-up for native and degalactosylated IgG1 and EG2-hFc

Using a 96-well V-bottom plate, all trials were performed in duplicate with a 50 µL final volume. See **Table 2.7** for plate set-up. The negative assay control (**NAC)** and assay control (**AC)** wells received 10 µL of UDP-Gal donor, 10 µL of GlcNac, 5 µL of CP and 20 µL assay buffer each. The assay blank (**AB)** received 50 µL of assay buffer. The coupling phosphatase control (**CPC**) received 20 µL of assay buffer, 5 µL of CP and 25 µL of 0.1 mM UDP. The **IgG1** and **EG2-hFc** wells received 10 µL of UDP-Gal donor and 5 µL of CP. The target protein content for each Mab was 0.5 nmol of protein. Assay buffer was used to top up to 45 µL. Each of **AC**, **IgG1** and **EG2-hFc** received 5 µL of GalT. **NAC** received 5 µL assay buffer instead. The plate was covered with sealing-film and incubated at 37°C for 1 hour.

Table 2.7 Plate layout for GalT activity with Mabs IgG1 and EG2-hFc as acceptors and UDP-gal as donor. All conditions were performed in duplicate

	1	2	3
A	CPC	NAC	NAC
B	AB	AC1$_{GlcNAc}$	AC2$_{GlcNAc}$
C		IgG1-1	IgG1-2
D		EG2-hFc-1	EG2-hFc-2

2.10.5. Phosphate detection by Malachite Green for all GalT assays

After incubation, 30 µL of the Malachite Green Reagent A was mixed into each well followed by 100 µL of deionized water and 30 µL of the Malachite Green Reagent B. The plate was allowed to develop for 20 minutes at room temperature before loading into a plate reader set at 630 nm (absorbance) in endpoint mode. The Specific GalT activity was calculated using the following equation:

Equation (2.2)

$$Specific\ activity\ (pmol/min/\mu g = \frac{Phosphate\ released^{1}(nmol) \times \left(1000\frac{pmol}{nmol}\right)}{Incubation\ time\ (min)\ \times\ amount\ of\ GalT\ (\mu g)}$$

[1]Derived from the phosphate standard curve using linear equation and adjusted for blank

2.11. GalT trials with Mabs for glycan analysis

2.11.1. Reagent preparation

The assay Buffer (AB) was the same as in **2.10.1**. Other reagents included: 10 mM UDP-Gal (Sigma, St.Louis, MO) made up in DI water and GalT (10 µg/µL, G5507, Sigma, St.Louis, MO) diluted to 2.5 µg/µL in AB. The concentrations of Mabs after buffer exchange into AB were: [IgG1] = 20 µg/µL, [EG2-hFc] = 3 µg/µL, [partially reduced IgG1 pool] = 3.7 µg/µL.

2.11.2. Whole Mab *in vitro* galactosylation

Two microfuge tubes were set up; one for EG2-hFc and one for IgG1. Each tube received 10 µL of 10 mM UDP-Gal and 10 µL of 2.5 µg/µL GalT. In order to have sufficient glycans for analysis, 90 µg (1.8 µg/µL) of Mab was targeted for loading in a 50 µL final volume. To achieve this 30 µL of EG2-hFc was loaded into one tube while 4.5 µL of IgG1 and 25.5 µL AB were loaded into the other. The tubes were placed in the incubator at 37⁰C overnight. After incubation, a Protein A clean up and in-solution glycan analysis were performed as described earlier.

2.11.3. Partially reduced IgG1 *in vitro* galactosylation

50 µL of the partially reduced IgG1 pool (3.4 µg/µL) generated in **2.8** was placed in a microfuge tube. 10 µL of 10 mM UDP-Gal and 10 µL of 2.5 µg/µL GalT were then added. The tubes were placed in the incubator at 37ºC overnight. After 18 hours, the tubes were removed from the incubator, cleaned up by Protein A and separately run on non-reducing prep SDS-PAGE gels. The bands corresponding to 50, 100, 125, and 150 kDa were excised and in-gel glycan analysis was performed as described earlier.

Chapter 3 – HPLC method development for higher resolution and throughput with hydrophilic interaction liquid chromatography

3.1. Abstract

Many analytical tools exist for determining microheterogeneic glycan structures and isomeric forms. They include capillary electrophoresis, carbohydrate microarrays, mass spectrometry and liquid chromatography. The HPLC method called hydrophilic interaction liquid chromatography (HILIC) is ideal for determining the microheterogeneity of glycans as they present on glycoproteins. Using a fluorescent label, HILIC is capable of distinguishing individual unit construction of glycans and when coupled with an ever growing comprehensive literature database stored at the NIBRT (National Institute for Bioprocessing Research and Training), findings are easily comparable across multiple sites. The old HILIC method used in the Butler lab was low throughput with >3 hour run times and degrading resolution over column life. A new column was employed, on original equipment, and new flow/gradient structure developed which increased throughput 3 fold with a much higher resolution including the identification of multiple isomeric forms that were previously unresolved.

Keywords Hydrophilic interaction chromatography, glycan analysis, 2-aminobenzamide, recombinant protein, monoclonal antibody

3.2. Introduction

Hydrophilic interaction liquid chromatography (HILIC) has been widely used as a principal form of N-glycan analysis in industrial and academic institutions (Gilar et al. 2011, Doherty et al. 2012). Previously known as normal phase HPLC it uses a polar stationary phase of 50 mM ammonium formate, and a mobile phase of acetonitrile. When a polar gradient is applied to the column, the analytes are eluted in a defined manner, which allows for structural determination and bond configuration (Royle et al. 2008). Isolated glycans are detected via an attached fluorescent label with specific excitation and emission values. The 2-aminobenzamide (2-AB) fluorescent label is very sensitive (Karlsson et al. 2008) allowing for low glycans titres to be evaluated. Glycan profiles generated by this method are assessed Glucose Unit (GU) values derived from a standard curve of a partially hydrolyzed dextran sample. GU values correspond to the oligomeric nature of the dextran reported in that peak; GU=1 has one glucose unit, GU=2 has 2 glucose, GU=3 has 3 glucose, etc. These GU values can then be interpreted through the use of an online database provided by the National Institute for Bioprocessing Research and Training in Dublin, Ireland which maintains a cumulative record of all published data using HILIC and other orthogonal glycan analytical methods for comparison.

Some of the deficiencies in the HILIC-HPLC method can be the long run duration, which results in low throughput and high solvent usage.

Other issues are that the resolution of peaks can be hampered when GU values closely overlap as well as peak erosion over the life of a column. New UPLC methods have remedied most of these issues (Ahn et al. 2010) but require a substantial capital investment. For HPLC users the solution comes in the form of new column development and method optimization.

Original methods in the lab used a 5 µm bead size TSKgel Amide-80 column from Tosoh (Grove City, OH) with run times exceeding 200 minutes. Separation efficiencies of this column were poor, resulting in the overlap of many glycan moieties and without baseline resolution between peaks. In this section a new 3.5 µm bead Waters (Milford, MA) Amide-80 column was employed and new method devised to shorten the run time, reduce solvent usage, and most importantly increase resolution between glycan structures.

The new method was able to resolve previously unidentified structures in several complex glycan samples from insect mimic sf9 cultures producing hemagglutinin antigen. Insect sf9 cell cultures typically produce paucimannose glycans on the recombinantly expressed proteins. Mimic sf9 cultures have been engineered with other glycosyltransferases such that more mammalian-like glycan structures can be formed (Jarvis et al. 1998). These human-like glycans are then better suited for injectable therapeutics due to lower immunogenicity lending to longer serum half-lives. The new method was also tested on a

more conventional mammalian cell culture product of recombinant monoclonal antibody glycans, specifically a humanized NS0 derived Mab.

3.2.1.   Objectives

The objectives of the experiments outlined in this chapter were to develop a new high throughput HILIC-HPLC method for glycan analysis without the introduction of any new instrumentation.   This included higher resolution, less solvent waste and repeatability.

3.3. Results

3.3.1. Method development

The original method (Method 1) using a 5 µm particle size had a flow rate of 0.4 mL/min and a gradient duration of 152 minutes. The washout steps to ensure a clear column with no carryover to subsequent samples extended the run time to 200 minutes. Switching over to a 3.5 µm particle size column required a new method (Method 2) with new flow rate and gradient to be determined (solvents did not change). In order to calculate these new values the following equations, provided by Waters, were employed with results summarized in **Table 3.1**.

Equation (3.1)

$$FlowRate(2) = FlowRate(1) \times \frac{Diameter(2)^2}{Diameter(1)^2} \times \frac{ParticleSize(1)}{ParticleSize(2)}$$

Equation (3.2)

$$GD(2) = \frac{GD(1) \times Length(2)}{Length(1)} \times \frac{Diameter(2)^2}{Diameter(1)^2} \times \frac{FlowRate(1)}{FlowRate(2)}$$

Where all variables with (1) refer to method 1 values and all variables with (2) refer to method 2 values. GD is gradient duration.

Table 3.1 Flow rate and gradient duration values for HILIC protocol with either 5 µm or 3.5 µm columns run on Waters HPLC

Feature	5.0 µm Tosoh Method 1	3.5 µm Waters Method 2
Flow rate	0.4 mL/min	0.57 mL/min
Gradient Duration	152 minutes	106.4 minutes

It should be noted that only the particle size changed in the new column; the length and diameter of the column remained constant at 250 mm and 4.5 mm respectively. Preliminary test runs with a standard dextran ladder indicated that separation was efficient in the new column with sufficient separation between peaks to allow for higher throughput flow rates. The calculated flow rate of 0.57 mL/min was increased to 0.86 mL/min while still running within acceptable pressure limits; <3000 psi. This new flow rate along with the 106 minute gradient resulted in the separation of 19 dextran peaks when the standard was run. This range of

GU values covers the glycans that may be encountered with recombinant glycoproteins where the typical range of GU values is 4-12. For example a fully sialylated, fucosylated, tetra-antennary structure has a GU value of 11.9. However, having 19 peaks elute in that time frame would elute glycans too quickly forcing some overlap when samples were run. To optimize peak separation and run duration it was determined that a maximum of 13 dextran peaks would be sufficient to provide an overlapping standard curve while encompassing all possible glycan variants.

With these factors in mind the gradient and gradient duration were altered to achieve optimum performance. Method 1 had a gradient of 20-58% 50 mM ammonium formate. When used with the 3.5 μm column, the elution profile of a standard dextran ladder produced the 19 dextran peaks. The small intervals between peaks translated into decreased accuracy with respect to GU calculations. GU calculations are based on a fifth order polynomial equation fit to the glucose peaks from a dextran ladder and that greater distances between peaks yields more accurate results for GU values. Method 1 could also generate up to 19 glucose peaks; however the long duration (200 min) meant peak spacing was not compromised as much. Optimal results for method 2 were found when the run time was decreased from 106 minutes to 48 minutes and gradient changed from 20-58% to 20-50%. This new gradient yielded the desired

13 glucose peaks upon standard injection. The standard dextran ladders from methods 1 and 2 can be seen in **Figures 3.1** and **3.2** respectively. In both methods the peaks were sharp with single peaks appearing at each dextran oligomer.

The washout steps after the gradient were also optimized with a decrease from 44 to 16 minutes resulting in a run time of only 64 minutes, more than a threefold decrease compared to method 1. Washout optimization was confirmed by running blanks after standard dextran injections and noticing no carry-over peaks. In addition to flow and gradient characteristics, the sample injection volumes were lowered from 100 μL to 25 μL. Excitation and emission wavelengths were not changed. The fully optimized conditions compared to original method are found in **Table 3.2**.

Figure 3.1 Standard dextran ladder profile from 5 μm column run with HILIC-HPLC method 1. Peaks are identified as 1→13 and correspond to the Glucose Unit value. 100 μL injection volume
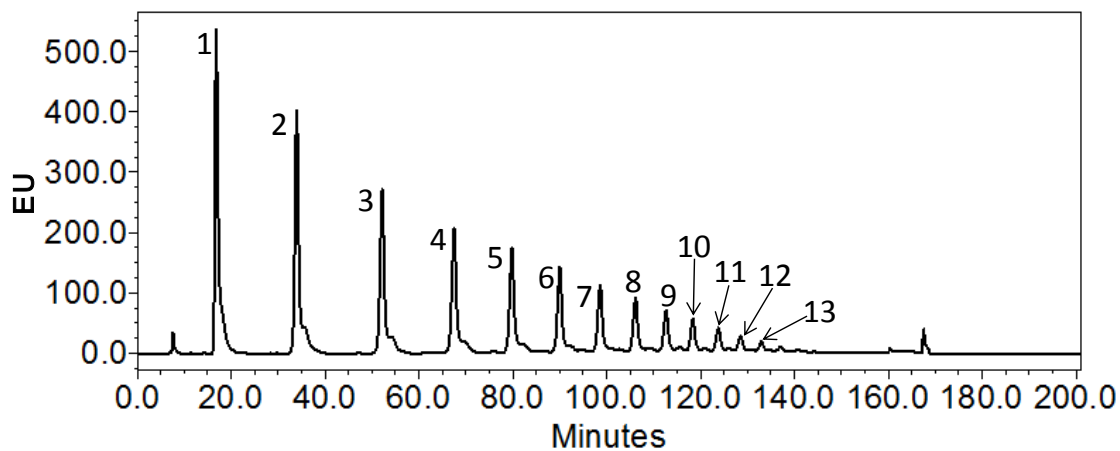
Figure 3.2 Standard dextran ladder profile from 3.5 μm column run with HILIC-HPLC method 2. Peaks are identified as 1→13 and correspond to the Glucose Unit value. 25 μL injection volume
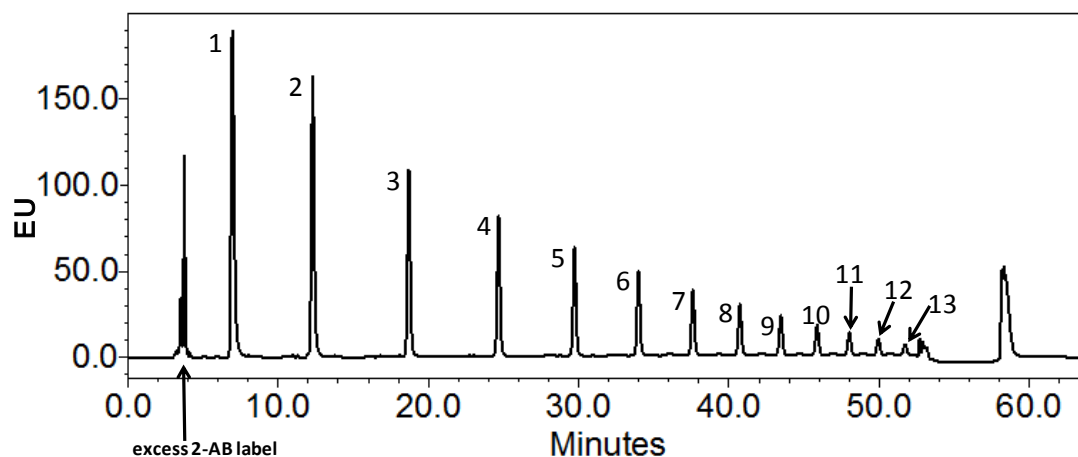
Table 3.2 Final optimized conditions for method 2 with 3.5 µm particle size column from Waters compared to method 1 with 5 µm column from Tosoh

Feature	5.0 µm Tosoh Method 1	3.5 µm Waters Method 2
Flow rate	0.4 mL/min	0.86 mL/min
Gradient Duration	157 minutes	48 minutes
Gradient buffer A% (50 mM Ammonium formate pH4.4)	20-58	20-50
Run time	200 minutes	64 minutes
Injection volume	100 µL	25 µL
Column ID	4.5 mm	4.5 mm
Column length	250 mm	250 mm
Column temp	30°C	30°C
Exc/Ems	330/420 nm	330/420 nm

3.3.2. Recombinant glycoprotein trials

Two samples were used to test the suitability of Method 2 vs Method 1: 1) a hemagglutinin H5 antigen produced in mimic sf9 insect cells and 2) a humanized IgG1 monoclonal antibody produced in NS0 cell culture.

3.3.2.1. *H5 antigen*

Figures 3.3 and **3.4** show glycan profiles generated using methods 1 and 2 respectively for the same sample of H5 antigen produced in mimic insect cell culture. As evidenced in method 1 (**Figure 3.3)** the peaks are slightly rounded at the top and not fully resolved to baseline with all significant peaks eluted by 100 minutes run time. The identified peaks are listed in **Table 3.3**. Approximately 70% of the glycans were biantennary and variably galactosylated. High mannose structures were also identified, making up ≈ 30% of glycans. When the same sample was run by method 2, it generated the profile found in **Figure 3.4**. The differences between method 1 and method 2 are clearly seen when comparing both profiles. The peaks are well defined and sharp with resolution to baseline occurring in most cases. Equally important is that the high resolution allowed a higher throughput; all significant peaks were eluted by 44 minutes of run time; no peaks appeared after 44 minutes. All identified peaks can be found in **Table 3.4**.

Method 2 identified 19 peaks compared to 12 with Method 1. The higher resolution of Method 2 allowed quantification of peaks that were overlapped or shouldered in Method 1. In Method 2, variably galactosylated biantennary glycans were predominant making up ≈ 90% of the structures. High mannose structures comprised only 10% of overall structures. This discrepancy in composition of the same sample when analysed by Methods 1 and 2 is tremendous and will be discussed later on.

Figure 3.3 Hemagglutinin H5 glycans produced in mimic sf9 cells run on Waters HPLC with HILIC method 1 (5 µm column). Purified H5 processed with PNGase F followed by 2-AB labelling of released glycans
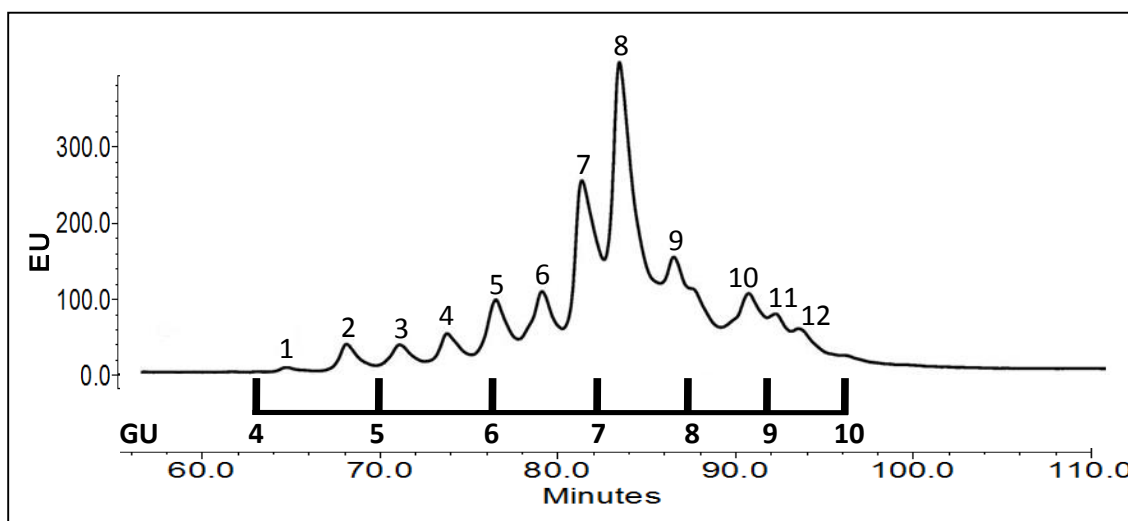
Figure 3.4 Hemagglutinin H5 glycans produced in mimic sf9 cells run on Waters HPLC with HILIC method 2 (3.5 μm column). Purified H5 processed with PNGase F followed by 2-AB labelling of released glycan
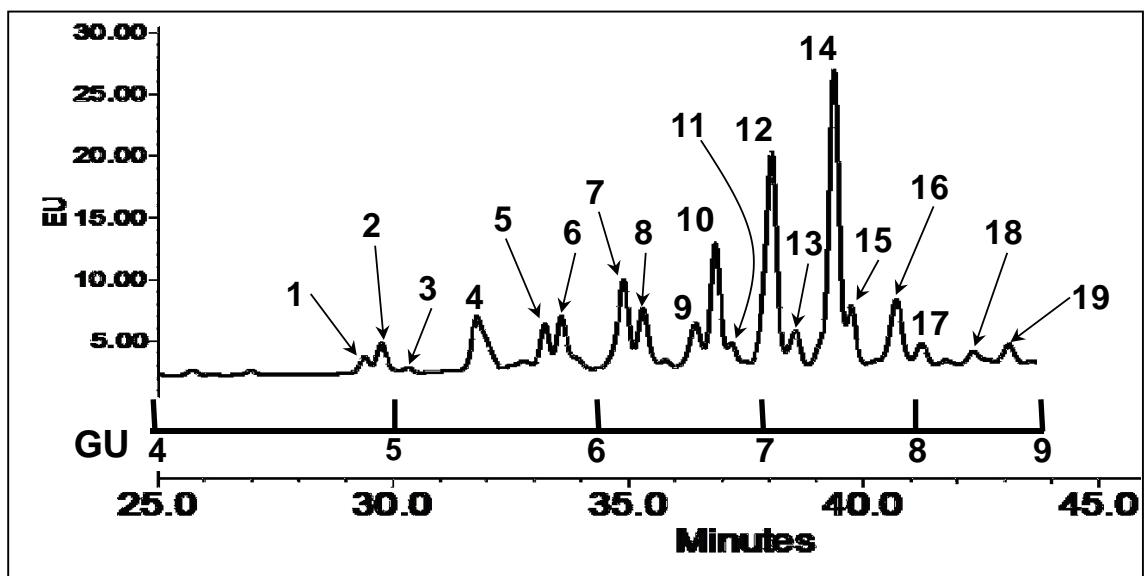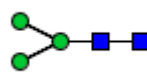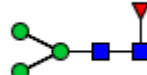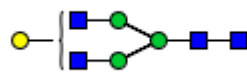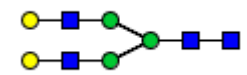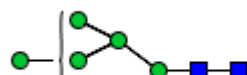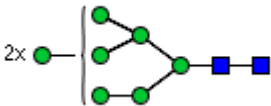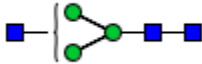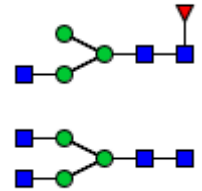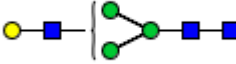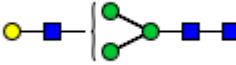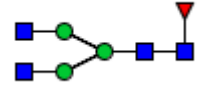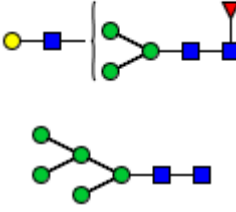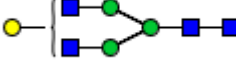
Table 3.3: Structure identification of glycans present on H5 antigen and relative percent area when run with HILIC Method 1. GU and relative percent area values are averages from 2 runs of the same sample with RSD < 10% in all cases.
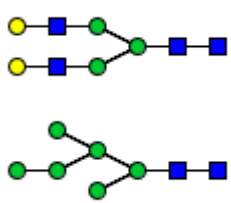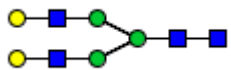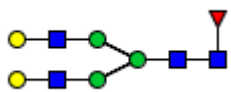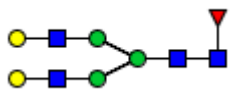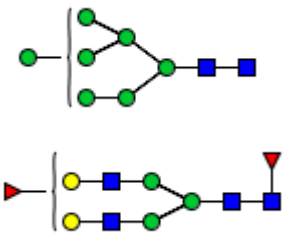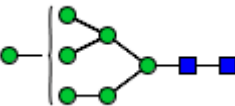
Peak#	GU value	Structure ID		Relative % area
1	4.32	M3		0.7
2	4.78	F(6)M3		2.4
3	5.21	A1		2.6
4	5.62	F(6)A1		3.4
5	6.05	A2G1		6.2
6	6.48	F(6)A2G1		7.5
7	6.87	A2G2		15.8
8	7.25	F(6)A2G2		28.5
9	7.84	M7		14.6

10	8.70	M8		8.3
11	9.04	?*		3.6
12	9.33	M9		6.3

*this structure is unidentified; exoglycosidase digestion suggests it is galactosylated

Table 3.4: Structure identification of glycans present on H5 antigen and relative percent area when run with HILIC Method 2. GU and relative percent area values are averages from 2 runs of the same sample with RSD < 10% in all cases

Peak#	GU value	Structure ID		Relative % area
1	4.89	F(6)M3		1.1
2	4.96	A1		2.2
3	5.42	F(6)A1 and A2		5.9
4	5.65	A1G1		1.1
5	5.76	A1G1		3.1
6	5.85	F(6)A2		4.7
7	6.19	F(6)A1G1 and M5		7.3
8	6.30	A2G1		4.7

9	6.61	F(6)A2G1 and M5A1		3.7
10	6.73	F(6)A2G1		8.5
11	6.82	F(6)A2G1		1.6
12	7.08	A2G2 and small amount of M6		17.5
13	7.23	A2G2		2.7
14	7.49	F(6)A2G2		21.1
15	7.61	F(6)A2G2		3.8
16	7.93	M7 and some F(6)A2G2F(2)1		6.0
17	8.12	?*		1.8
18	8.52	?*		1.6
19	8.79	M8		1.8

*these structures are unidentified; exoglycosidase digestion suggest they are galactosylated

3.3.2.2. *Ig*G1

The same sample of 2-AB labelled glycans from IgG1 produced in NS0 cell culture was analysed with both methods. **Figure 3.5** shows the glycan profile as run with HILIC Method 1. This profile resembles the expected profile of an IgG1 with the major peak identified at GU 5.92 being F(6)A2, peak 4, a fucosylated non-galactosylated biantennary complex glycan. It is a well-defined single peak with no shoulder. The second major peak identified at GU 6.67 is F(6)A2G1, peak 7, fucosylated mono-galactosylated biantennary complex glycan. The shape of this peak includes a right side shoulder, suggesting that another species of glycan may be present; however the shoulder and main peak body are integrated as one unit and therefore given only one GU value. The third largest peak identified at GU 7.58 is F(6)A2G2; peak 9, a fucosylated, digalactosylated biantennary complex glycan. This peak does not have a shoulder and does not resolve to baseline. Also of interest is that for the remaining smaller peaks, they are slightly rounded and not always resolved to baseline. All peaks were identified in **Table 3.5**; all identities have been confirmed through exoglycosidase digestions and comparison to published data provided by the Glycobase database. The identities of peaks were limited to those glycans which comprise more than 0.5% of the overall structures present on the IgG1 molecule.

The glycan profile of the same IgG1 sample run with HILIC Method 2 can be seen in **Figure 3.6** with identified peaks listed in **Table 3.6**. The most pronounced difference in **Figure 3.6**, compared to **Figure 3.5**, is the sharpness of peaks and the resolution to baseline for most of them. Of the three major peaks, peak 4 (F(6)A2) and peak 9 (F(6)A2G2) are sharp and well isolated from the larger sialylated species. Of particular interest are peaks 7 and 8; these represent the isomeric forms of F(6)A2G1. In Method 1 (**Figure 3.5)** peak 7 has a right side shoulder; this shoulder becomes fully resolved when using Method 2 (**Figure 3.6**). This level of separation allows for the identification of more isomeric forms and overlooked species of glycans with more confidence. It can be noted that the same glycans are not always found by both methods nor in the same quantity. However, more confidence can be place on Method 2 in which the peaks are better resolved and sharper.

Figure 3.5 IgG1 glycans produced in NS0 cells run on Waters HPLC with HILIC Method 1 (5 μm column). Protein A purified IgG processed with PNGase F followed by 2-AB labelling of released glycans
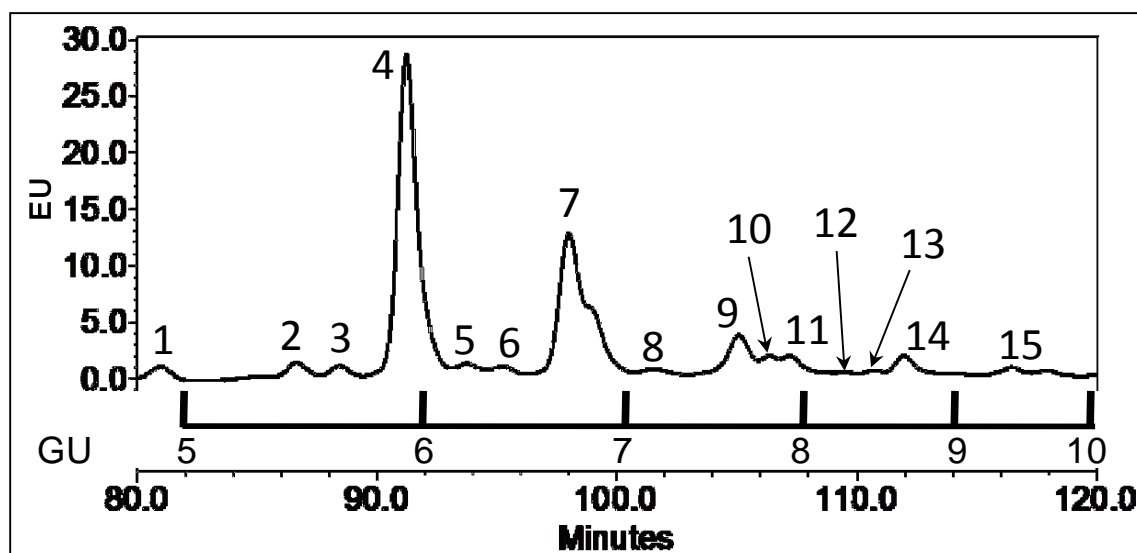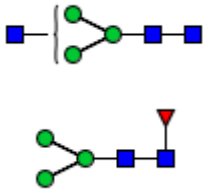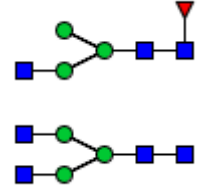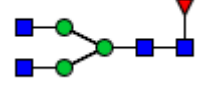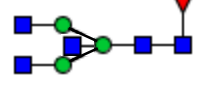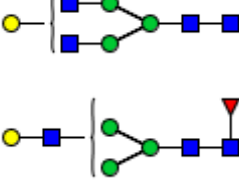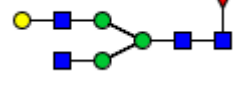
Table 3.5: Structure identification of glycans present on NS0 produced humanized IgG1 and relative percent area when run with HILIC Method 1. GU and relative percent area values are averages from 2 runs of the same sample with RSD < 10% in all cases

Peak#	GU value	Structure ID		Relative % area
1	4.93	A1 and F(6)M3		1.9
2	5.45	F(6)A1 and A2		3.3
3	5.63	A1G1		2.0
4	5.92	F(6)A2		40.1
5	6.19	F(6)A2B		2.4
6	6.36	A2G1 and F(6)A1G1		2.1
7	6.67	F(6)A2G1		26.4
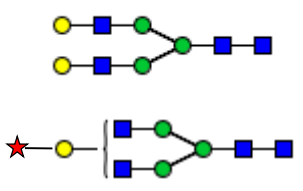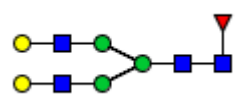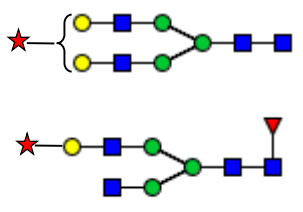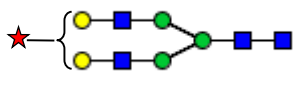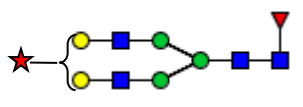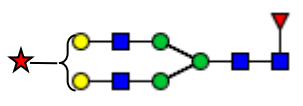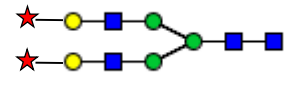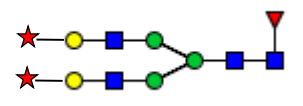
8	7.11	A2G2 and some A2G1S1		1.9
9	7.58	F(6)A2G2		6.8
10	7.87	A2G2S1 and F(6)A2G1S1		4.1
11	7.92	A2G2S1		1.6
12	8.21	F(6)A2G2S1		0.7
13	8.39	F(6)A2G2S1		0.9
14	8.58	A2G2S2		4.1
15	9.32	F(6)A2G2S2		1.6

Figure 3.6 IgG1 glycans produced in NS0 cells run on Waters HPLC with HILIC Method 2 (3.5 µm column). Protein A purified IgG processed with PNGase F followed by 2-AB labelling of released glycans
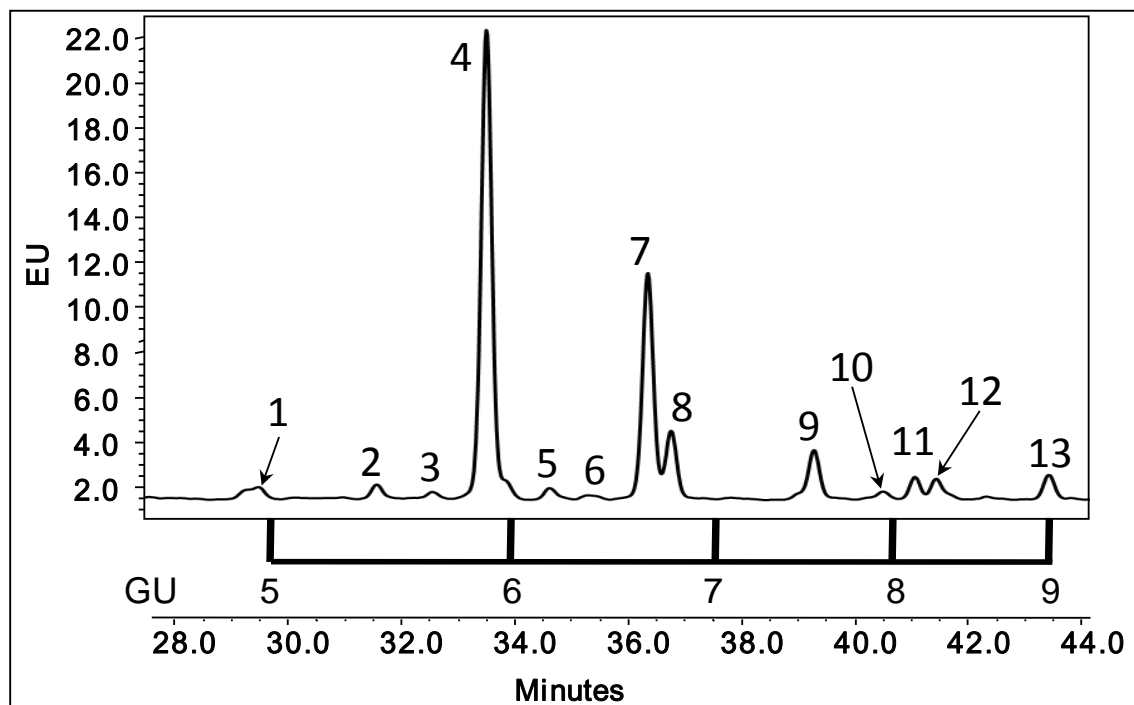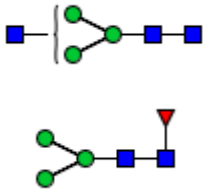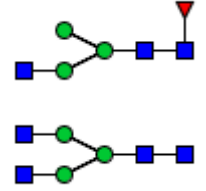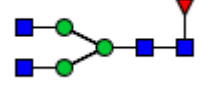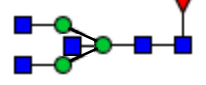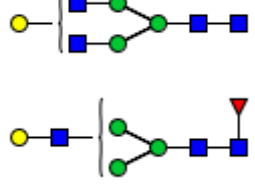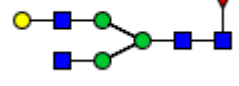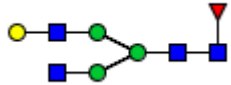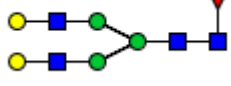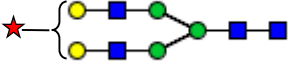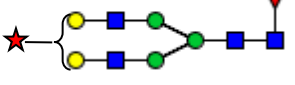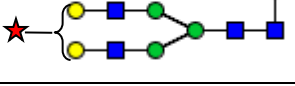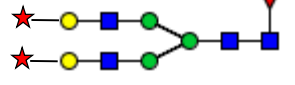
Table 3.6: Structure identification of glycans present on NS0 produced humanized IgG1 and relative percent area when run with HILIC Method 2. GU and relative percent area values are averages from 2 runs of the same sample with RSD < 10% in all cases
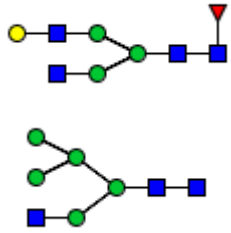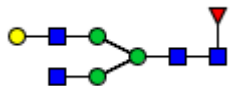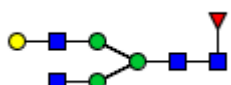
Peak#	GU value	Structure ID		Relative % area
1	4.94	A1 and F(6)M3		1.7
2	5.40	F(6)A1 and A2		1.3
3	5.63	A1G1		<1.0
4	5.87	F(6)A2		36.2
5	6.15	F(6)A2B		1.1
6	6.33	A2G1 and F(6)A1G1		<1.0
7	6.62	F(6)A2G1		17.4

8	6.74	F(6)A2G1		5.5
9	7.50	F(6)A2G2		4.3
10	7.90	A2G2S1		<1.0
11	8.10	F(6)A2G2S1		1.7
12	8.23	F(6)A2G2S1		1.9
13	8.97	F(6)A2G2S2		1.9

3.4. Discussion

High throughput methods are particularly desirable when running a great number of samples from multiple users. The original HILIC method using a 5 µm bead amide column was sufficient for glycan determination. However the new columns and resins allow for higher resolution of peaks and therefore more reliable data to be obtained rapidly. Optimally a UPLC (Ultra Pressure Liquid Chromatography) instrument could be employed which could generate data in a fraction of the time, with low solvent usage and high resolutions (Ahn et al. 2010). This is possible due to the ability of UPLCs to operate with column media less than 2 µm in diameter at pressures exceeding 10000 Psi. Alternatively capillary electrophoresis, lectin microarrays and mass spectrometry could be used to determine glycan structures from a multitude of recombinant proteins (Szabo et al. 2011; Park et al. 2013; Snovida et al. 2010); however the capital investment for these technologies is very high for academic research labs and therefore undesirable. A lower cost alternative was targeted, a new method with a new column for the current HPLC instruments. One of the issues with the older 5 µm columns was the rounding of peaks after repeated usage. This rounding not only affected the integrity of integrated peak area but also the resolution of individual peaks from their neighbours. This effect has not been seen with the new 3.5 µm column to the same extent. The 5 µm column generally lasted 4-

5 months (1000 runs) before resolution was too poor to continue. The 3.5 μm column lasts approximately 10 months (2000 runs) or longer before needing to be replaced. This increase in longevity is not necessarily due to the size of the bead but rather the composition of the column resin. This is a reflection of switching from a Tosoh to Waters manufacturer. When comparing new 5 μm vs. 3.5 μm columns, significant differences are not seen in peak sharpness but are apparent in resolution. In order to get the same resolution in the 5 μm column we would need to increase the run time to allow for proper separation. At a current run time of over 3 hours, that was not a practical goal for optimization.

After calculating and modeling Method 2 for a Glucose Unit range of 1-13, it was able to outperform Method 1 in less than one third the time while utilizing 69% of the solvent (80 mL vs 55 mL). The time, solvent usage and increase in precision are paramount to this new method.

When examining the trial samples of H5 antigen glycans there are discrepancies between the identification and quantity of some of the peaks. With Method 1, high mannose glycans account for ≈ 30% and in Method 2 only ≈ 10%. Further to this, Man8 and Man9 species are not identified at all in the Method 2 data set; no significant peaks were eluted past the 45 minute mark in the Method 2 sample where these two glycans would be expected. The difference in high mannose content is not due to sample degradation but may be attributed to the fact that in Method 1 there is no

baseline resolution between these peaks, contributing to apparent increased peak areas. The other clear difference with regard to H5 antigens run on these two methods is that more peaks can be identified in Method 2 than in Method 1. These peaks were always present in the sample however were overlapping. The separation of these peaks gives greater credibility to the assay and the reproducibility of the data.

The power of the HILIC-HPLC method places great weight on the use of the Glucose Unit values and their comparisons to published data as held in the Glycobase database (Campbell et al. 2008). One known issue with the database is that, by design, it accumulates published data and therefore can produce ranges of GU values for the same glycan depending on the source. As more data are published, the database becomes more valuable in that its confidence levels are higher but GU ranges still tend to exist. It is for these reasons that when looking at the data presented here, there are different values for some of the same glycans, which are not due to their isomeric forms or bond associations. For example in the H5 antigen sample the prominent peak, F(6)A2G2, can be found at 7.25 in Method 1 and 7.49 in Method 2. Likewise in the IgG1 sample, F(6)A2G2 can be found at 7.58 and 7.50 for Methods 1 and 2 respectively. The online Glycobase database provides a GU value of 7.55 ±0.05; within the range of values reported here. In every case the identities were confirmed by exoglycosidase digest and it appears that the H5 antigen run with Method

1 did have a problem with the run that went unnoticed initially. Even though all the structures are identified correctly, the GU values appear to have a shift in them of ≈ -0.3 units. Every run is standardized with a dextran ladder sample run at the beginning and end of each sample set to ensure no drift takes place as was the case here. The only other possible causes would be due to an older column or buffer composition. Regardless of the cause, the final structure IDs are solid. When a closer look is taken at the IgG1 sample, the GU values are much tighter and well within the range of the Glycobase data. **Table 3.7** gives the values of the main peaks from both methods as well as the Glycobase value and range. Overall the glycans reported herein are within expected ranges.

Method 2 yielded another positive over Method 1 when the injection volume was changed from 100 μL to 25 μL. The method for glycan purification and labelling takes 3-4 days requiring gel extraction and several drying steps. These steps can be minimized by using less initial glycoprotein to get sufficient quantities of glycan for the HPLC. As demonstrated in the data for dextran ladders and H5 antigen more resolution was obtained with Emission Unit (EU) values far less in Method 2. With H5 antigen the EU values (y-axis) were reduced 10 fold with greater separation being seen. In the case of the IgG1 data, the sample volume in both cases was set at 25 μL for comparison purposes. The IgG1

74

injected at 100 µL in Method 1 gave the same profile as seen in **Figure 3.5** with rounded peaks and inferior separation (data not shown).

Table 3.7 Summary of major IgG1 glycan GU values as determined by HILIC methods 1 and 2 compared to values from the Glycobase database.

Structure	Method 1 GU value	Method 2 GU value	Glycobase value ±SD
F(6)A2	5.92	5.87	5.89 ±0.04
F(6)A2G1	6.67	6.62	6.75 ±0.23
F(6)A2G1		6.74	6.75 ±0.23
F(6)A2G2	7.58	7.50	7.55 ±0.04
F(6)A2G2S1	8.21	8.23	8.13 ±0.19
F(6)A2G2S2	9.32	8.97	9.06 ±0.29

3.5. Conclusion

The development of high throughput methods are important for most assays and especially so for glycan analysis when multiple users are vying for instrument time. New resins have been developed to incorporate smaller bead sizes such that separation efficiency can be greatly improved upon. When this increased resolution is optimized with shorter run times and lower buffer usage the results can yield a more reproducible and accurate profile of the selected glycans.

As demonstrated herein, the separation has been greatly improved while reducing run times by more than threefold. This has been accomplished using only 25% of the original sample volume with a reduction of buffer usage by 30%. The new method is sufficient to analyse all 2-AB labelled glycans with GU values in the range of 1-13. Without investing in new capital equipment or new technology, the efficacy of the HILIC-HPLC has been greatly improved and culminated in a very reliable, robust method for glycan analysis.

Note The methods described herein were employed in two published papers in which I am a co-author. The glycan analysis portion of the Kim et al. (2013) paper was performed by me and Katrin Braasch equally using Method 1 and the 5 μm column.

Kim, D. Y., Chaudhry, M. A., Kennard, M. L., Jardon, M. A., Braasch, K., Dionne, B., Butler, M. and Piret, J. M. (2013), Fed-batch CHO cell t-PA production and feed glutamine replacement to reduce ammonia production. Biotechnol Progress, 29: 165–175. doi: 10.1002/btpr.1658

The glycan analysis in the Lin et al. (2013) paper was performed solely by me and used both methods 1 and 2.

Lin S-C, Jan J-T, Dionne B, Butler M, Huang M-H, et al. (2013) Different Immunity Elicited by Recombinant H5N1 Hemagglutinin Proteins Containing Pauci-Mannose, High-Mannose, or Complex Type N-Glycans. PLoS ONE 8(6): e66719. doi:10.1371/journal.pone.0066719

Chapter 4 – A low redox potential affects monoclonal antibody assembly and glycosylation in cell culture

Chapter 4 - Preface

Having optimized the HILIC-HPLC method using the glycans from a variety of recombinant proteins, experiments could now be performed where higher throughput could be achieved. This was crucial to evaluating the multiple conditions and replicates of the following NS0 trials. Along with higher throughput came the higher resolution, which allowed for more glycan species to be separated and identified while minimizing the amount of sample required. By reducing the sample load amount from 100 µL to 25 µL, samples could be prepared using less initial protein prior to deglycosylation by PNGase F. In the following NS0 work, harvest materials from duplicate flasks no longer needed to be pooled to attain sufficient glycans for analysis.

4.1. Abstract

The glycosylation and intracellular assembly of Mabs is very important in ensuring consistent glycan profiles, which are essential for efficacy and effectiveness. To better understand how these factors may be influenced by a lower redox potential, an IgG1 producing NS0 cell line was grown in the presence of varying concentrations of the reducing agent dithiothreitol (DTT). Cultures were monitored for growth and culture redox potential (CRP) with glycan heterogeneity determined using a HILIC-HPLC method. Macroheterogeneity was unchanged in all conditions whereas the Galactosylation Index (GI) decreased by as much as 50% in cultures with lower CRP or higher DTT levels. This shift in GI is reflected in more agalactosylated and asialylated species being produced. Mab assembly and assembly intermediate levels were determined using radioactive isotope ^{35}S incorporated into nascent IgG1 molecules. The assembly pathway for this IgG1 was shown to progress via HC$\rightarrow$HC$_2$$\rightarrow$HC$_2LC\rightarrow$HC$_2LC_2$ in all conditions tested and autoradiographs highlighted that the ratio of heavy chain dimer to heavy chain monomer increased greatly over time for cultures with higher DTT concentrations. The increase in heavy chain dimers and lower GI appear to be correlated, possibly due to disruption of the disulfide bonds at the higher levels of assembly. A change in the assembly pathway may alter

the final IgG glycan pattern and possibly lead to control mechanisms that influence glycan profiles of monoclonal antibodies.

4.2. Introduction

The N-glycosylation of a therapeutic recombinant protein can have a pronounced effect on function *in vivo*. A major contributor to the binding efficiency of monoclonal antibodies (Mabs) to cellular receptors is the glycan attached to the Fc region of the Mab. Although production techniques of Mabs from mammalian cell culture have been well characterised, product quality and consistency are dependent upon the variable profile of the glycosylation pattern (Del Val et al. 2010). This glycan microheterogeneity that exists in the final product can have variable effects on therapeutic efficacy. The control of parameters that affect glycosylation during the cell culture process is important to reduce batch-to-batch variability as well as to enhance the production of glycoforms identified with desirable activities. As a result, many studies have been performed to identify and manipulate the culture parameters that affect glycosylation patterns of recombinant glycoproteins (Hossler et al. 2009) and to derive the desired glycan structures.

The dissolved oxygen concentration is one specific process parameter that has been studied extensively. Lowering the dissolved oxygen (DO) concentration has been shown to decrease the extent of galactosylation in Mabs with little to no effect on Mab productivity (Kunkel et al. 1998). For a therapeutic antibody, lower levels of galactosylation on IgG1 decrease the activity of complement dependent cytotoxicity (CDC) (Werner et al. 2007). Kunkel et al. showed that when DO was decreased to 10% in a chemostat culture of hybridoma cells there was an increase in the production of agalactosylated Mabs compared to cultures maintained at 50% or 100% DO (Kunkel et al. 1998). One explanation for this effect is that the low DO caused a shift in the intracellular redox balance with a consequent effect on cellular metabolism. When DO is lowered in cell culture, a shift in the culture redox potential (CRP) may disrupt disulfide bonds, which may have a profound effect in the synthesis of immunoglobulins because of the structural proximity of the consensus glycan to an interchain disulfide bond. A disturbance in disulfide bond formation may cause a change in the accessibility of galactosyltransferases and subsequent effect on galactosylation.

In another study (Serrato et al. 2004), it was shown that an oscillating DO, that mimics what may occur in heterogeneous large scale manufacturing runs, does indeed influence the overall glycan microheterogeneity. As cultures were exposed to an oscillating DO, the

transitory periods between low and high oxygen enhanced sialylation and tri-antennary structures. A proposed explanation for these results is that the oscillations caused a shift in the internal redox balance of the cells thereby altering the glycan pathway. Although CRP was not measured directly, the effects of a shifting DO environment could be related to metabolic changes under reducing conditions. This reducing environment may be responsible for altering both the cell's protein folding mechanisms and glycan processing.

Unlike pH or DO, CRP is not a parameter that is measured routinely and is thus not very well understood although attempts have been made (Meneses-Acosta et al. 2012). In Meneses-Acosta et al. the CRP was controlled at specific values and compared to cultures maintained at constant DO. Their findings indicated that reducing conditions (redox <0.0 mV) enhanced cell culture performance with respect to specific growth rate and overall Mab concentration although no glycan analysis was performed to determine product quality. It was determined that control strategies involving CRP could be employed to maximize cell growth and productivity by shifting CRP during cell culture operations.

It has been reported that the intracellular redox state of mammalian cells has an impact on protein folding and disulfide bond formation during monoclonal antibody production (Pluschkell et al., 1995, Guo et al., 2008, Liu et al., 2010). The disruption of these bonds may impact on

glycosylation by allowing or eliminating any steric hindrances affecting access of glycosyltransferases. Although protein structures are synthesized in the endoplasmic reticulum they may be subsequently modified in the Golgi. Mabs enter the Golgi fully folded, but the possibility remains that a reducing environment may allow disulfide bond disruption and therefore alter structural access to the glycosyltransferases.

In order to better study the effect of altered redox potentials on protein synthesis in a cell culture system, a reducing agent such as dithiothreitol (DTT) may be introduced into the medium. DTT has previously been shown to alter the glycan macroheterogeneity of recombinant tissue plasminogen (tPA) resulting in the production of primarily fully glycosylated tPA (type I) (Allen et al. 1995). The mechanism for this is proposed to be through the delayed formation of a disulfide bond that would extend the exposure of a specific glycan site. Without the disulfide bond, the oligosaccharyltransferase adds the consensus primary glycans to the nascent polypeptide chain in the endoplasmic reticulum (ER). The oxidizing environment of the ER can be altered with DTT in the culture medium resulting in misfolded proteins and therefore lower production rates but the effect can be reversed when the reducing agent is removed (Lodish et al., 1993). The redox environment of the Golgi is not as well understood but it is likely that some change in the redox balance would affect the post-translational modifications occurring therein. A shift

to a more reducing environment within the Golgi could cause changes in structure to increase or decrease the access of glycosyltransferases to any protein.

The objectives of the work presented here were to determine the effects of a reducing agent on cell culture performance, glycosylation profiles and assembly of a humanized immunoglobulin (IgG1) produced from a transfected mouse cell line (NS0). In addition, the levels of IgG1 intermediates were monitored under various reducing conditions to determine any relationship between disulfide bonding and changes in glycan microheterogeneity. The results are important for understanding the effects of redox potential on the control of antibody assembly and glycosylation.

4.2.2.   Objectives

The objectives here were to determine the effect a reducing agent and lower culture redox potential had on NS0 cell cultures in terms of productivity, growth and glycosylation of the main IgG1 product. In addition, the mechanism by which IgG1 forms through disulfide bonding was also sought after to determine if any links could be made between formation and resulting glycan profiles.

4.3. Results

4.3.1. Cell culture performance in the presence of reducing agent

Preliminary studies were performed with dithiothreitol (DTT) and β-mercaptoethanol (β-ME) to determine a suitable reducing agent and concentration to induce a low redox potential with minimal effect on cell culture performance. At 1 mM β-ME the cultures exhibited one third the viable cell density (VCD) and an initial CRP = -6 mV (ΔCRP=-20 mV) compared to the control at +14 mV. At lower β-ME concentrations; 0.25 and 0.50 mM, the initial CRP were 9 and 5 mV respectively in cell-free media, which did not highlight as great a change in CRP as did DTT. Cultures supplemented with 1 mM DTT cultures grew to a VCD within 85% of the control with a ΔCRP = -85 mV. As a result, DTT was chosen for subsequent experiments because of the greater change of CRP under conditions that did not affect culture performance appreciably. A range of DTT concentrations was further tested to determine the effect on growth of this NS0 cell line in the chemically defined media. It was determined that VCD and viability were comparable to control cultures at concentrations < 1 mM DTT. The cell growth rate and Mab productivity were not significantly different at these concentrations of DTT over 4 days; although at 0.25 mM DTT there was a slight but significantly enhanced growth rate at day 2. The VCD of the control culture (1.8×10^6 cells/ml)

and viability (95%), at day 4 were comparable to values with an initial supplementation of DTT up to 0.75 mM DTT (**Figure 4.1a**). All cultures were harvested on day 4 when viabilities were > 90%. The high cell viability reduced the possibility of protease or glycan digestion of the product in the supernatant due to cell lysis.

Figures 4.1 a,b,c NS0 cell culture growth characteristics with varying concentrations of a reducing agent. T-flasks were inoculated at 2.5 x 10^5 cells/mL in 30 mL chemically defined protein free media supplemented with DTT. Growth was at 37^0C and 10% CO_2. Cells were harvested on day 4. Error bars represent ±SD (n=6) for all conditions. **a** viable cell densities and viabilities; determined by automated trypan blue exclusion method, **b** pH profiles measured with offline probe, **c** culture redox potentials (CRP) measured with offline redox probe

Figure 4.1a
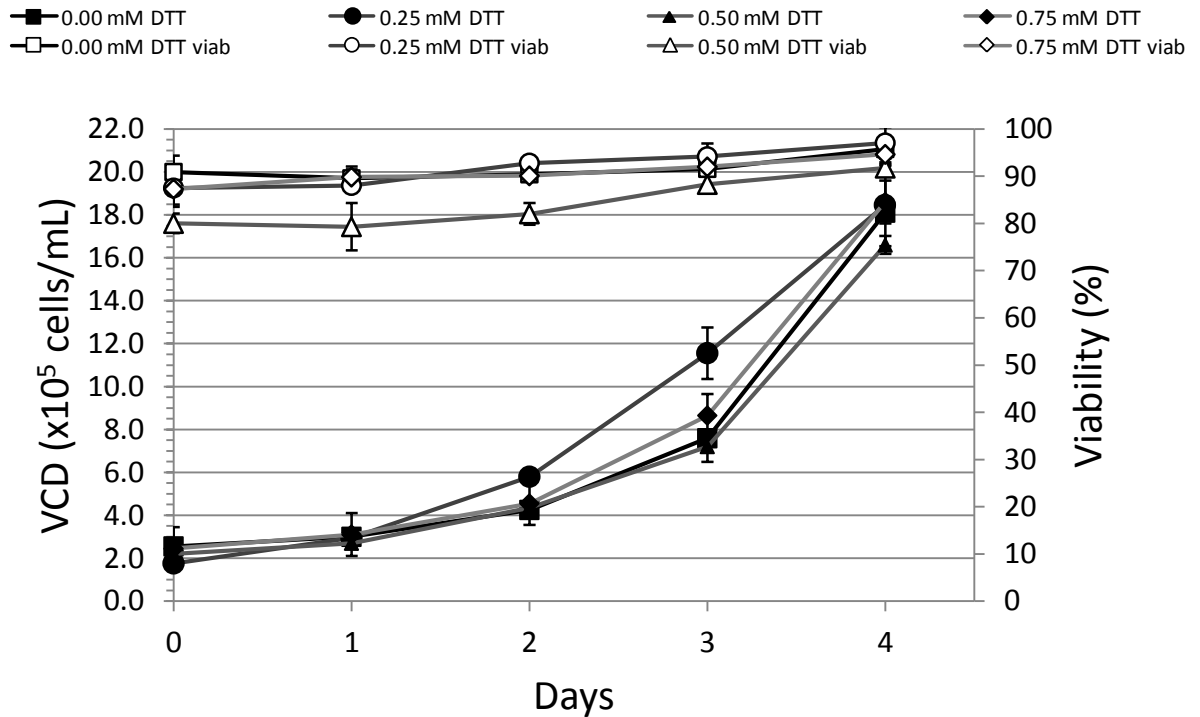
4.3.2. Cell culture antibody production

The antibody titres, final integral of viable cell density (IVCD) and specific productivities (Q_{Mab}) from these cultures are shown in **Table 4.1**. The final antibody titre measured from the harvested media at day 4 was 89.7 mg/L for the control culture and increased slightly but significantly to 110 mg/L for the 0.25 mM DTT supplemented culture, although the Mab titres at higher DTT concentrations were not significantly different from the control. Specific antibody productivities were calculated for each culture with little significant difference identified. However the IVCD was significantly higher at 0.25 mM DTT compared to control.

Table 4.1 Titre, IVCD and specific antibody production rates of day 4 NS0 cell cultures grown in the presence of DTT. Titres determined by absorbance at 280 nm post-Protein A purification. All standard errors were <5% of the mean values (n=3)

[DTT]	0 mM	0.25 mM	0.50 mM	0.75 mM
Titre (mg/L)	89.7	108.8	83.8	83.1
IVCD (x10^9 cells/day/L)	2.52	3.04	2.37	2.68
Q_{Mab} (pg/cell day)	35.6	35.8	35.4	31.0

4.3.3. Culture pH

Using a calibrated pH probe offline, basal media was measured at time of inoculation to have a pH of 7.2. Addition of DTT had no effect on this initial pH. However, there was a significant difference in the rate of decrease of pH over the 4 days of culture. The pH of the control culture decreased from the initial value of 7.2 to 6.95 as compared to a sharper decline to pH 6.8 for all DTT-supplemented cultures. (**Figure 4.1b**).

Figure 4.1b pH profiles measured with offline probe
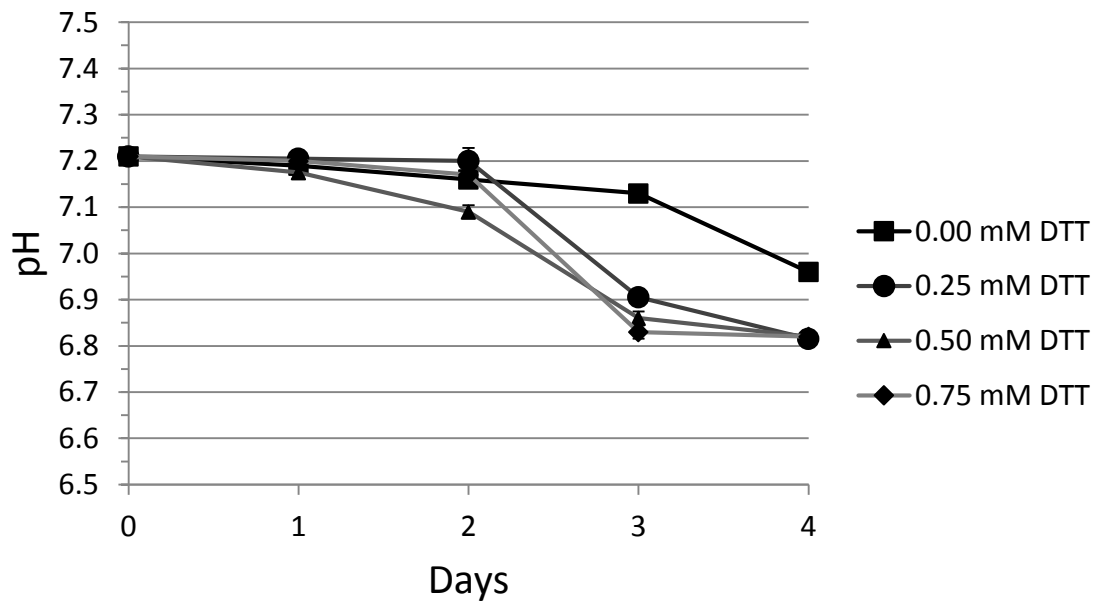
4.3.4. Redox and product stability in the presence of reducing agent

Offline measurements using a standard ORP probe calibrated with fresh basal media showed an expected decrease in media culture redox potential (CRP) prior to inoculation when DTT was introduced, day 0 in **Figure 4.1c**. The decrease in CRP was directly related to the concentration of DTT added; the range was measured between +14.3 mV and -59.2 mV for the control and 0.75 mM DTT cultures respectively on day 0. After inoculation, there was a decrease in CRP during the course of all the cultures with no crossover of values so that after 4 days the values ranged between -80 mV for the control to -110 mV for DTT supplemented cultures. There was a consistent spike increase in CRP on day 3 which could be explained by a shift in cell metabolism. The shift was seen in all cultures across multiple trials and is therefore not an errant point but no further experiments were performed to determine its cause. The lowest CRP recorded was for the 0.75 mM DTT culture at CRP = -110 mV, which was within the normal CRP range of 100 mV to -140 mV for mammalian cell growth as previously reported (Meneses-Acosta et al. 2012).

Figure 4.1c Culture redox potentials (CRP) measured with offline redox probe
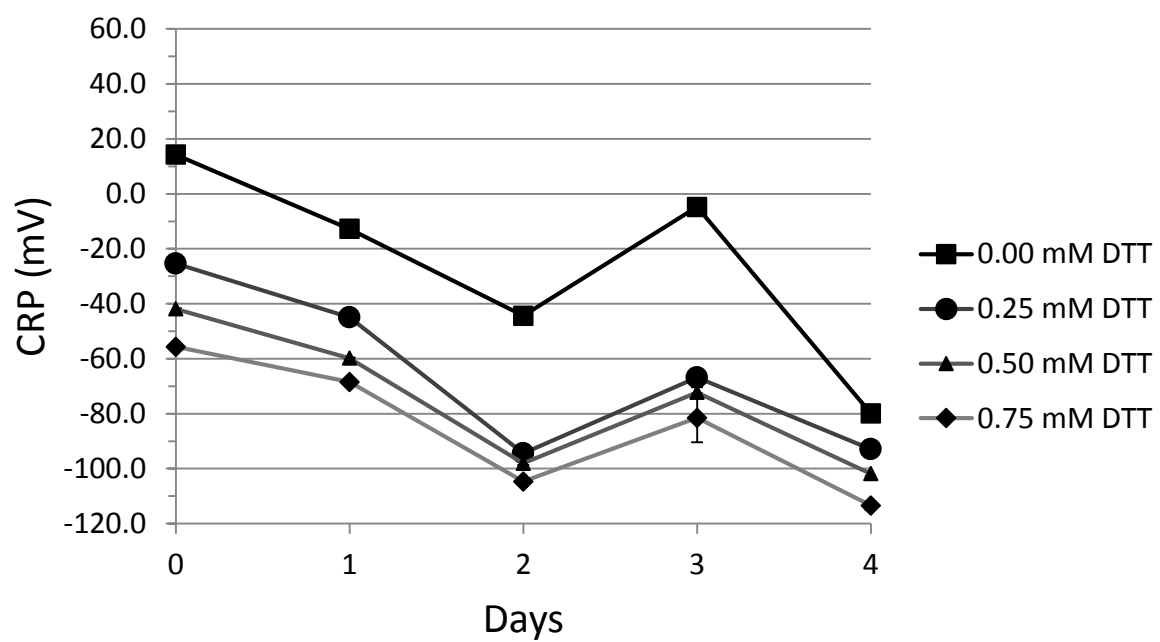
In order to determine if these low CRPs had an effect on the IgG1 product's structure within the supernatant, a non-reducing SDS-PAGE gel was run (**Figure 4.2**) with non-purified harvest supernatant. The most intense band is located at 150 kDa, which corresponds to the intact IgG1. Less intense, lower molecular weight bands are present for all lanes at 50 kDa (heavy chain) and 25 kDa (light chain); these unbound fragments are normally present in the supernatant. The density profiles of the gels from DTT-supplemented cultures were identical to the control with respect to IgG fragments of heavy and light chain in the harvest material. This indicated that there was no Mab reduction taking place in the supernatant post-secretion as a result of DTT. It is evident from these results that cell culture parameters or performance were not greatly affected due to the addition of DTT with the exception of the CRP.

Figure 4.2 Non-reducing SDS-PAGE of IgG1 in supernatant from cultures grown in the presence of DTT. Equal volumes of 4 culture supernatants were mixed 1:1 with non-reducing sample buffer and loaded into wells of a 4-12% polyacrylamide precast gel and run at 25 mAmps for 1 hour. Gel was stained with Coomassie Blue. Lane 1= 0 mM DTT, 2 = 0.25 mM DTT, 3 = 0.50 mM DTT, 4 = 0.75 mM DTT
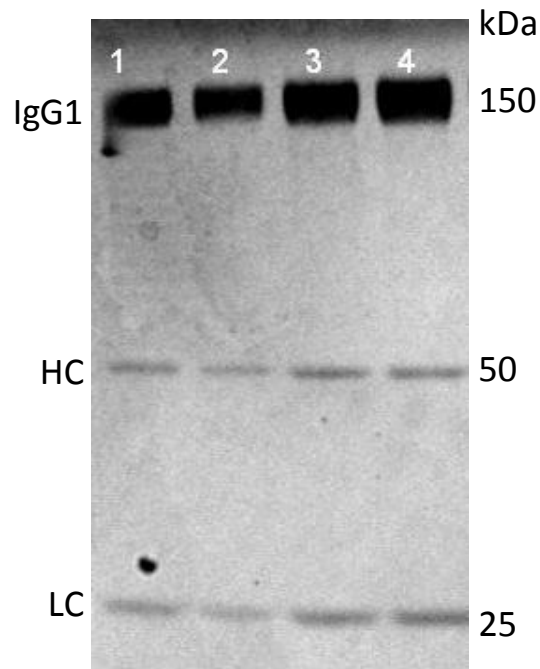
4.3.5.   Glycan Analysis

IgG glycan profiles, as determined by HILIC analysis, produced from Mabs secreted in control and DTT supplemented NS0 cell culture are shown in **Figure 4.3**. The chromatogram has been normalized to the fucosyl agalactosylated (G0F) peak in order to highlight the difference in galactosylation profiles by addition of DTT. **Figure 4.3** is representative of repeated glycan analyses; the results summarized in **Table 4.2** show the assigned structures corresponding to each peak based upon Glucose Unit (GU) values derived from the online NIBRT Glycobase 3.1.

Figure 4.3 Overlaid normalized HILIC-HPLC glycan profiles of NS0 cultures producing IgG1 in the presence of DTT. Supernatant was filtered then purified on a Protein A column. Glycans were cleaved with PNGaseF and isolated prior to labeling with 2-aminobenzamide. Samples were then loaded on a 3.5 μm amide column running a 50 mM ammonium formate/acetonitrile gradient. Glucose Units were generated by use of a standard dextran ladder and compared to values in the NIBRT Glycobase
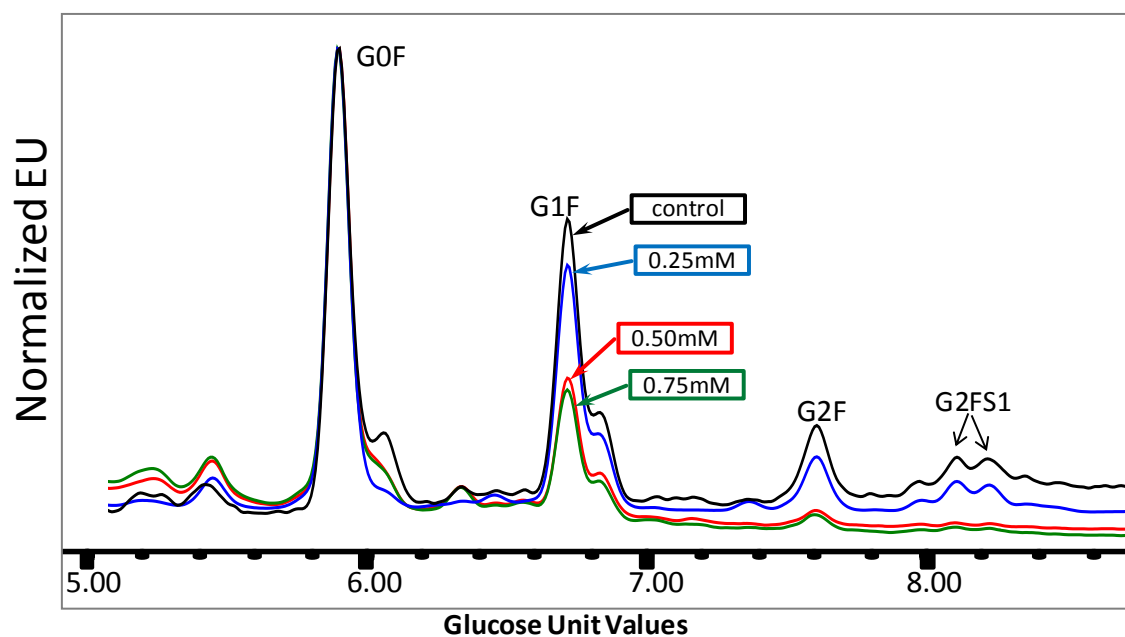
Table 4.2 Glycan profile peaks expressed as percent area from NS0 cultures producing IgG1 in the presence of DTT. Integrated peak areas include GU values between 4 and 9.

		Area %*			
GU value	Structure ID	0 mM	0.25 mM	0.50 mM	0.75 mM
4.39	M3	3.35 ±0.1	4.27 ±3.2	7.75 ±6.7	11.1 ±11.1
4.93	F(6)M3	6.78 ±4.6	11.3 ±1.5	15.8 ±6.7	9.97 ±1.0
5.40	G0	1.48 ±0.5	3.15 ±2.2	3.53 ±1.0	3.41 ±0.7
5.63	A1G1	4.26 ±0.0	2.85 ±0.0	4.83 ±0.0	6.10 ±0.0
5.86	F(6)G0	42.0 ±7.9	43.8 ±4.1	47.8 ±16.5	50.8 ±16.3
6.36	G1	3.78 ±0.0	1.40 ±0.0	1.96 ±0.2	1.59 ±0.0
6.62	F(6)G1[1]	23.9 ±2.8	22.9 ±4.8	18.0 ±3.5	18.1 ±1.1
6.73	F(6)G1[2]	6.56 ±0.9	7.85 ±1.5	5.84 ±2.6	5.00 ±0.3
7.50	F(6)G2	6.64 ±0.8	4.77 ±1.8	3.07 ±2.4	2.56 ±0.2
8.10	F(6)A2G2S1[1]	2.60 ±0.3	2.41 ±1.2		
8.23	F(6)A2G2S1[2]	2.49 ±0.6	1.98 ±1.2		
8.97	F(6)A2G2S2	3.12 ±0.6	2.50 ±1.0		

*±SD, average of n=3
[1] isomer forms of terminal residues on 6-antenna
[2] isomer forms of terminal residues on 3-antenna

The predominant peak in all samples was of F(6)G0 Mab with decreasing peak areas for F(6)G1 and F(6)G2 glycans. Species of glycan containing one or two sialic acid residues (S) also appeared to a greater extent in the control sample. As the [DTT] was increased, the Mabs' glycans showed less sialylation or none at all. The other major glycan peak was of the base structure F(6)M3. This compound is formed due to either low levels of glycosylation initially or product degradation. It is unlikely that these glycans are due to product breakdown due to the high cell viability at harvest and limited residence time of the antibody in culture. Therefore it would appear that glycosylation machinery was simply not functioning to its full extent. There was a higher level of variability in some peaks such as F(6)G0 in the 0.50 mM and 0.75 mM DTT samples; however when coupled to the F(6)M3 and M3 peaks % area it became clear that when less F(6)G0 was being produced, the swing in glycosylation was to even simpler structures. A shift in fucosylation was also noted for the cultures when exposed to an altered redox state. As [DTT] increased the percent of fucosylated glycans decreased, as seen in **Table 4.3**. This may in part also be due to a partially functioning glycosylation pathway. In order to simplify glycan profiles across multiple experimental conditions, a Galactosylation Index (GI) was generated for each profile. The GI incorporates all peak areas for those species that have either none, 1 or 2 galactose residues on the biantennary arms of the glycans. This NS0 cell

line does not produce any detectable levels of tri- or tetra- antennary glycan species.

Table 4.3 GI values and % fucosylated glycans for NS0 cultures producing IgG1 in the presence of DTT as determined by HILIC analysis

[DTT] (mM)	GI*	% Fucosylated*
0.00	0.314 ±0.017	94.1 ±5.8
0.25	0.270 ±0.070	92.2 ±6.5
0.50	0.161 ±0.067	86.5 ±6.0
0.75	0.161 ±0.008	83.5 ±15.4

* ±SD, average of n=3

Table 4.3 shows the GI values of Mab glycans of cultures grown in the presence of DTT. The average GI value for control cultures was 0.314 which decreased by 20% in the 0.25 mM DTT culture and by nearly 50% in the 0.5 mM DTT supplemented cultures. There was also an 85-100% decrease in the sialylated glycan structures at higher DTT concentrations. A higher concentration of DTT (0.75 mM) did not appear to cause any further decrease in GI. The drop in GI and the high degree of variability in the 0.50 mM DTT cultures' GI values may indicate that this level is near a threshold limit for the cell where upon the redox balance has been shifted from a predominantly oxidized to reduced state.

4.3.6.　　　Radiolabelling IgG intracellular intermediates

Radiolabelled cultures were prepared to (1) determine the assembly pathway for this NS0 cell line and (2) determine any changes in assembly intermediate concentrations in the presence of DTT. **Figure 4.4** shows the change in the profile of radioactive bands taken from cell lysates over a period of 60 minutes following the addition of ^{35}S methionine and cysteine in a control culture. Intracellular samples were processed by Protein A purification so that only fragments with a heavy chain (HC) component would appear, i.e. no solo light chain fragments. Bands are clearly present at 50 kDa; monomer of heavy chain (HC), 100 kDa; heavy chain homodimer (HC-HC), 125 kDa; three-quarter IgG intermediate with one light chain (HC-HC-LC) and 150 kDa; the full IgG1. The appearance of multiple bands in the regions of 50 kDa and 125 kDa is explained by the nature of non-reducing SDS-PAGE; proteins are not reduced or fully denatured and therefore may assume slightly different confirmations when running through the gel matrix. These types of banding patterns are also present in non-radiolabelled samples. Absent from the gel is a band at 75 kDa that would represent a half IgG intermediate of HC-LC. These data suggests that the IgG1 is assembled initially by the formation of a HC homodimer followed by the attachment of the 2 LC independently to form the final IgG1.

Automated densitometry analysis, with correction for background, was performed on similar bands from non-reducing SDS-PAGE gels of cell lysates taken from DTT-free or DTT-supplemented cultures. It was noted that there were significant changes in the ratios of HC homodimer to HC monomer, which were compared between all cultures (**Figure 4.5**). In all cases, the density of the homodimer band increased over the 60 minutes compared to the monomer band. This suggests that the monomer is transient and forms dimer quickly after translation. In the control culture, the ratio of dimer/ monomer increased from 2 to 3 over the 60 minutes of the experiment. For the 0.25 mM DTT supplemented culture the ratio increased only slightly from 1.8 to 2.2 during the same period. For 0.50 mM and 0.75 mM DTT cultures there was a dramatic increase in the rate of dimer formation/accumulation from an initial dimer/monomer ratio of 2 to > 6. This represents significantly more dimer formation than monomer in the presence of DTT.

Figure 4.4 Autoradiograph of ^{35}S (cys/met) radiolabelled intracellular IgG and IgG assembly intermediates post-ProteinA clean-up run on non-reducing SDS-PAGE; samples shown here are from a control culture with no DTT
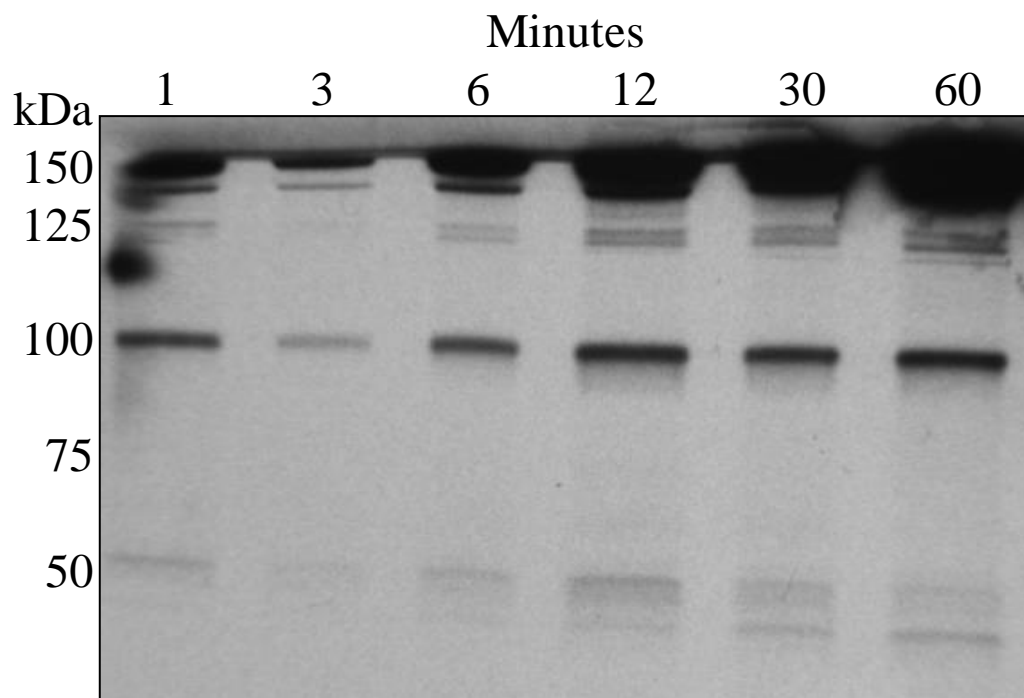
Figure 4.5 Ratio of ^{35}S (cys/met) radiolabelled HC dimer /HC monomer over time when exposed to varying concentrations of DTT. Automated densitometry comparison of dimer vs. monomer band densities from SDS-PAGE autoradiograph for time points at 1, 3, 6, 12, 30 and 60 minutes. Error bars represent SD, n=2
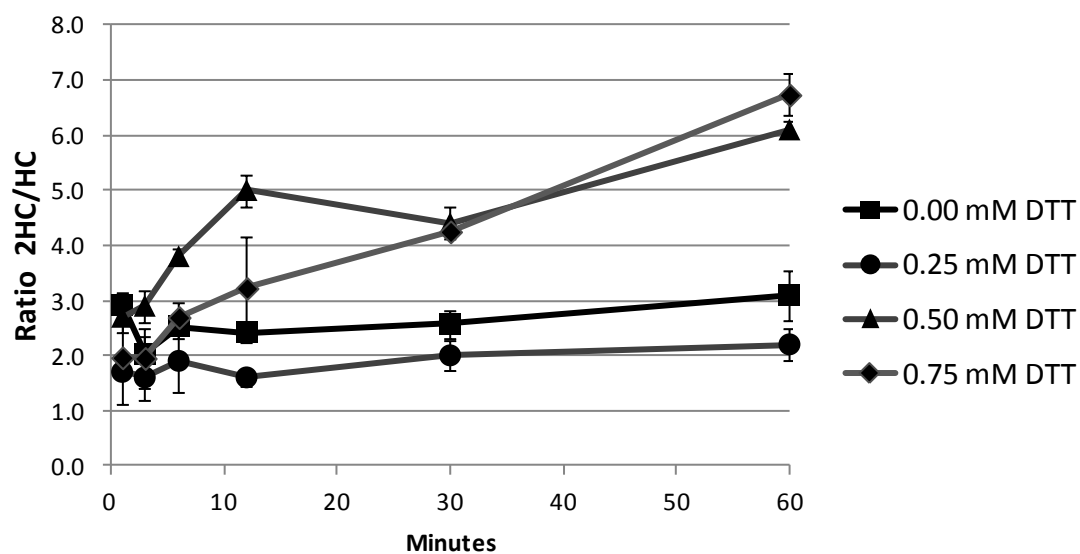
4.4. Discussion

Although redox potential is not a parameter that is routinely measured in mammalian cell cultures it is undoubtedly an important factor for the control of cellular metabolism. It is a difficult parameter to control because it is a function of dissolved oxygen, pH and the thiol/disulfide content of the media. Hwang and Sinskey (1991) showed that the ability to accumulate thiols in the medium during growth appears to be a universal characteristic of cultured mammalian cells and may be used to monitor cell growth.

In our experiments with an antibody-producing NS0 cell line we showed that the initial addition of dithiothreitol (DTT) to the media decreased the measured redox potential by up to $\Delta 50$ mV. This initial drop in CRP may be sufficient for effecting change in culture performance even if the DTT in the medium does not remain stable for the duration of culture. The culture redox potential (CRP) continued to decrease over the course of a batch culture by as much as 60 mV. These are similar values to those previously reported and can be explained by a gradual increase in extracellular SH/SS ratio as a product of cell growth and metabolism (Hwang & Sinskey 1991). Reducing conditions can improve cell culture performance as previously shown with increased viable cell densities, product titres and more efficient metabolism (Meneses-Acosta et al. 2012). In our experiments this was shown by supplementation of a culture with

0.25 mM DTT with an enhanced antibody titre. This enhancement was explained by an improved growth rate and overall integrated viable cell density (IVCD) rather than cell specific productivity (Q_{Mab}). Evidence for an effect on cellular metabolism was shown by a greater change in pH in DTT supplemented cultures that may be attributed to an enhanced rate of lactic acid production. Enhanced lactate production in mammalian cell cultures is an undesirable trait as it increases the osmolality of the medium and acidifies the environment leading to lower viabilities and early apoptosis (Li et al. 2010).

It has been shown previously that concentrations of DTT > 2 mM can cause intracellular misfolding of proteins and accumulation in the endoplasmic reticulum (ER) resulting in a decreased product titre (Lodish et al., 1993). In our experiment the concentrations of DTT were lower (<0.75 mM) and there was no apparent decrease in Mab titre. In fact, at 0.25 mM DTT there was an increase in Mab titre, which concurs with enhanced antibody titres observed under reducing conditions in a hybridoma culture (Meneses-Acosta et al. 2012). The increased titre at 0.25 mM DTT was related to an enhanced growth rate rather than an enhancement of specific productivity. This result and the change in culture pH suggest that DTT affected cellular metabolism rather than specific events in the ER as suggested by Lodish et al. (1993). The addition of DTT had no direct effect on initial pH of the culture. However, the

altered metabolism caused a small difference in pH at the end of the culture but not enough to suggest a difference that could contribute to altered glycosylation profiles (Müthing et al., 2003, Borys et al., 1993).

The profile of glycan structures on an antibody is important for its functional activity and role as a biopharmaceutical. Defining cell culture parameters that can alter glycan structures in a predetermined manner is crucial for Mab development. Redox potential is one parameter that may affect the final glycan profile. In our experiments we show that DTT caused reduced galactosylation of the isolated antibody corresponding to a ≈50% decrease in the galactosylation index (GI) and a consequent reduction in sialylation. These observations are compatible with previously reported data that showed a gradual decrease of GI of a murine antibody from 0.56 to 0.37 as the dissolved oxygen level of a bioreactor was reduced from 100 to 10% air saturation (Kunkel et al. 2000). Although the GI values were slightly higher for the murine antibody, the phenomenon of decreased galactosylation under low redox potential is consistent.

Our experiments established that glycan microheterogeneity is altered by DTT but not macroheterogeneity. Primary glycosylation occurs on nascent HC in the ER during translation (Bergman et al., 1978). The lack of appearance of a low molecular weight band corresponding to a non-

glycosylated structure suggests that heavy chains were occupied very quickly after synthesis.

The microheterogeneity of the consensus glycan in an immunoglobulin (IgG1) can be related to its position in the interstitial space between the CH2 domains of two heavy chains. The heavy chains are held in close proximity by two disulfide bonds in the hinge region that are close to the glycan site (Liu & May 2012). This close proximity of the two heavy chains can reduce the accessibility of glycosyltransferase enzymes particularly the galactosyltranferase (GalT) that adds the terminal galactose to form the G1 or G2 structures. It might be expected that a reducing environment induced by DTT could prevent or delay the formation of the disulfide bonds in IgG1 thereby granting greater accessibility to glycosyltransferases. However, the results both with the effect of DTT and with dissolved oxygen suggest the opposite.

One explanation is that the GalT has lower activity under reducing conditions with a consequent reduced level of galactosylation. The decreased activity of the enzyme could be due to low availability of the UDP-Gal substrate, mis-localization of the GalT enzyme or GalT's inactivation. GalT, a transmembrane protein located in the trans-Golgi, functions by first binding the donor UDP-Gal which, alters the conformation of the enzyme to accept an oligosaccharide with a terminal

GlcNAc residue (Qasba et al. 2008). If the sugar nucleotide pool were low or the GlcNAc residue unavailable, then galactosylation could be reduced.

The glycan profiles under reducing conditions also showed an increase in smaller glycan species like M3 and F(6)M3 (**Table 4.2**). These are the core structures of complex biantennary glycans to which N-acetylglucosamine (GlcNAc), galactose and N-acetylneuraminic acid are added sequentially. The higher content of these precursors suggest that the activities of other glycosylation enzymes may be hindered by the reducing environment imposed by DTT, perhaps in a similar way to GalT. An alternative explanation may be related to alterations to the assembly pathway of IgG1. Radiolabelling studies were performed to isolate IgG1 intermediates and determine the assembly pathway. Several conformations of Mabs are possible within the ER and Golgi; monomers of light chains (LC) and heavy chains (HC), HC-HC homodimer and HC-LC heterodimer (Bergman et al., 1979). IgG1 synthesis pathways are cell line specific in terms of folding and assembly. Two predominant assembly pathways have been proposed (Percy et al., 1975, Elkabetz et al., 2008, O'Callaghan et al., 2010) wherein the first pathway progresses through a half-Mab intermediate where one heavy chain and one light chain bind first and then couple to form the final IgG1. The second potential pathway occurs through the formation of a heavy chain homodimer intermediately followed by light chain addition yielding the final IgG1 form. The pulse-

labelling experiments were designed to distinguish between these potential pathways and the conclusion was made that the preferred assembly pathway for this particular IgG1 is HC→HC$_2$→HC$_2$LC→HC$_2$LC$_2$. This IgG1 assembly pathway is consistent for all cultures in the presence or absence of DTT. Assembly pathways can vary depending on the cell line and culture conditions. Bergman et al. demonstrated that immunoglobulin assembly may be cell line specific or IgG class specific; IgG1 and IgG2 produced in 2 different murine cell lines had initial assembly pathway intermediates of HC-HC dimer and HC-LC respectively (Bergman et al., 1979). These data have been supported by further research (Elkabetz et al. 2008; O'Callaghan et al. 2010) however assembly still remains a cell line specific course of events.

The ER is known to have an oxidizing environment with a regulated redox balance systems, including glutathione, in place to counteract external pressures (Van Lith et al. 2011). In contrast, the redox balance system within the Golgi is not well understood (Mesecke et al. 2008) and small changes in redox potential may impact Golgi operations either directly or indirectly.

Densitometry analysis of the radiolabelled intermediates showed a 200-350% increase in the dimer to monomer ratio of HC$_2$/HC in the cells of DTT supplemented cultures respectively over 60 minutes. It may be that this is an independent event from the reduced galactosylation.

However, it is possible that the relative increase in heavy chain dimers is resulting from the breakdown of intact IgGs and might suggest an imbalance of structures within the Golgi that are less susceptible to the activity of the GalT enzyme.   If this were the case, it offers a possible mechanism of action for generating low GI cultures of IgG1 in the presence of DTT.   DTT may create a higher proportion of the observed HC dimers which have reduced binding capabilities to GalT.   This may lead to sufficient delay in the formation of fully formed IgG1 to cause the reduction in galactosylation (**Figure 4.6**).   The final fully formed IgG1 is re-established prior to secretion from the cell.

Figure 4.6 Possible mechanism of action for generating low GI cultures of IgG1 in the presence of reducing agents. DTT creates a higher proportion of 2HC dimers that may have a conformation with reduced binding to the GalT enzyme. The final fully formed IgG1 is re-established prior to secretion from the cell
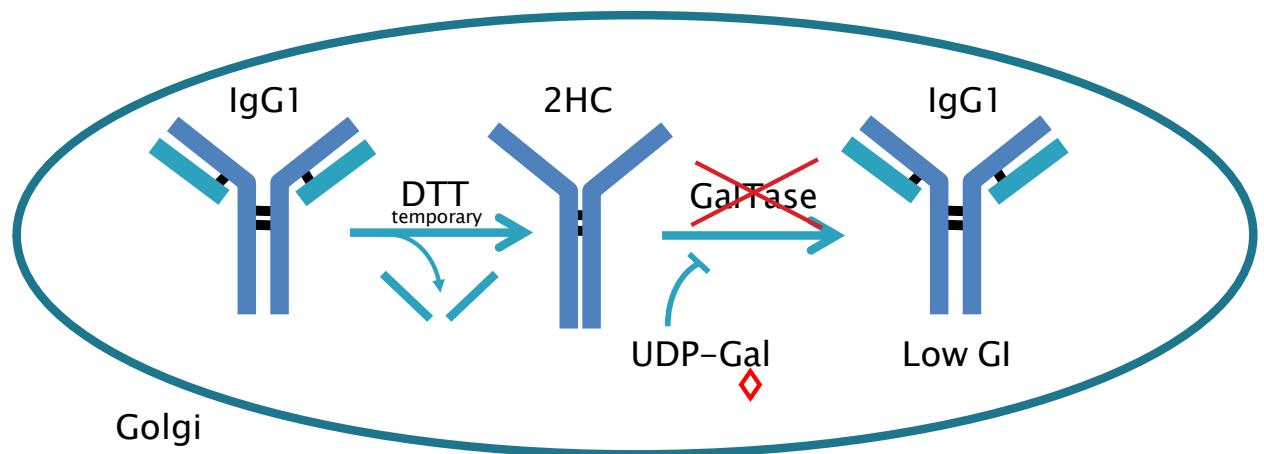
4.5. Conclusion

CRP is not a well defined parameter in mammalian cell cultures but could be a useful measure in predetermining product quality attributes. A lower culture redox potential caused decreased galactosylation of the glycan on a Mab, by low dissolved oxygen or an added reducing agent. Furthermore, the lower redox potential increased the proportion of heavy chain dimers during assembly. These may be independent events or it may be suggested that the different ratios of intermediates are less susceptible to galactosylation. Although the mechanism of action is not well defined it may become important to monitor CRP levels in order to maintain consistent product quality and to control glycan heterogeneity.

Chapter 5 – Comparison of multiple cell lines and antibodies when placed under the influence of a reducing agent

5.1. Abstract

It has been demonstrated that decreasing the culture redox potential in an NS0 IgG1 producing cell line with dithiothreitol (DTT) has a negative effect on galactosylation. Trials were performed to determine if the effect seen in NS0 was general to other mammalian cell lines and antibody types using two CHO cell lines: 1) DP-12 expressing anti-IL-8; a humanized IgG1 and 2) EG2-hFc; a novel chimeric camelid 80 kDa antibody. No change in growth profile or productivity were observed in either cell line with variable levels of DTT up to 1 mM. The only culture parameter that did exhibit a shift from one condition to the next was the CRP, in a [DTT] dependent manner. Despite consistent growth between cultures, the reduced CRP did have an effect on glycan profiles as determined by HILIC-HPLC methods. A 7% increase in fucosylated species was detected in DP-12 cultures at higher [DTT] with no corresponding changes in galactosylation index (GI) values. DTT did not affect the glycosylation of the EG2-hFc antibody; GI or % fucosylated. The glycan analysis of EG2-hFc did reveal an intriguing profile with an exceptionally high GI of 0.625 with a predominant F(6)G2 peak. This represents a 2.5 fold increase over the GI of DP-12 (0.245) and 2 fold over NS0 (0.314). EG2-hFc's higher GI value

111

and smaller MW may translate into better *in vivo* activity as a therapeutic. Overall it would appear that the CRP effect on glycosylation observed with the NS0 cell line was not shown for the CHO cells

Keywords: monoclonal antibody, glycosylation, camelid, culture redox potential, galactosylation, HILIC, Chinese Hamster Ovary

5.2. Introduction

Previous work performed with NS0 cell culture showed that a change in the culture redox potential by adding dithiothreitol could have an effect on the glycosylation profile of a humanized IgG1 monoclonal antibody. This effect was most significant with regard to the Galactosylation Index (GI) which decreased at lower redox potentials. Despite the shift in GI, there were no substantial changes to other measured parameters including growth rates, specific production rates and pH of the culture. To pursue this inquiry further and determine if these redox effects were universal, two more cell lines were chosen for experimentation. The first was a Chinese Hamster Ovary (CHO) cell line, which produced a human IgG1 similar to the product of the NS0 cell line. The second cell line was a CHO cell producing a novel single domain chimeric antibody.

The human IgG1 producing CHO DP-12 cell line was purchased from the American Type Culture Collection (ATCC)(ATCC-CRL-12445). It

is a CHO K1 (DHFR⁻) derived cell line expressing an anti-IL-8 antibody. These antibodies bind the chemokine interleukin 8 (IL-8) and prevent its binding to neutrophils. This binding of Mab to IL-8 prevents induction of chemotaxis (Leong et al. 2001) and/or inhibition of tumor progression (Mian et al. 2003). This antibody varies from the humanized IgG1 of NS0 by having a fully human amino acid sequence in its makeup of heavy and light chains, i.e. no murine regions. These differences can be found in the variable regions of the Mab and not in the Fc domain where the characteristic Asn-297 N-glycan site resides. As with the NS0 IgG1, the only site for N-glycosylation is at Asn-297 on the DP-12 IgG1 heavy chains.

DP-12 was listed as an attached culture when received from the ATCC. Upon entry into the Butler lab it was shifted from a DMEM 10% FBS culture medium to a serum free BioGro medium supplemented with 0.5% yeast hydrolysate. The adaptation took place over seven passages with a continual decrease of serum in the media. Only the freely suspended cells were transferred to new vessels, which in the end resulted in a fully suspended, serum-free culture. The selection pressure of methotrexate was not introduced to the DP-12 cells in the Butler lab. Serum-free adaptation resulted in similar growth profiles to those reported by others (Heinrich et al. 2011; Beckmann et al. 2011). It should be noted that the previous work done with NS0 cells in Chapter 4 and the chemically defined medium used were proprietary to Abbvie Inc. and

despite tremendous effort could not be grown for extended passages with the BioGro media. Likewise DP-12 cells could not be grown in the Abbvie CD media. Other culture parameters were maintained, as seen in Chapter 4, for consistency such as temperature and CO_2 levels.

The anti-IL-8 CHO cell line may perform similarly to the NS0 cells in serum free suspension cultures; however there is a key difference in how the cell line was manipulated to attain its ability for Mab production. The NS0 cell line has been engineered to incorporate only one copy of the transfected heavy and light chains with selection pressure provided by antibiotic resistance (Hartman et al. 2007). HC, LC and antibiotic resistance genes were all placed on the same plasmid for transfection. Selection pressure was removed when a stable cell line was chosen and not introduced during any subsequent sub-cloning activities. The DP-12 cell line used here originates from CHO K1(DHFR$^-$), which uses medium components and methotrexate (MTX) as its selection pressure. DHFR$^-$ cell lines are incapable of DNA synthesis via the *de novo* pathway and must rely on the salvage pathway instead. This salvage pathway requires supplementation into the media of hypoxanthine and thymidine (HT). All pre-transfection cells are supplemented with these components for growth. After transfection the supplements are removed from the media thereby only allowing the cultivation of cells which have incorporated the exogenous *dhfr* into their genome. The incorporation of the *dhfr* gene also

increases the chances that the HC and LC genes were also incorporated. To further enhance the *dhfr* transfection efficiency methotrexate is used. Methotrexate is a DHFR inhibitor and works in a concentration dependent manner; as more MTX is added only the cells with high levels of DHFR will survive (Kaufman et al. 1979). High levels of DHFR are attributed to CHO cells that have high expression of *dhfr* genes or many integrated copies of the *dhfr*. High production/copy number of *dhfr* should be associated with similar results for the HC and LC components that sat on the same initial plasmid. In this manner DP-12 cells can have hundreds of copies of the HC and LC sequences integrated randomly throughout the genome. This may have a positive or negative effect on productivity and the function of host cell genes.

The second cell line examined for comparison to the NS0 results was designated as EG2-hFc. The monoclonal antibody produced was specific for human epidermal growth factor receptor (EGFR) (Bell et al. 2010). The binding of the anti-EGFR antibody inhibits the signalling that would allow for cancer cells to proliferate (Mendelsohn 2001). The marketed blockbuster therapeutic with the same mechanism of action is cetuximab. Cetuximab is a chimeric IgG1 produced in a murine-derived Sp2/0 cell line. The sales of cetuximab exceeded $1 billion US in 2012; however its effectiveness may be limited by its ability for tissue penetration (Lee 2010) and the presence of $\alpha(1,3)$–galactose (α-gal) on the Mab (Chung et al. 2008).

These α-gal moieties are highly immunogenic in humans (Galili 2013) and are produced in non-primate cell lines. The Sp2/0 host cell line for cetuximab is known to produce this α-gal whereas CHO cell lines typically do not. With these factors in mind, the EG2-hFc was engineered into a CHO host cell with a reduced size of 80 kDa, compared to an IgG1 150 kDa. This was accomplished through the fusion of camelid and human antibody components (Zhang et al. 2009).

Camelid antibodies consist of only 2 heavy chains (Hamers-Casterman et al. 1993) sporting three domains; V_H, C_H2 and C_H3. The C_H domains resemble very closely the IgG1 C_H and therefore were substituted by human Fc regions while maintaining the camelid V_H domain (Zhang et al. 2009). The total size of each heavy chain is 40 kDa and each forms inter-disulfide bonds to form the final 80 kDa structure. This smaller structure can potentially have better tissue penetration with no adverse effect on binding affinity (Wesolowski et al. 2009). The newly fused human Fc (hFc) region lacks the C_H1 domain but retains the single N-glycan consensus sequence (Asn-X-Ser/Thr) and undergoes proper glycosylation according to its CHO host cell machinery. This glycosylation is important for the newly acquired ability to activate the antibody dependent cell cytotoxicity (ADCC) pathway.

The parental cell line of EG2-hFc is CHO-DXB11 (DHFR$^-$). Unlike the selection process performed on DP-12 anti-IL-8, EG2-hFc underwent

an antibiotic selection process similar to that of the NS0 cell line. Puromycin was used to select for clones that had incorporated the exogenous DNA containing a puromycin resistant gene and Mab HC sequence (Agrawal et al. 2012). Surviving cells are those that had sufficient production of puromycin resistance and therefore likely to have some expression of the desired Mab. It is unknown how many copies of the gene sequences have been incorporated but it is expected that the number is fewer than in DP-12 anti-IL-8 cells due to lack of an amplification process by methotrexate. This cell line grows well with the Biogro media supplemented with hypoxanthine and thymidine; these components are necessary due to the lack of DHFR.

Both the DP-12 anti-IL-8 and EG2-hFc cells are derived from a CHO K1 cell line. When compared to NS0 cultures they have very similar growth characteristics such as doubling times, viability, pH profiles, and productivity. Differences do arise however when comparing final product quality attributes like Mab glycosylation. NS0 is derived from a murine source and therefore has the ability to produce Mabs with terminal α-1,3-galactose (Sheeley et al. 1997) which, as mentioned earlier, is undesirable due to its immunogenicity. CHO cells, derived from hamsters, generally do not produce this glycan variant. Initially it was thought that they lacked the gene for α-1,3-galactosyltransferase (Jenkins et al. 1996) but

this may no longer be the case as some studies have found α1,3-gal on commercially available Mabs made in this cell type (Bosques et al. 2010).

Terminal sialic acid is also an important sugar residue which generates different glycan profiles between the two cell lines in three ways. Firstly, NS0 produces Mabs with glycans terminated with both N-acetylneuraminic acid (NeuAc) and its hydroxylated form N-glycolylneuraminic acid (NeuGc), favouring the latter, whereas CHO cells produce NeuAc and very low levels of NeuGc (Baker et al. 2001). The desired product here is the NeuAc because when NeuGc is introduced into humans it can elicit an immunogenic response (Zhu & Hurst 2002) which in turn could cause quick clearance of a therapeutic in vivo. Secondly, CHO cells tend to sialylate recombinant proteins more often than NS0 which would make them preferred for production of a therapeutic where serum longevity was desired (Zhang et al. 2010). Thirdly, CHO cells tend to bond sialic acid to galactose via an α-2,3 configuration instead of α-2,6 as found in human and NS0 samples (Kilgore et al. 2008). This difference has not been shown to contribute to any immunogenicity or other quality attributes like protein aggregation.

One trait common to both cell lines is the production of high mannose structures (Hills et al. 2001, Pacis et al. 2011). High mannose glycans include species with 5 or more mannose residues. The appearance of these glycans indicates that a glycosylation pathway disruption has

occurred, stunting the trimming and elongation of the glycan but still secreting the full Mab. High mannose species are usually unwanted because they shorten the Mab half-life *in vivo* (Goetze et al. 2011).

In tandem these two cell lines were exposed to the same conditions as previously applied to NS0 cells with varying amounts of DTT in the batch media to lower the initial culture redox potential (CRP). The literature is extremely limited with regard to CHO cells in variable redox conditions allowing for novel research to be done and generate a new knowledge base that may have an impact on product quality and consistency.

5.2.2.   Objectives

The objectives for the work presented here were to investigate whether or not the CRP associated shift in glycan patterns seen in NS0 cultures was specific to cell line/antibody type or could be applied to two other mammalian cell lines. This was completed by using two CHO cell lines; an IgG1 producer and a chimeric camelid Mab producer. A secondary objective was to characterize the novel single domain Mab with respect to its glycan profile which had not yet been examined.

5.3. Results

5.3.1.　　Cell culture performance in the presence of reducing agent

The addition of DTT up to 1 mM to the Biogro media had little effect on the growth of the CHO DP-12 anti-IL-8 cell line. The DP-12 anti-IL-8 cell line maintained viabilities >90% until harvest on day 4 with VCD ranging from 28-35 x 10^5 cells/mL at time of harvest (**Figure 5.1a**). The lowest peak VCD was recorded by the 1 mM DTT culture followed by 0.75 mM and 0.50 mM DTT cultures. DTT concentrations higher than 0.50 mM may have a negative impact on cell growth. The highest VCD occurred in the 0.25 mM DTT culture at 34.5 x 10^5 cells/mL; recall the peak VCD from the NS0 data was also in the 0.25 mM DTT culture. The semi-log plot (**Figure 5.1b**) shows consistent exponential growth throughout the culture for all conditions with R^2 values > 0.98 in all cases. The growth of DP-12 cultures exhibited a consistent specific growth rate with a mean $\mu = 0.61$ ± 0.02 d^{-1}.

The CHO EG2-hFc cell line was more variable where after day 2 the different culture VCDs diverged but in no apparent trend with respect to the [DTT]. From the outset all EG2-hFc cultures behaved differently than DP-12 with their growth reaching ≈ 20 x 10^5 cells/mL by day 2 (see **Figure 5.2a**) compared to < 10 x 10^5 cells/mL by DP-12 cell cultures. EG2-hFc cultures reach their peak VCDs on day 3 and then begin to decline in some

instances compared to rising VCDs in DP-12. The EG2-hFc 0.50 mM DTT culture had the lowest VCD peaking at 26.7 x 10^5 cells/mL while the control culture had the second lowest peak VCD at 33.3 x 10^5 cells/mL. The 0.25 mM, 0.75 mM and 1 mM DTT cultures all exhibited peaks greater than 37.0 x 10^5 cells/mL. Viabilities were maintained > 90% at time of harvest for all conditions. The semi-log plot of the EG2-hFc data (**Figure 5.2b**) illustrates that exponential growth was only observed through day 3 (R^2>95) when VCD reached between 30-40 x10^5 cells/mL, approximately the same range of DP-12 VCD reached on day 4. The mean growth rate generated through day 3 was μ=0.82 ±0.05 d^{-1}.

Peak VCDs and integral of viable cell density (IVCD) for both cell lines are summarized **Table 5.1**. There was no significant difference (p> 0.05) in the IVCD with a CRP change in each culture. When both cell lines are compared to one another however, there is an IVCD increase of 23-88% by EG2-hFc cultures. These data represent duplicate flasks during three runs of each condition.

Figure 5.1 a,b,c,d DP-12 anti-IL-8 cell culture growth characteristics with varying concentrations of a reducing agent. Shake flasks were inoculated at 2.5 x 10^5 cells/mL in 30 mL Biogro media supplemented with DTT. Growth was at 37^0C and 10% CO_2. Cells were harvested on day 4. Error bars represent ±SD (n=6) for all conditions **a** viable cell densities and viabilities; determined by automated trypan blue exclusion method **b** semi-logarithmic plot of viable cell densities **c** pH profiles measured with offline probe using a 3-point calibration **d** culture redox potentials (CRP) measured with offline redox probe calibrated with fresh basal media

Figure 5.1a Viable cell densities and viabilities of DP-12
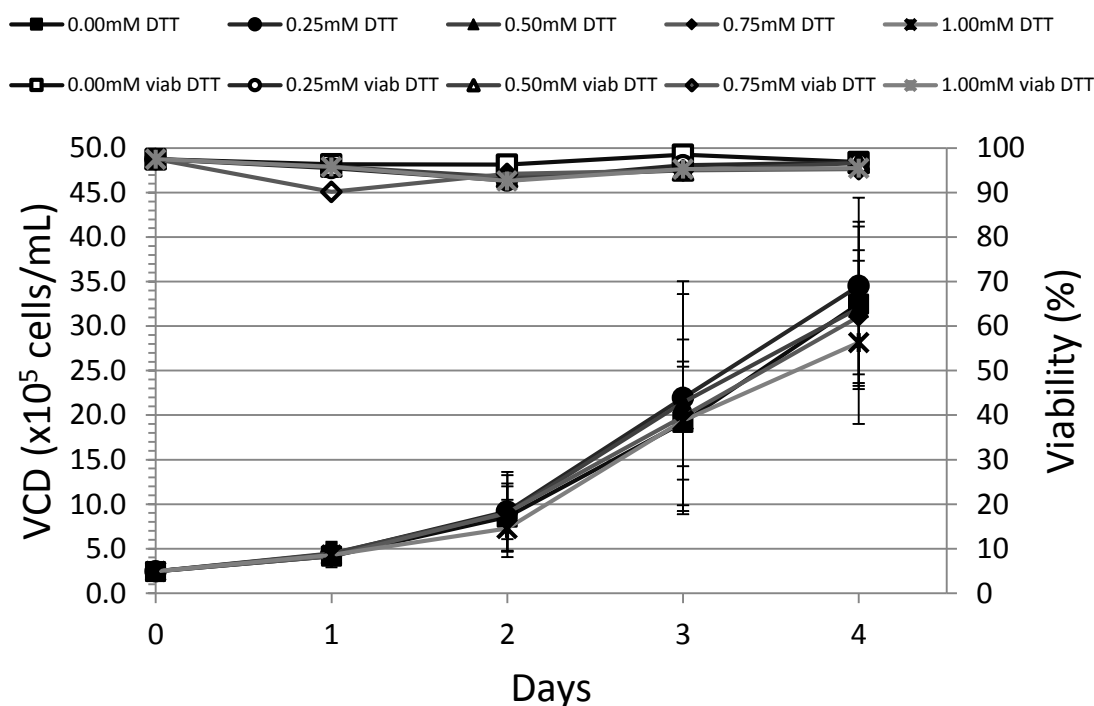
Figures 5.2 a,b,c,d EG2-hFc cell culture growth characteristics with varying concentrations of a reducing agent. Shake flasks were inoculated at 2.5 x 10^5 cells/mL in 30 mL Biogro media supplemented with DTT. Growth was at 37^0C and 10% CO_2. Cells were harvested on day 4. Error bars represent ±SD (n=6) for all conditions **a** viable cell densities and viabilities; determined by automated trypan blue exclusion method **b** semi-logarithmic plot of viable cell densities **c** pH profiles measured with offline probe using a 3-point calibration **d** culture redox potentials (CRP) measured with offline redox probe calibrated with fresh basal media

Figure 5.2a Viable cell densities and viabilities of EG2-hFc
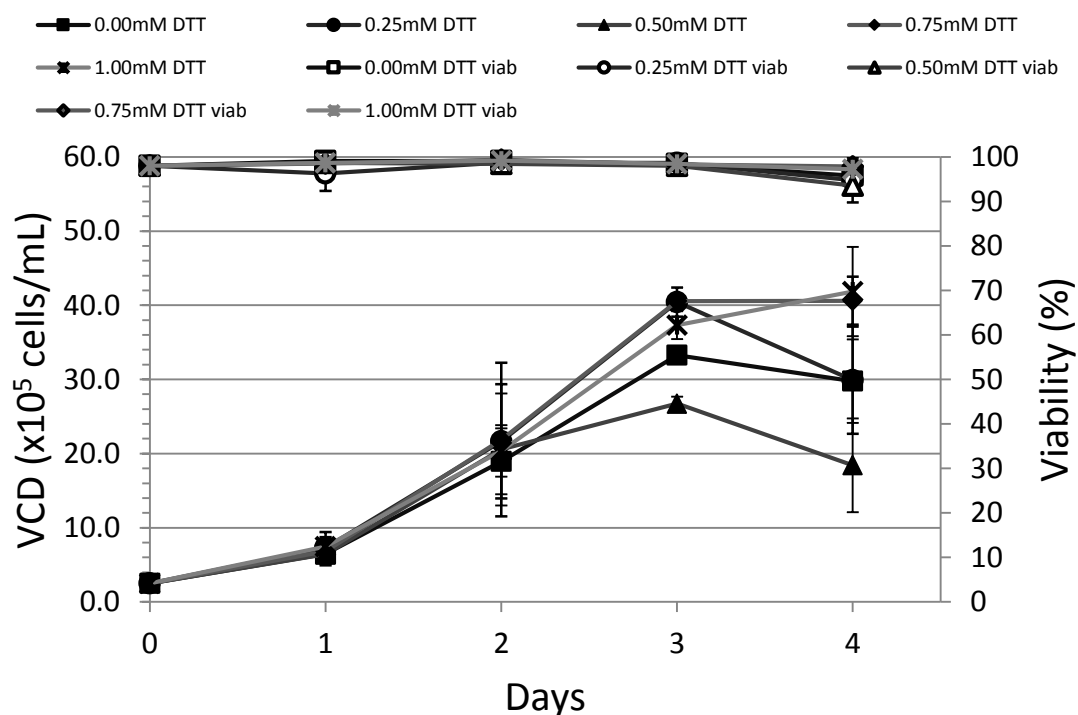
Figure 5.1b Semi-logarithmic plot of DP-12 viable cell densities
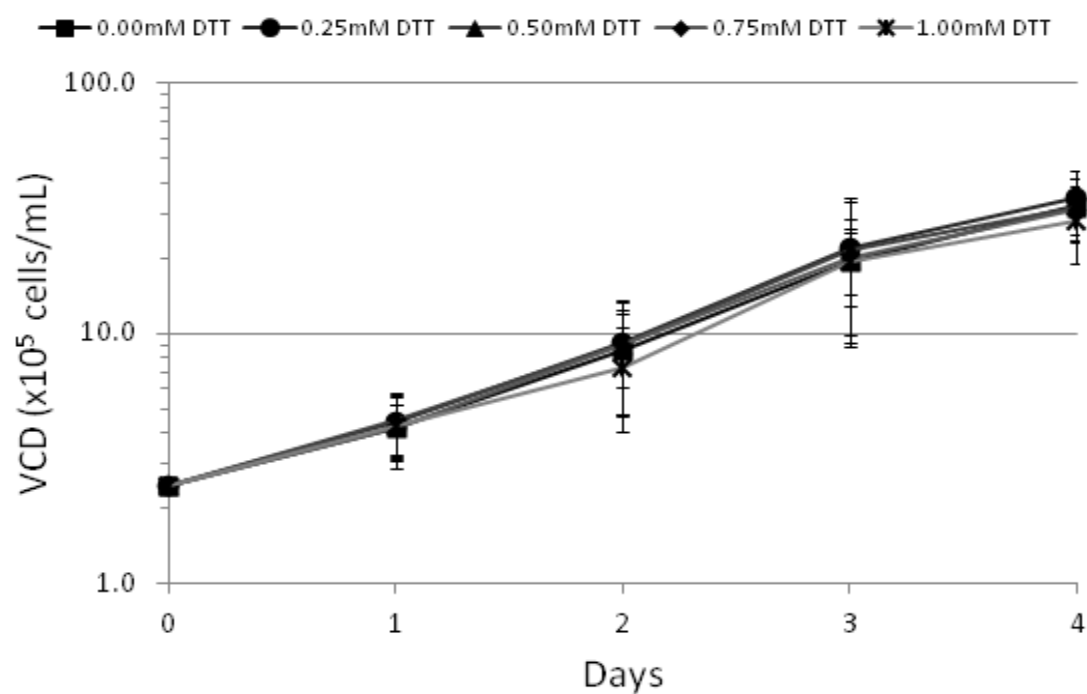
Figure 5.2b Semi-logarithmic plot of EG2-hFc viable cell densities
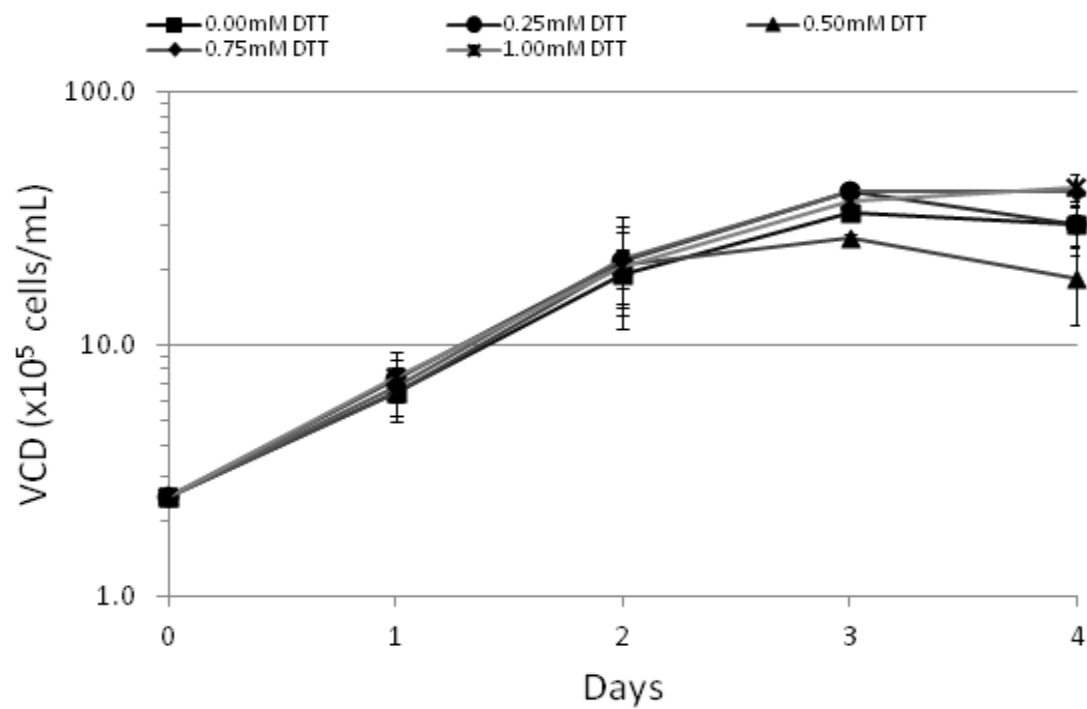
Table 5.1 Summary of peak VCD, IVCD and productivity values for cell lines DP-12 anti-IL-8 and EG2-hFc at varying DTT concentrations. Titres determined by absorbance at 280nm post-Protein A purification. Average values from n=6 runs

	[DTT] (mM)	Peak VCD (x10⁵cells/mL)	Viability %	Titer* (mg/L)	IVCD (x10⁹cells/day/L)	Q_{Mab}[1] (pg/cell/day)
				Values at time of harvest		
DP-12	0.00	32.5	97	71.8 ±3.4	4.94	14.5
	0.25	34.5	97	72.1 ±4.3	5.40	13.4
	0.50	32.1	97	71.9 ±2.3	5.21	13.8
	0.75	31.1	95	70.1 ±3.5	4.98	14.1
	1.00	28.2	96	68.5 ±4.0	4.63	14.8
EG2-hFc	0.00	33.3	96	67.9 ±3.7	7.48	13.1
	0.25	40.4	95	61.9 ±2.1	8.56	11.0
	0.50	26.7	94	68.6 ±1.9	6.42	14.3
	0.75	40.6	98	61.3 ±1.3	9.08	9.9
	1.00	41.9	97	61.2 ±1.9	8.73	11.1

* ±SD,

[1] Q_{Mab} for DP-12 is based on harvest values (day 4), EG2 is based on day 3 IVCC and titre; when exponential growth was occurring

5.3.2.　Cell culture antibody production

As determined by A280 after protein A clean-up, **Table 5.1**, the DP-12 cell line produced $\approx$ 70 mg/L of Mab for each condition, the lowest being from the 1 mM DTT culture at 68.5 mg/L indicating no significant change ($p > 0.05$) in final titer. These values, together with the integral of viable cell density (IVCD), generated specific productivities (Q_{Mab}) > 13.4 pg/cell/day. The lowest Q_{Mab} was in the 0.25 mM DTT culture at 13.4 pg/cell/day and the highest was with the 1 mM DTT culture at 14.8 pg/cell/day.　The control condition had a value of 14.5 pg/cell/day. Overall productivity did not vary significantly with the added DTT in the media, with $p > 0.05$ between control and all tested conditions.

The EG2-hFc cell line had greater IVCDs than DP-12 but lower overall titers. Due to the non-exponential growth through day 4, the EG2-hFc Q_{Mab} in **Table 5.1** was calculated using day 3 values of IVCC and titre. The Q_{Mab} did show significant differences between culture conditions varying from a low of 9.9 pg/cell/day in the 0.75 mM DTT condition to a high of 14.3 pg/cell/day in the 0.50 mM DTT condition. Despite these significant differences, there was no trend in titre or specific productivities with respect to varying DTT concentrations in either cell line tested. No significant deleterious effects were noted for these two parameters at any DTT concentration tested.

5.3.3. Culture pH

The pH profile for all conditions of the DP-12 anti-IL-8 cell line (see **Figure 5.1c**) were not significantly different from the control culture with a gradual decrease in pH over the course of the run from a starting pH of 7.4 to pH 7.0 after 4 days. Starting pH of the Biogro media is 7.4 before the addition of the DTT. The addition of DTT lowered the initial pH of the media slightly in a concentration dependent manner. The decrease in pH was greatest in the 1 mM DTT condition at 0.06. The control culture dropped in pH from 7.4 to 6.93 after 4 days with a similar drop of approximately 0.5 pH units over the course of the trial for all DTT containing flasks. The lowest pH was recorded in the 0.75 mM DTT flask at 6.89.

The EG2-hFc pH profiles (see **Figure 5.2c**) were similar to the DP-12 in that they too had the concentration dependent drop in starting pH after addition of the DTT. Starting pH values ranged from 7.38 in the control to 7.29 in the 1 mM DTT culture. The drop in pH over the course of the run in the control was 7.38 to 6.84. All EG2-hFc cultures dropped in pH in the range of 0.5-0.6 pH units. The lowest pH were recorded in the 0.25 mM and 0.75 mM DTT cultures with pH = 6.77 while the 1 mM DTT culture had pH = 6.80 and the 0.50 mM flask finished with a pH of 6.85.

Figure 5.1c DP-12 pH profiles measured with offline probe
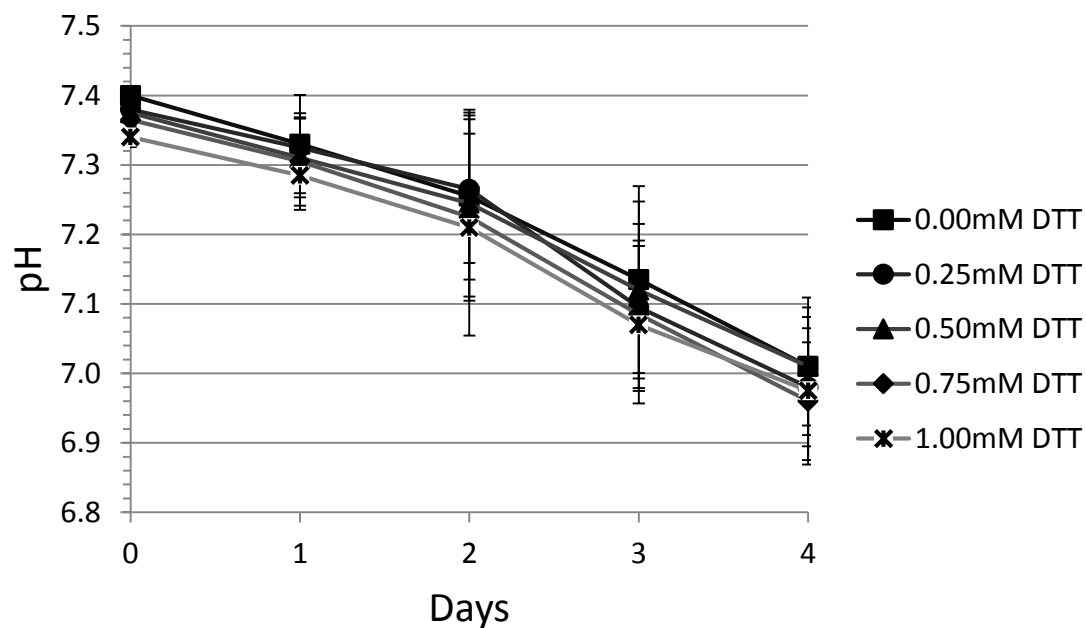
Figure 5.2c EG2-hFc pH profiles measured with offline probe
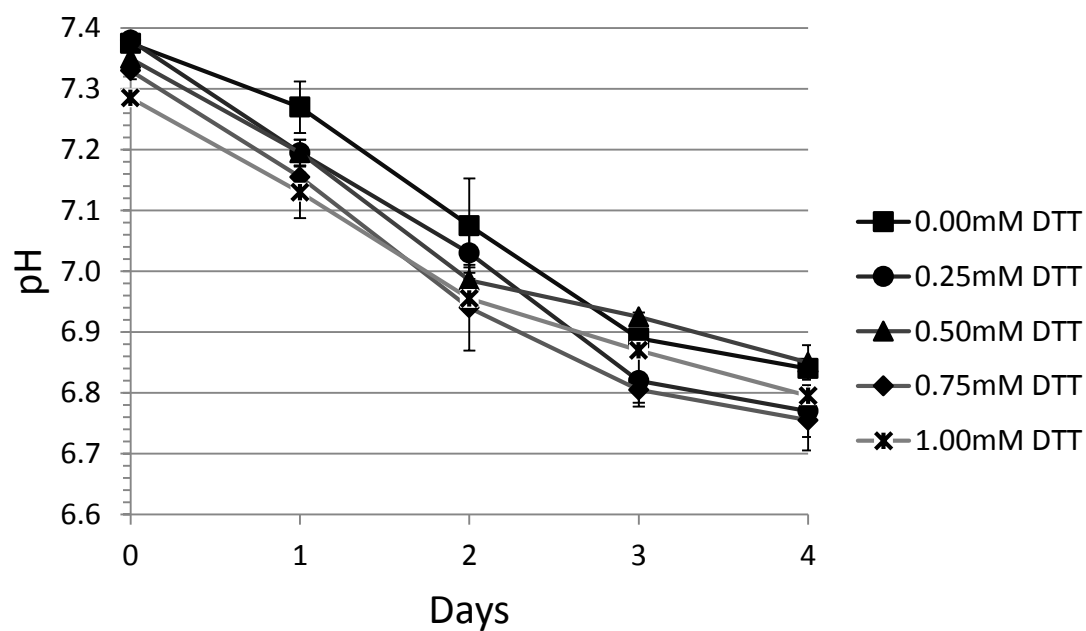
5.3.4. Redox and product stability in the presence of reducing agent

The DP-12 anti-IL-8 cell line showed a [DTT] dependent drop in CRP when DTT was first added to the medium (see **Figure 5.1d**). Biogro media prior to DTT supplementation had a CRP of between 10-35 mV. The control culture for these experiments had an average CRP = 21.0 mV ±0.5. When DTT was added the initial CRP dropped for each experimental culture condition to a low of -8.5 ±2.3 mV in the 1 mM DTT condition. As the run progressed the CRPs continued to decline daily until harvest. The control culture had a final CRP of -30.8 ±6.9 mV and the lowest CRP was determined in the 1 mM DTT culture at -56.6 ±4.7 mV. All other conditions fell within these two values at time of harvest. Examining the figure, it can be seen that the decrease in CRP is uniform between all cultures for the duration of the run save one data point; there is a crossover on day 3 between the control and 0.25 mM DTT cultures. The CRPs of the control (-21.7 ±4.2 mV) and 0.25 mM DTT culture (-20.6 ±2.1 mV) gave no indication that this cross over point influenced the antibody productivity or glycosylation profile. The average change in CRP for all cultures was -49.0 ±3.6 mV. The lowest CRPs reached and overall drop in CRPs for all cultures can be seen in **Table 5.2**.

Table 5.2 Summary of CRP values for cell lines DP-12 anti-IL-8 and EG2-hFc at varying DTT concentrations as measured by offline redox probe

	[DTT] (mM)	Lowest CRP (mV)*	↓ in CRP over 4 day culture (mV)*
	0.00	-30.8 ±6.9	-51.8 ±7.4
	0.25	-32.2 ±1.3	-48.3 ±2.8
DP-12	0.50	-36.8 ±1.6	-44.0 ±0.9
	0.75	-51.5 ±8.3	-53.1 ±7.6
	1.00	-56.6 ±4.7	-48.1 ±2.5
	0.00	-56.8 ±4.7	-66.8 ±4.5
	0.25	-64.2 ±10.4	-65.1 ±11.0
EG2-hFc	0.50	-77.1 ±9.1	-72.4 ±10.1
	0.75	-89.0 ±6.3	-74.8 ±3.6
	1.00	-95.2 ±6.9	-76.0 ±6.5

* ±SD, average of n=6

The EG2-hFc cell line exhibited the same initial drop in CRP upon addition of DTT to the media. The control culture without DTT had a starting CRP = 10.0 ±0.3 mV. The lowest initial CRP occurred at 1 mM DTT culture at -19.2 ±0.4 mV. All other conditions fell within these two values (see **Figure 5.2d**). After one day of culture there was a large decrease in all CRPs of ≈45 mV. This large decrease compared to the DP-12 data is likely due the increased growth rate exhibited by the EG2-hFc cell line. On subsequent days the decrease in CRP continued in smaller increments. The small increase in CRP of one control replicate in trial #1 on day 3 was not deemed significant. This type of CRP increase was also noted with NS0 cells as well but not seen in DP-12 cultures. The cause of the increases remains unexplained. The harvest CRPs ranged from -56.8

±4.7 in the control to the lowest CRP of -95.2 ±6.9 in the 1 mM DTT culture. It must be noted that even though the standard deviations between these replicate runs is sometimes high, this is inherent to the redox method used due to different calibration cycles between runs. Different lots of media were used between runs and factors such as agitation, headspace or age of media in the supply bottle can play a role on the level of dissolved oxygen in the media. Minimizing these effects was essential to the experiments but could not be eliminated entirely. This also contributes to the large range of CRP in Biogro media. The individual duplicates that were run in each of the three trials had relative standard deviations of less than 10% with a majority less than 5%. These different CRP values between runs were taken into account when performing the glycan analysis to determine if the CRP value itself influenced the glycan profile. An important feature is that the decrease in CRP is consistent between cultures for the entire run with no crossover of values. The average drop in CRP for all EG2-hFc cultures was -71.0 ±4.8 mV. The lowest CRP values and overall drop in CRP for all cultures can be seen in **Table 5.2**.

Figure 5.1d DP-12 culture redox potentials (CRP) measured with offline
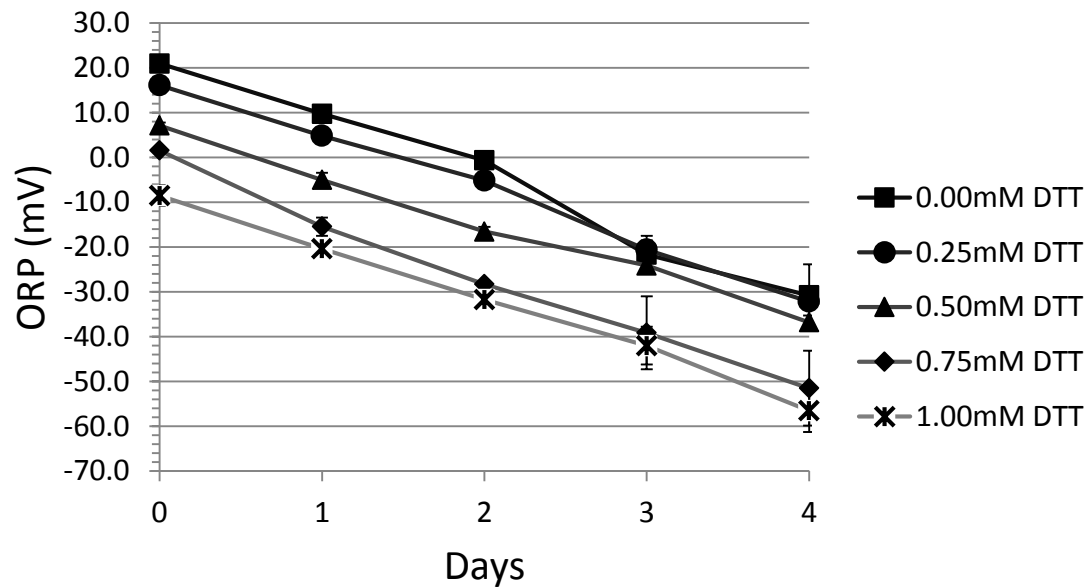
redox probe

Figure 5.2d EG2-hFc culture redox potentials (CRP) measured with

offline redox probe
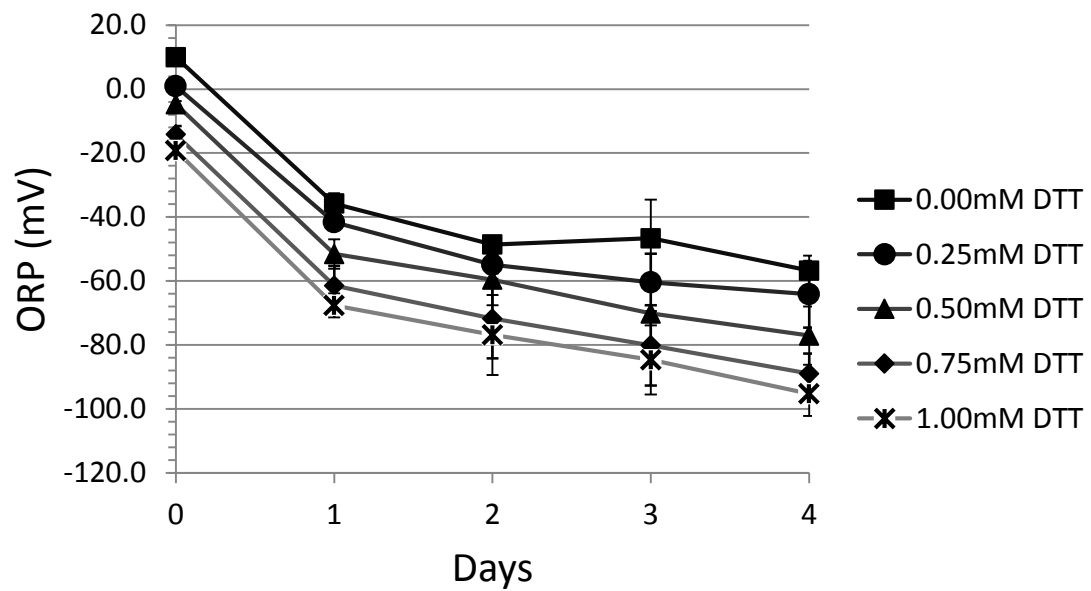
5.3.5. Glycan Analysis

The glycan profile of the Mabs produced by the DP-12 anti-IL-8 cell line is very similar to other IgG1 high producing cell lines including the NS0 cell line tested earlier. An example of the HILIC-HPLC profile for the 0 mM culture can be seen in **Figure 5.3**. The main peak identified as FG0 represents a fucosylated biantennary structure with terminal GlcNac residues on both arms and no galactose. The second largest peak is identified as FG1, which has the same base structure as FG0 but with one galactose residue on either of the arms. The other most notable peak is identified as FG2. This is the fucosylated base structure with two terminal galactose residues. In typical IgG1 profiles of high producing cell lines, FG0, FG1 and FG2 are the three main peaks in descending order. **Table 5.3** is a summary of all peaks identified in the HILIC-HPLC analysis using a set standard of integration parameters. Integration parameters included peaks between the GU values of 4-9. Peaks with less than 1% area were not included in the table and as a whole contributed less than 5% of the total area and had no effect on the overall analysis of glycans. This is not to say that the peaks were not present, only that they were insignificant with overall profiling efforts. This is the case for the F(6)M3 peaks missing in 0.50, 0.75 and 1 mM DTT cultures and the A1G1 peak omitted in the 0.75 mM DTT culture. Other noteworthy peaks sometimes associated with

IgG1 that are not present in the DP-12 cell line include high mannose glycans and bisecting GlcNAc species; each with less than 1% area.

Looking at the values from the control culture, we can see that the non-fucosylated G1 peak is quite large in some instances at 8.9% area but is variable from run to run with a standard deviation of 4.7%. This gives an RSD >50%. This variability is not seen in the three main peaks of FG0, FG1 and FG2 where the RSV <11%. This G1 peak consistently decreases in size as the DTT concentration increases from a high of 8.9% to a low of 2.8% in the 1 mM DTT culture. This would suggest perhaps that fucosylation is affected by the presence of DTT or by the shift in redox conditions. **Figure 5.4** depicts an overlay of every culture condition for DP-12 normalized to the FG0 peak where the shift in fucosylation is apparent by the decrease in peak height for the G1 species as [DTT] increases.

Figure 5.3 HILIC-HPLC profile of 2-AB labelled glycans cleaved from IgG1 produced in a 0 mM DTT culture of DP-12 anti-IL-8 cells. In-solution PNGaseF digestion was performed on protein A purified IgG1 prior to isolation and labelling of glycans by 2-aminobenzamide. HILIC was run with a 50 mM ammonium formate/acetonitrile gradient and GU were generated by use of a standard dextran ladder and compared to values in the NIBRT Glycobase
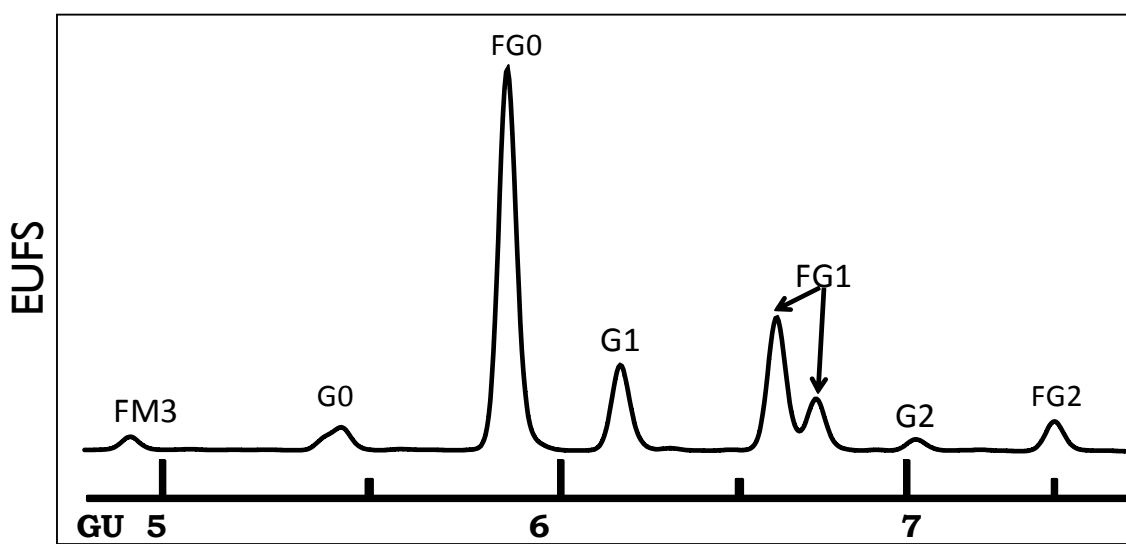
Table 5.3 Glycan profile peaks expressed as % area from DP-12 anti-IL-8 cultures in the presence of DTT. Integrated peak areas include GU values between 4 and 9.

GU value	Structure ID	Area % *				
		0 mM	0.25 mM	0.50 mM	0.75 mM	1.00 mM
4.93	FM3	2.4 ±0.2	2.6 ±0.8			
5.43	G0	4.9 ±0.7	5.0 ±0.8	4.9 ±0.5	4.8 ±1.9	3.5 ±1.0
5.86	FG0	50.0±3.6	48.3 ±0.4	50.7 ±0.0	54.1±4.7	46.5 ±3.7
5.93	A1G1	4.0 ±1.4	4.8 ±1.9	4.0 ±1.4		3.8 ±1.2
6.16	G1	8.9 ±4.7	7.7 ±4.3	6.0 ±4.0	3.5 ±1.5	2.8 ±0.2
6.61	FG1[1]	19.7±1.2	19.5 ±0.8	21.1 ±0.6	22.3±2.5	26.7 ±0.2
6.73	FG1[2]	8.7 ±1.4	8.9 ±0.9	9.7 ±0.1	9.5 ±1.2	11.6 ±0.7
7.49	FG2	4.7 ±0.4	5.5 ±0.3	5.6 ±0.1	5.9 ±1.3	7.1 ±0.7

* ±SD, average values from n=3
[1] isomer forms of terminal residues on 6-antenna
[2] isomer forms of terminal residues on 3-antenna

Figure 5.4 Overlaid normalized HILIC-HPLC glycan profiles of DP-12 anti-IL-8 IgG1 produced in the presence of DTT. Supernatant was filtered then purified via Protein A column. Glycans were cleaved with PNGaseF and isolated prior to labeling with 2-aminobenzamide. Samples were then loaded on a 3.5 μm amide column running a 50 mM ammonium formate/acetonitrile gradient. Glucose Units were generated by use of a standard dextran ladder and compared to values in the NIBRT Glycobase
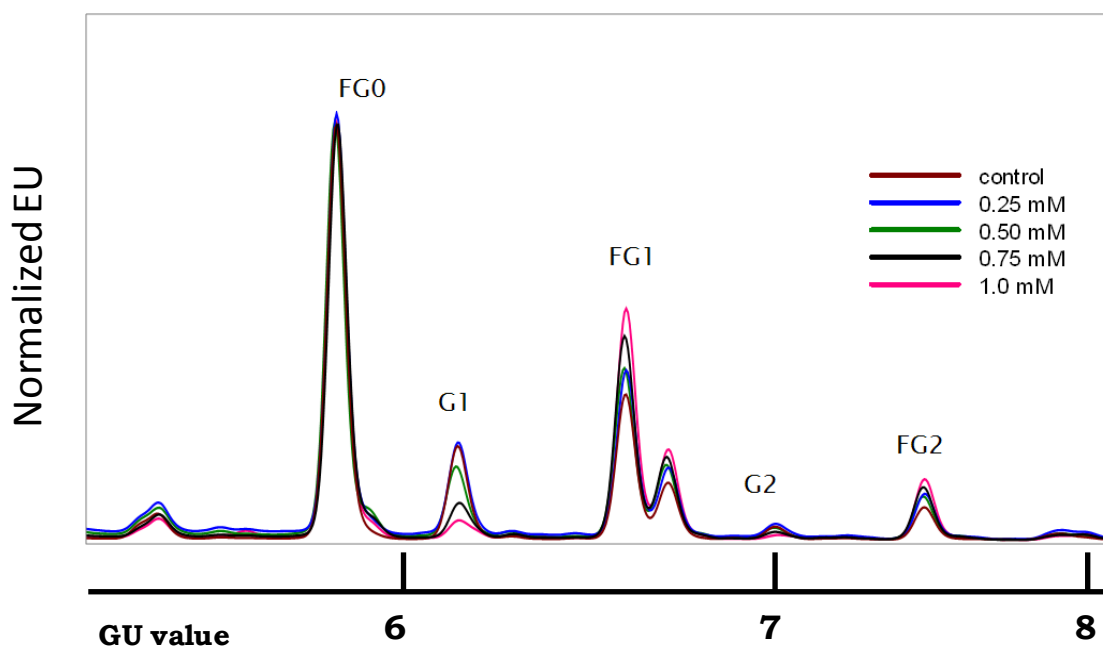
The G2 peak identified in **Figure 5.4** is for identification purposes but comprises <2% of total area for any sample. The size of the G2 peak follows the same trend as the G1 peak in that it recedes while the FG2 peak gets larger as the [DTT] increases. The shift in fucosylation can be seen in **Table 5.4** where the values of overall fucosylated structures have been calculated as well as the Galactosylation Index (GI) for each cell culture tested. The calculated GI makes it easier to determine the effect of CRP on galactosylation. GI in the control is 0.245 which increases slightly in the 0.25 mM and 0.50 mM DTT cultures to 0.254 and 0.255 respectively. GI then drops in the 0.75 mM DTT culture to 0.235 before rebounding to a high of 0.290 in the 1 mM DTT culture. This data would suggest no correlation between GI and change in CRP; however there exists a possible exception above 1 mM DTT. See discussion for further explanation.

Table 5.4 GI values and percent fucosylated glycans for DP-12 anti-IL-8 cultures producing IgG1 in the presence of DTT as determined by HILIC analysis

	[DTT] (mM)	GI*	% Fucosylated*
DP-12	0.00	0.245 ±0.009	86 ±1.2
	0.25	0.254 ±0.001	85 ±0.1
	0.50	0.255 ±0.004	87 ±0.6
	0.75	0.235 ±0.040	92 ±0.4
	1.00	0.290 ±0.010	92 ±3.9
EG2-hFc	0.00	0.625 ±0.015	84 ±12.5
	0.25	0.705 ±0.068	89 ±14.8
	0.50	0.628 ±0.086	81 ±15.9
	0.75	0.695 ±0.120	84 ±15.0
	1.00	0.723 ±0.106	85 ±17.8

* ±SD, average of n=3

The EG2-hFc glycan analysis revealed a profile where the predominant peak was FG2 with smaller peaks at FG1 and FG0. This is in contrast to the profile observed in IgG1 that had smaller peak areas for FG2. **Figure 5.5** depicts a representative glycan profile of a control culture of EG2-hFc antibodies. The biantennary base structures of the glycans found in EG2-hFc are the same as in the IgG1 glycans with most glycans being fucosylated with variable galactosylation. Due to the higher level of galactosylation there is also more sialylation of these glycans as evidenced by the large peaks at higher GU values than for FG2. Using the same HILIC-HPLC method and integration parameters as with DP-12 glycans, the chromatograms of representative EG2-hFc runs from all [DTT] tested have been overlaid in **Figure 5.6** and the identities of the individual glycans and peak areas have been summarized in **Table 5.5**.

Figure 5.5 HILIC-HPLC profile of 2-AB labelled glycans cleaved from chimeric camelid antibodies produced in a 0 mM DTT culture of EG2-hFc cells. In-solution PNGaseF digestion was done on protein A purified IgG1 prior to isolation and labelling of glycans by 2-aminobenzamide. HILIC was run with a 50 mM ammonium formate/acetonitrile gradient and GU were generated by use of a standard dextran ladder and compared to values in the NIBRT Glycobase
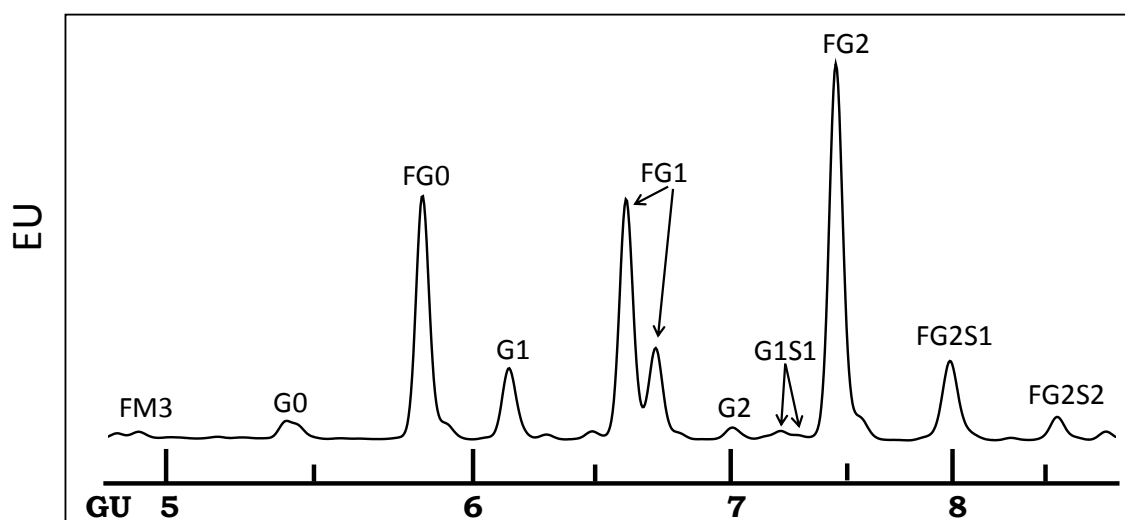
Figure 5.6 Overlaid normalized HILIC-HPLC glycan profiles of EG2-hFc

antibodies produced in the presence of DTT. Supernatant was filtered

then purified via Protein A column. Glycans were cleaved with PNGaseF

and isolated prior to labeling with 2-aminobenzamide. Samples were

then loaded on a 3.5 µm amide column running a 50 mM ammonium

formate/acetonitrile gradient. Glucose Units were generated by use of a

standard dextran ladder and compared to values in the NIBRT Glycobase
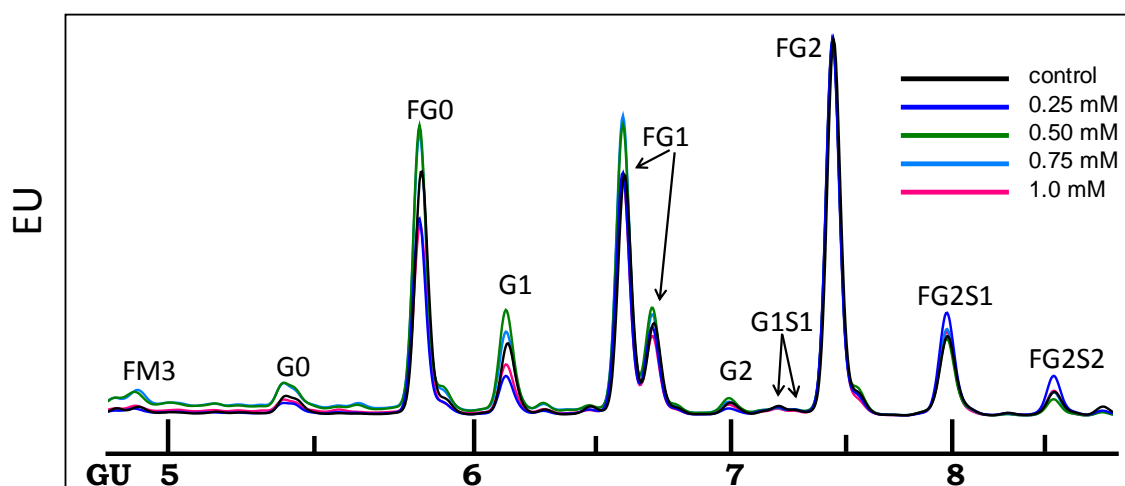
Table 5.5 Glycan profile peaks expressed as % area from EG2-hFc cultures in the presence of DTT. Integrated peak areas include GU values between 4 and 9.

| GU value	Structure ID	Area %*				
		0 mM	0.25 mM	0.50 mM	0.75 mM	1.00 mM
4.92	FM3	2.2 ±0.3				
5.41	G0	3.4 ±1.5	2.1 ±0.1	3.7 ±0.9	2.4 ±0.2	1.7 ±0.5
5.66	A1G1			2.1 ±0.1		
5.86	FG0	17.7±4.2	13.0±6.6	16.0±8.8	13.1±9.9	11.9±8.3
6.18	G1	5.5 ±1.1	3.8 ±0.2	6.6 ±2.0	5.1 ±1.3	4.2 ±1.0
6.34	FA1G1		2.0 ±0.1	2.3 ±0.4	2.0 ±0.0	
6.52	A2BG1?			2.5 ±0.7		
6.61	FG1	17.1±3.4	16.7±6.1	16.8±6.1	15.9±6.3	16.3±7.6
6.73	FG1	7.9 ±0.3	6.7 ±2.2	6.9 ±2.2	5.9 ±2.0	6.0 ±2.4
7.07	G2	5.6 ±5.1	6.1 ±5.7	6.4 ±6.2	6.7 ±6.7	6.1 ±5.8
7.23	G1S1	2.4 ±0.5	2.3 ±0.5	2.3 ±0.4	2.4 ±0.5	2.3 ±0.4
7.37	G1S1	2.1 ±0.1	2.0 ±0.0	2.1 ±0.2	2.2 ±0.2	1.9 ±0.1
7.49	FG2	25.5±10.2	28.1±9.5	23.8±8.9	26.4±10.7	28.9±10.4
7.68	G2S1	2.5 ±0.7	2.8 ±1.2	2.7 ±1.0	3.1 ±1.6	2.8 ±1.2
8.03	FG2S1[1]	9.6 ±2.0	12.4±2.5	9.1 ±3.0	10.7 ±5.1	12.3±4.5
8.29	FG2S1[2]		2.3 ±0.5	2.1 ±0.2	2.6 ±0.8	2.5 ±0.6
8.58	FG2S2	3.6 ±1.8	5.6 ±2.4	3.6 ±2.2	5.1 ±3.8	5.6 ±4.4
8.84	FG2S2		2.0 ±0.0		2.0 ±0.0	2.0 ±0.0

* ±SD, average values from n=3
[1] isomer forms of terminal residues on 6-antenna
[2] isomer forms of terminal residues on 3-antenna
? this is a plausible structure though not identified through exodigests

143

Using the same integration parameters as with DP-12, peak areas < 1% were not identified. These areas do not alter the overall analysis or downstream calculations as does that for GI. Despite numerous runs on the HPLC there is always a high level of variability with the EG2-hFc glycan profiles as exhibited in the standard deviation values for all samples. The variability can be partially attributed to the fucosylation pattern of the glycans. For example in the 0 mM culture, the RSV is 46% and 24% for G0 and FG0 respectively. When these peaks areas are combined the RSV drops to below 13% between culture runs suggesting that the variability of these two peaks can be attributed to a fucosylation event taking place or not. This variable fucosylation does not account for every glycan species' high deviation values therefore other factors must be considered.

Due to the high variability, the tabular data does not provide much in terms of emerging trends influenced by CRP. In order to simplify the results, GI values were calculated along with % fucosylation and presented in **Table 5.4**. There is no trend (increasing or decreasing) with respect to % fucosylation in EG2-hFc cell culture when DTT is added to the media. The GI values show more consistency than the individual glycans and begin as low as 0.625 in the 0 mM culture to a high of 0.723 in the 1 mM DTT culture. These values may suggest a trend towards more galactosylation at lower redox states however when a student t-test is

applied the p-value > 0.05 thereby making the shift in GI unpredictable from run to run.

It should also be noted that no α-1,3 galactose was detected in any of the antibodies produced. This was confirmed by performing exodigestions on the 2-AB labelled glycans using a β-galactosidase which removes all β-galactose residues while leaving any α-gal residues in-place. The dominant peaks all shifted to the base structures of $GlcNAc_2Man_3GlcNAc_{(1-2)}$(data not shown). No residual peaks were found in the GU regions where mono and bi-antennary α-gal would reside.

5.4. Discussion

As evidenced by the NS0 data presented previously, culture redox potential can have a significant effect on glycosylation profiles while maintaining otherwise characteristic cell culture parameters such as viable cell density, pH and titre. It is important to determine if these effects are universal to mammalian cell cultures regardless of cell line and recombinant protein expressed. To address these questions a series of experiments were designed which incorporated two other cell lines producing two different types of monoclonal antibodies.

5.4.1.   Growth, productivity and redox potential

DP-12 anti-IL-8 cultures were not affected in any uniform manner by the DTT in the Biogro media. All cultures ran with mean growth rates of 0.62 d^{-1} ±0.02, which is within the range of 0.2 to 1.0 d^{-1} seen in the work of Heinrich et al. in 2011. Productivities were slightly increased over Heinrich et al. values (6-13 pg/cell/day) with an average of 14.1 ±0.6. (Heinrich et al. 2011). These results are comparable to those obtained from the NS0 cell line in that little to no change was observed due to the influence of changing CRP. EG2-hFc cultures did perform differently from one another but unfortunately no correlation was found between CRP levels and these fluctuations in growth profiles.

146

The Q_{Mab} values for both DP-12 and EG2-hFc are on the low end of what have been recently seen in industrial processes in the range of 10-50 pg/cell/day (Butler & Meneses-Acosta 2012) but more importantly they do not fluctuate in any uniform manner with the imposed change in CRP. The lack of a correlation between Q_{Mab} and CRP in all three cell lines (NS0 included) is notable because it has been shown that [DTT]> 0.1 mM can keep the redox potential of the ER in a reduced state (Van Lith et al. 2011). This reduced state may lead to less protein folding and secretion thereby decreasing productivity. The absence of a productivity decrease in the cell lines tested here with levels higher than 0.1 mM DTT may suggest that other redox regulatory pathways have been engaged such as high turnover of glutathione or increased activity of chaperone folding proteins (Chakravarthi et al. 2006; Appenzeller-Herzog et al. 2010). The higher Q_{Mab} and different growth profiles (VCD, IVCC) in DP-12 compared to EG2-hFc is due to it being a different cell type, despite both being CHO. However, built into the selection process are other contributing factors such as DP-12 being screened as an industrial production cell line(ATCC CRL-12445) and possibly by the selection pressure used when the clones were selected (Misaghi et al. 2013). With regards to its industrial origins, commercial cloning and screening techniques generally outperform those of academic labs due to the large number of clones that can be screened thereby resulting in a higher probability for success. With respect to

147

selection pressure, in Misaghi et al. they showed a differences in production levels for CHO DHFR⁻ cells when puromycin or methotrexate was used. What has not yet been determined is if these changes in productivity can be correlated to the number of gene copies present in the individual cell lines; recall that MX amplifies the number of *dhfr* genes with an associated rise in the number of integrated HC and LC genes. If the selection pressure can influence productivity, it may also affect other phenotypic parameters like glycosylation.

One concern for non-CRP related influences was the starting pH of the cultures. There was a dose dependent drop in all starting pH when DTT was added to Biogro media but values were within the setpoint of 7.4 ±0.1 and therefore deemed not a significant variable. This drop in initial pH was not observed when using the Abbvie CD media with NS0 cells. Of significance was the decrease in pH over the course of the cultures. In both cell lines the pH drops by as much as 0.4 in DP-12 and 0.6 in EG2-hFc. This was independent of the DTT concentration. The larger drop in pH seen in EG2-hFc was likely due to its elevated growth rate and increased lactate production. In any event, the two cell lines reach pH levels that have been shown to affect glycan patterns of recombinant proteins when culture pH<7.2 (Borys et al. 1993; Müthing et al. 2003) showed increased agalacto and monogalacto species of recombinant proteins at a pH below 7.2. This might explain the DP-12 results as

evidenced by the low GI, as would the low GI generated by NS0 glycans. In both these cases the final pH of the cultures were below 7.1. In stark contrast to this however was the relatively high GI maintained by the EG2-hFc cultures despite having pH<6.9. If low pH decreases GI then clearly another factor plays a more prominent role in sustaining galactose residues on glycans, some possibilities include intracellular redox potential, up regulation of glycan machinery or protein backbone structure.

As already mentioned, much like the NS0 data, neither the DP-12 nor EG2-hFc cultures were influenced by DTT in a concentration dependent manner with respect to growth or productivity. This is despite the different initial CRPs in the individual conditions. A drop in the basal media CRP was documented according to how much DTT was added, like NS0 cultures. Unaltered basal media has been shown to have levels of CRP ranging from 10-35 mV. Over the range of [DTT] tested, the drop in CRP was ≈30 mV in each cell line on day 0. The differences in starting redox values are likely due to the inherent difficulty in measuring redox potential off-line (Pluschkell & Flickinger 1995). There are no alternatives to offline measurement for redox when using small flasks; however if bioreactors are incorporated it would become possible for online measurements and perhaps even control of the CRP much in the same way DO or pH are controlled (Meneses-Acosta et al. 2012).

The large decrease in CRP exhibited by EG2-hFc but not by DP-12 in the first 24 hours was likely attributed to the higher cell growth of EG2-hFc. This large decrease early on may have an effect on the very few Mabs produced in this time; however it is of minor consequence to the overall Mab population. More importantly was to evaluate the absolute values of CRP for each cell line and the overall drop in CRP during the 4 day culture.

The lowest absolute CRP in a DP-12 culture was -59.9 mV in one replicate of a 1 mM DTT culture, compare this to the highest final CRP in NS0 cells at -79.9 mV in the control and we can see that there is no overlap at all on day 4. The EG2-hFc cultures, with the high initial drop in CRP, ranged from -56.8 to -95.2 mV on day 4 thereby demonstrating some overlap in values compared to NS0; specifically the 0.75 mM and 1 mM DTT EG2-hFc cultures. The NS0 data suggested that a redox threshold may exist near a CRP of -100 mV (50 mM DTT) that would affect the GI of Mabs. This value was never reached in DP-12 and was only approached by the EG2-hFc 1 mM DTT culture; only one replicate ever reached < -100 mV. This leaves open the possibility that a threshold does exist around -100 mV as no trend in altering the GI for DP-12 or EG2-hFc were observed. Taking into account individual replicates, their redox values and the associated glycan profiles revealed no new glycan patterns or changes in GI that would suggest an influence by absolute CRP values.

The CRP drop in the DP-12 control was -51.8 mV compared to –66.8 mV in EG2-hFc control and -94.2 mV in the NS0 control. The drop in the NS0 culture was high in comparison to the others; however it retained a higher GI value than the DP-12 culture which produced an antibody very similar in structure and size. None of the DP-12 cultures exhibited as high a drop in CRP with an average of only -49.0 ±3.6 mV. Similarly, the EG2-hFc cultures had lower drops as well averaging only -71.0 ±4.8 mV. Considering there is no discernable trend in GI that corresponds to [DTT] in DP-12 and EG2-hFc cultures but one does exist with NS0 cells, it is plausible that the overall drop in CRP was not the major contributing factor to change in galactosylation. The natural change in CRP over the course of a culture was likely due to the release of anti-oxidants and reducing enzymes into the media (Trexler-Schmidt et al. 2010; Kao et al. 2010); however when runs are terminated at high viabilities (>90%) it is unlikely that the amount of natural reducing agents released through cell lysis is sufficient to cause a decrease on their own. In order to evaluate if the drop in CRP or if absolute CRP values can affect the glycan patterns of recombinant proteins, cultures may have to be run with lower harvest viabilities targeted and possibly include a low dissolved oxygen parameter to ensure CRP < -100 which may contribute to changing the glycan patterns observed.

5.4.2. Glycosylation of monoclonal antibodies

DP-12 anti-IL-8 Mabs have the same structure as IgG1 produced in NS0 cells with one glycosylation site available at Asn-297 on the Fc region. Differences can arise when different cell lines are employed to produce similar recombinant proteins (Lifely et al. 1995) but in this case the glycan profile is very similar to that of glycans produced in NS0 with a predominant FG0 peak but with a slightly lower GI at 0.245 vs. 0.314 in NS0, in the controls. In the NS0 data a ≈ 50% decrease in the GI was observed as [DTT] increased. With DP-12 we see no correlation between [DTT] and GI except in the 1 mM DTT condition where ($p < 0.01$) GI increases to 0.290±0.010. This opposite reaction to galactosylation in CHO DP-12 in the presence of lower CRP, compared to NS0, is unexpected but more likely to do with the host cell than the antibody. The GI in CHO EG2-hFc mirrors the DP-12 results with respect to no observable trend linked to [DTT] but EG2-hFc has a higher GI ($p < 0.05$) in the 1 mM DTT condition at 0.723. It would appear that the change in galactose profiles at 1 mM DTT is cell line dependent; detected in CHO but not NS0. Having the capability to manipulate the amount of galactose residues on the glycans of Mabs is desirable (Dalziel et al. 2014; Gramer et al. 2011) depending on its end use as a therapeutic.

One significant difference between NS0 and CHO DP-12 is the change in the level of fucosylation when DTT is added to each condition.

In NS0 the percentage of fucosylated glycans decreases as [DTT] increases but with extremely high variability and is not deemed significant. In contrast the DP-12 glycans exhibit a 7% increase in fucosylation in the 1 mM DTT condition with a p <0.5. This significant effect may have an impact on how the IgG1 is used as a therapeutic as binding efficiencies are affected by the presence of a core fucose (Shinkawa et al. 2003; Kanda et al. 2007; Mizushima et al. 2011; Ferrara et al. 2011). An increase in fucosylated glycans would adversely affect any IgG1 where the mechanism of action is to elicit an ADCC response. This increase in fucose moieties can be correlated to a decrease in CRP, thereby making the monitoring of CRP in some cell lines necessary to detect impending changes in fucose patterns. EG2-hFc, like NS0, does not show any significant change in % fucosylation when [DTT] are changed; it does however show great variability from run to run. This variability, as mentioned earlier, is decreased when fucosylated and non-fucosylated glycans of the same structure are grouped together; like G0 and FG0, G1 and FG1, etc. This is not a DTT or CRP determined event as there is high variability in all conditions. The cause of the variance is likely at the level of fucosyltransferase activity within the Golgi of the cells. The causes of the fluctuations in this activity are unknown at this time.

Perhaps the most interesting aspect of the EG2-hFc glycan analysis is the reversed HILIC-HPLC peak profile. Unlike normal IgG1s, including

the commercially available analog to EG2-hFc (cetuximab) with its low GIs (Jefferis 2012), the EG2-hFc cells produce glycoforms that are much more desirable as therapeutics with a predominant FG2 peak and GI = 0.625±0.015 while lacking some undesirable traits like terminal α-1,3 galactose which has been determined to be immunogenic (Berg et al. 2014). This high GI also contributes to higher levels of sialylation. EG2-hFc had as much as 22% of the glycans species sialylated, compared to < 1% from DP-12. The type of sialic acid residues found on the CHO derived glycans was, as determined by their GU value, the expected NeuAc however the α-2,3 vs. α-2,6 bond determination was not done due to a broad spectrum sialidase being used during the exodigestions which cleaved both types of bonds.

Theoretically the high GI, higher sialic acid content, non-existence of α-1,3 galactose and smaller tissue penetrating size of the EG2-hFc would make it an ideal candidate for therapeutic use. Higher GI can translate into increase receptor binding affinities (Houde et al. 2010; Raju & Jordan 2012) and increase serum half-life (Raju et al. 2001) while increased sialylation can contribute to an anti-inflammatory response *in vivo* (Anthony et al. 2008; Kaneko et al. 2006). Currently the two products on the market for EGFR, cetuximab and trastuzumab, both target solid tumours where penetration efficiency is crucial (Beckman et al. 2007; Jain

et al. 2005) for efficacy. EG2-hFc could substantially increase this penetration efficiency.

The overall glycan profile does not vary under DTT conditions and any influence exerted by different selection methods (methotrexate vs. puromycin) is unlikely as these are common methods for industrial cloning. This high GI is unique among monoclonal antibodies and its cause is unknown. The most likely answer could be found in the structure of the camelid antibody. Despite having a similar humanized Fc region to IgG1, the difference in overall molecular weight is big enough to alter the activity of glycosyltransferases. It has been demonstrated previously that steric hindrance can affect glycan patterns when interfering molecules are present (Narasimhan et al. 1985) with β-1,4 galactosyltransferase (β-1,4 GalT). The small 80 kDa size of EG2-hFc and how it is configured around the Asn-297 site may allow for β-1,4 GalT to be unimpeded and placed in contact with the N-glycan site more often leading to higher GI. Alternate explanations for the high GI may include overexpression of β-1,4 GalT in EG2-hFc or higher than normal UDP-Gal donor pools. Further research will need to be done to define the exact cause.

5.5. Conclusion

Previous work suggested that CRP monitoring may be crucial for NS0 cultures due to the decrease in Mab galactosylation when CRP levels

dropped over the course of a batch culture. The endeavour here with CHO DP-12 anti-IL-8 and EG2-hFc cultures was to determine if this effect occurred in other mammalian cell cultures or antibody type. To this end it was demonstrated that no CRP dependent shift in GI emerged in DP-12 IgG1. However a variable level of fucosylation was noted in IgG1 with a decrease in CRP suggesting more than one glycosylation enzyme/pathway may be affected by external redox potentials. Trends were not observed with respect to GI or fucosylation in the novel camelid Mab EG2-hFc when CRP changes were imposed. Perhaps the most noteworthy aspect of the camelid antibody was the high GI produced. The improved therapeutic profile could give the EG2-hFc Mab a substantial advantage over the current commercial material. More research needs to be done to determine the reasons for increased galactosylation and determine if these can be applied elsewhere. As for the universality of CRP's influence on glycosylation, it appears that differential effects will be observed with various cell lines and antibody types. This may require future cell lines to undergo process development efforts to determine the susceptibility of clones to CRP and establish an acceptable level of glycan variability. It may also be possible to control the CRP in such a manner as to define the glycan patterns by design rather than by chance.

Chapter 6 – β-1,4 galactosyltransferase activity under reducing conditions and with whole and partially reduced monoclonal antibodies

5.1. Abstract

The most variable monosaccharide of the glycans observed in NS0 and CHO cultures under lower redox conditions is galactose, whose significance has yet to be fully determined in therapeutics but whose determination on glycans can be explored. Through a series of *in vitro* assays using purified Mabs of IgG1 and EG2-hFc, the impact and activity of a soluble β-1,4 galactosyltyransferase (GalT) was examined. The primary goal was to further elucidate the mechanism of action previously proposed where lower redox potentials could affect the Galactosylation Index of an NS0 IgG1. To this end, NS0 IgG1 was determined to reduce through the loss of light chains followed by reduction of inter-heavy chain disulfide bonds. The resulting intermediate fragments ($50_{HC}, 100_{2HC}, 125_{2HCLC}$ kDa) were also treated with GalT and it was found that the smaller fragments showed less galactosylation than the 125 kDa or whole IgG1 Mabs. The results of the reduction pathway and fragment interaction with GalT support the hypothesis that NS0 IgG1 could undergo a structural shift whereupon GalT has less access to the N-glycan site of

the Fc region. The secondary goal of determining GalT affinity to IgG1 and the humanized camelid antibody EG2-hFc revealed a nearly 10 fold higher interaction with the EG2-hFc. The cause for the higher activity may be due to overall size difference or point mutations in the Fc region of EG2-hFc.

Keywords glycosylation, β-1,4 galactosyltransferase (GalT), monoclonal antibodies, hydrophilic interaction liquid chromatography (HILIC), malachite green, redox potential, disulfide bonds

6.2. Introduction

Altering the CRP on multiple cell lines and antibody types had no universal effect on glycosylation. With variable levels of galactosylation and fucosylation in the NS0 and CHO cell lines examined, a drilling down to the core glycosylation pathway components will hopefully clarify why some events occur while others do not, specifically examining galactosylation. The glycan profiles of therapeutic Mabs have been well studied in recent years (Raju & Jordan 2012) with the role of galactose being muddled in conflicting reports as to its importance in pharmacokinetics (Lux & Nimmerjahn 2011). The most recent findings point to a correlation between CDC and galactose heterogeneity but not with ADCC (Hodoniczky et al. 2005). Differential effects attributed to

158

individual residues are wide spread with many causes plausible. One explanation for varying glycan profiles of Mabs is that the glycosylation pathway has been altered by culture parameters or media components leading to shifts in microheterogeneity. This may not be the case as seen when polyclonal IgGs from the same sample with glycans on both the Fc and Fab regions were analysed, the Fc glycans were hypogalactosylated while the Fab glycans were galactosylated and sialylated (Holland et al. 2006). This would suggest that the machinery is behaving normally, including donors and enzymes, but that the position of the N-glycan is at issue. The Asn-297 N-glycan site on the Fc region of IgG is in close proximity to interchain disulfide bonds, which may sterically hinder access to glycosyltransferases, like β1,4-galactosyltransferase (GalT). In order to address the shift in GI seen with NS0 IgG1 via lowered CRP and the high GI seen in EG2-hFc, an examination of β1,4-GalT activity is required.

β1,4-galactosyltransferases are transmembrane proteins located in the *trans*-Golgi of mammalian cells. Seven β1,4-GalT have been identified with the best studied form being GalT-1 (Hennet 2002; Qasba et al. 2008). Its mechanism of action, put simply, is to bind in sequence the metal ion Mn^{+2}, the donor UDP-Gal and then substrate GlcNAc (in mono or oligosaccharide form). After substrate binding, the galactose is transferred to GlcNAc followed by release of UDP, Mn^{+2} and GlcNAc-Gal complex. GalT enzymes are present in all mammalian cells, including CHO and NS0,

159

producing similar IgG glycan patterns in standard conditions. The differences observed in the GI of NS0 IgG1 after the introduction of a reducing agent could have several intervening factors such as lower GalT mRNA; however previous results have shown that mRNA levels do not fluctuate even when agalactosylated species arise (Jeddi et al. 1996); this turns the focus to GalT activity. GalT activity was tested in two manners 1) GalT in a reducing environment and 2) GalT with intermediate forms of IgG substrate.

There is a possibility that the decrease in GalT activity with NS0 Mabs under reducing conditions could be a direct effect of the dithiothreitol on the GalT, such as a reduction of the 2 disulfide bonds (Yen et al. 2000) in GalT-1. An *in vitro* assay was devised to test for DTT effects on GalT activity using a free phosphate detection method.

The second determination of GalT activity included the use of IgG intermediate forms, including the degradation products from a reducing environment: HC (50kDa), HC-HC dimer (100kDa), and HC-HC-LC (125kDa) molecules. The premise was that a more accessible Fc and Asn-297 would undergo galactosylation with more efficiency than the intact IgG. Interchain disulfide bonds have been shown to interfere with macroheterogeneity of glycoproteins like tissue plasminogen activator (tPA) (Allen et al. 1995) and hemagglutinin-neuraminidase (McGinnes & Morrison 1997) by allowing more access to oligosaccharyltransferase and

160

there may be a similar opportunity for GalT. GalT has been shown to be sterically hindered by bisecting GlcNAc present on biantennary structures (Narasimhan et al. 1985) and possibly when in competition with N-acetylglucosaminyltransferase (Fukuta et al. 2000). This type of steric hindrance may have been present when a reducing agent was added to the NS0 cultures. From the NS0 results it was postulated that the reduced CRP caused a downward shift in GI. This event was initially attributed to a temporary reduction of the susceptible Mab disulfide bonds between LC and HC within the *trans*-Golgi. This in turn created a new conformation of the remaining HC dimer, which interfered with GalT binding the terminal GlcNAc resulting in no galactose added. In order to test this hypothesis, partial reduction assays were performed to determine the breakdown of IgG1 into its intermediates by using a reducing agent. Radiolabeling work had already shown that the formation of IgG1 went through the HC-HC dimer route prior to addition of LCs. The current work was to confirm the previously published results of IgG reduction: LC-HC-HC-LC (150kDa) → LC-HC-HC (125kDa) → HC-HC (100kDa) → HC (50kDa) (Hong et al. 2009; O'Callaghan et al. 2010) and to verify the NS0 IgG did the same. The accessibility of the intermediated structures was tested with GalT and results determined by HILIC.

In addition to GalT accessibility to IgG1 N-glycans, was the significant discovery that EG2-hFc had an unusually high GI. The

inherent structural differences of EG2-hFc are likely the cause of the high GI compared to DP-12 anti-IL-8 IgG seeing as both were produced in CHO cells with the same media and conditions. Notable structural differences include the lack of light chains in EG2-hFc and the shortened heavy chains lacking the CH1 domain resulting in an overall size of 80 kDa. This reduced size may enhance the ability of GalT to access the N-glycan, allowing for more complex glycosylation. The experiments performed here were to determine GalT activity on native and degalactosylated EG2-hFc and IgG1 *in vitro* to resolve the cause of the high GI.

6.2.2. Objectives

The first objectives of this chapter were to define the activity of GalT when under the influence of a reducing agent and to determine if GalT had differential activity on fragments of IgG1. The second objective was to examine the effect GalT had on the two different Mabs, IgG1 and EG2-hFc, to try and determine a mechanism by which the EG2-hFc achieved such a high GI.

6.3. Results

6.3.1. Galactosyltransferase activity when exposed to reducing conditions

One possibility for the shift to lower galactosylation observed in NS0 cultures may be a direct effect of DTT on GalT. The DTT may have a reducing effect *in vivo* on the disulfide bonds within the GalT thus disabling it. In order to test whether or not the concentrations of DTT used in cell culture were substantial enough for disruption, an *in vitro* assay was used. The assay used molar equivalents of monomer GlcNAc as the acceptor and UDP-galactose as the donor in an appropriate buffer solution containing Mn^{2+}. The concentration of DTT ranged from 0 mM to 1 mM, as in the experimental cultures grown previously, with negative and positive controls accounted for. The GalT activity in the control assay with no DTT has been normalized to 1 in Figure **6.1** and as the DTT concentration is increased the GalT activities fluctuate in both the up and down direction. There was a significant difference ($p<0.05$) between the 0 mM DTT and 0.75 mM DTT assays; however no correlation could be attributed to [DTT] and GalT activity. Normalized to the control where no DTT was present, the values fluctuated between 0.81-1.13 with %RSD<10% in every case. This data set would suggest that DTT at low concentrations does not inhibit the activity of GalT directly.

Figure 6.1 Normalized galactosyltransferase activity levels in the presence of DTT. Donor UDP-galactose, acceptor GlcNAc and phosphatase were mixed in wells with buffer containing Mn^{+2} prior to addition of GalT. After 1 hour incubation at 37°C, Malachite green reagents were added to detect the released free phosphates. Color was allowed to develop and wells were read at 630 nm
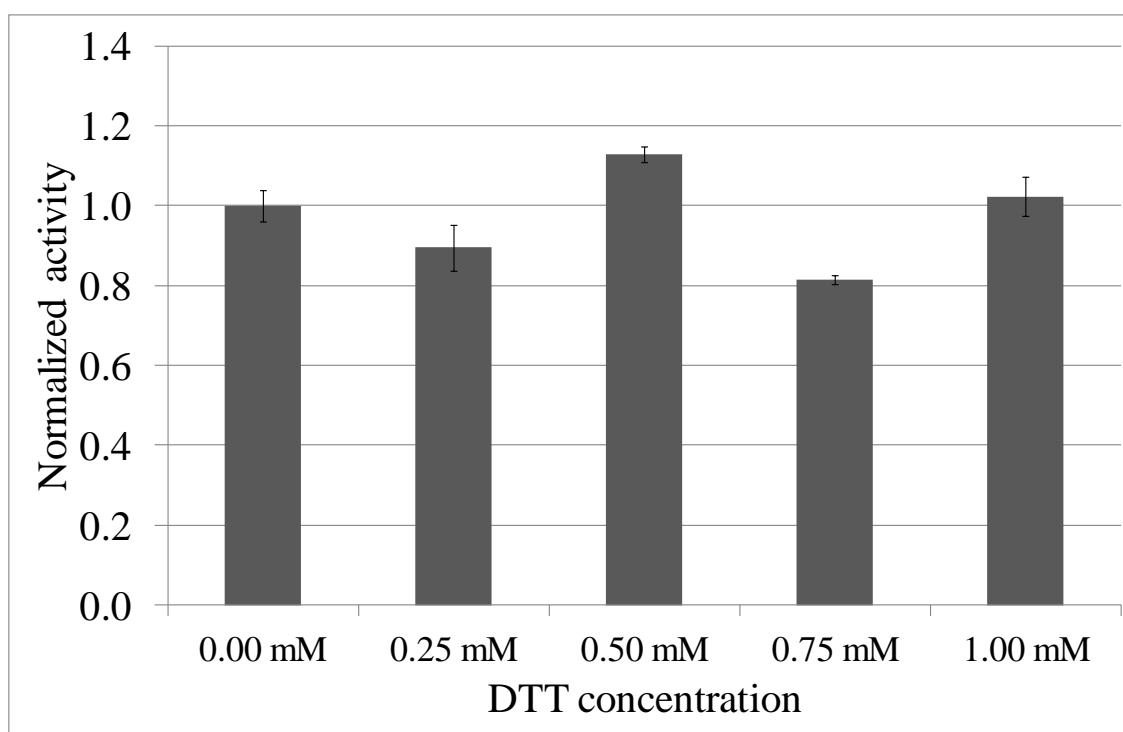
Error bars = ±SD, average of n=4

6.3.2.   Reduction pathway for IgG1 from NS0

The pathway for IgG disulfide bond formation was established previously by pulse radiolabeling nascent Mabs in NS0 cultures. This established that a HC dimer formed prior to addition of LCs. In order to confirm that the reduction pathway progressed in the reverse manner of its formation, a time course trial was setup to monitor the breakdown of IgG1 using DTT as the reducing agent. **Figure 6.2** shows an SDS-PAGE gel of IgG1 time course samples after exposure to 5 mM DTT and subsequent alkylation by 100 mM IAM. In a time dependent manner it was observed that the wholly formed IgG1 reduced from a 150 kDa structure to fragments of 125, 100, 50 and 25 kDa; no bands appeared at 75 kDa. Multiple bands were observed in the 125 kDa region of the gel. This was likely due to the non-reducing nature of the gel where the proteins do not fully denature and therefore several folded states may be present. The sizes of the top 3 bands are one 150 kDa band at the top followed by two 125 kDa bands running underneath. Densitometry analysis determined that as time progressed, the 150 and 125 kDa bands faded while the 50 kDa and 25 kDa bands intensified indicating the continuous reduction of IgG1 along the same path. Interestingly, the 100 kDa band has no significant change in density throughout the sample times suggesting that this species does not accumulate but is transient and less stable than the other intermediate forms. These results confirm

that the light chain to heavy chain disulfide bonds are more susceptible, leading to LC shedding first.

Figure 6.2 SDS-PAGE of partially reduced IgG1 by 5 mM DTT over time. Aliquots of IgG1 treated in 5 mM DTT were removed at various times followed by alkylation with IAM to prevent disulfide bond reforming. Samples were mixed 1:1 with non-reducing sample buffer and run on a non-reducing, 4-12% gradient precast SDS-PAGE gel at 25 mAmps for 1 hour followed by Coomassie Blue staining
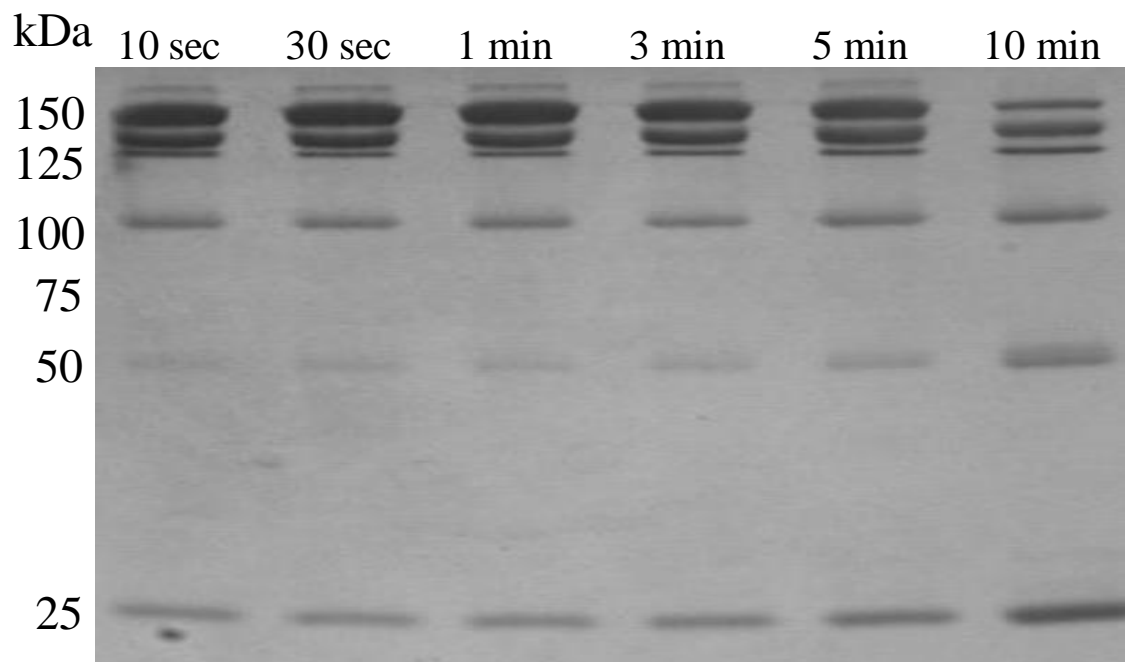
6.3.3. Partially reduced NS0-IgG1 fragments treated with GalT

With the IgG1 reduction pathway determined, the focus could now shift towards the low GI observed in NS0 cultures with lower culture redox potentials (CRP). Recall the hypothesis that the lower CRP caused a reduction of IgG1 in the Golgi resulting in the loss of light chains from the Mab. This in turn caused a conformational shift in the remaining HC dimer and sterically hindered the GalT from processing the glycans. To test this hypothesis, an *in vitro* method was devised where IgG1 was reduced to fragments (HC, HC_2, HC_2LC) by 5 mM DTT for 10 minutes followed by alkylation with 100 mM IAM to prevent disulfide bonds from reforming. This pool of fragments was then protein A purified and exchanged into GalT buffer containing Mn^{2+}. Donor UDP-gal and GalT were added and the reaction was carried out for 12 and 24 hour periods at 37°C before running samples on SDS-PAGE and excising the bands for in-gel HILIC analysis. Calculated GI of all fragments for both time points are found in **Table 6.1**. For reference, the untreated IgG1 (and all intermediate forms) had a GI = 0.310.

Table 6.1 Galactosylation Indexes of partially reduced IgG1 fragments treated with GalT. Protein A purified IgG1 was treated with 5 mM DTT followed by 100 mM IAM before being placed in solution with GalT and UDP-gal in appropriate buffer containing Mn^{+2}. Incubation proceeded for 12 or 24 hours at 37°C. Samples were then subjected to an in-gel HILIC analysis to derive the GI values

IgG1 fragment size	GI*	
	12 hr	**24 hr**
50 kDa	0.348 ±0.022	0.692 ±0.024
100 kDa	0.389 ±0.031	0.786 ±0.011
125 kDa	0.525 ±0.038	0.850 ±0.037
150 kDa	0.599 ±0.029	0.819 ±0.015

* ±SD, average of n=2

For each time point of 12 and 24 hours, the GIs increase with fragment size indicating that larger intermediates are more active with GalT. The largest GI increases in the 12 and 24 hour samples were observed in the 150 kDa (IgG1) and 125 kDa species respectively. The differences between the lowest and highest GI in each sample pool are 0.251 and 0.158 for 12 and 24 hours samples respectively. The lower differential in the 24 hour sample pool is likely due to near full galactosylation taking place; reaching a point where little substrate was available for GalT activity. The 12 hour sample gives a better representation of what may be occurring when substrate is not limited. The results are indicate that GalT has a propensity towards favouring

galactosylation of the 125 and 150 kDa species over the smaller 50 and 100 kDa species. This is in agreement with the proposed hypothesis.

6.3.4. GalT activity with native and galactosidase treated IgG1 and EG2-hFc

An investigation into the activity of GalT on the different Mabs was warranted due to the high GI seen in EG2-hFc. Molar equivalents of each protein A purified Mabs were exchanged into GalT buffer containing Mn^{+2} and assayed *in vitro* in the presence of GalT and UDP-gal. Released free inorganic phosphates from UDP→UMP cleavage by phosphatase were detected by malachite green with color measured at 630 nm. The specific activity was calculated using the following equation:

Equation (6.1)

$$specific\ activity\ (pmol/min/\mu g) = \frac{phosphate\ released\ (pmol)}{incubation\ time\ (min) \times amount\,of\ enzyme\ (\mu g)}$$

Where the amount of phosphate released is correlated to a standard curve based on the color measured at 630 nm. In tandem with this activity assay, a small amount of Mab (IgG1 and EG2-hFc) was treated with GalT for HILIC analysis to ensure that galactosylation was occurring as expected, the HPLC-HILIC profile can be seen in **Figure 6.3**.

169

Initial profiles, seen in **Figures 5.3** and **5.5**, have had most of their biantennary glycans shifted to a predominant FG2 peak after GalT treatment. The HILIC analysis does not give any quantitative data regarding the GalT activity because the time of exposure was too long and galactosylation was performed to near completion. It does however indicate that the GalT was active with the substrates provided, which was critical for upcoming activity assays.

The activity assay measured by Malachite Green phosphate detection generated quantitative values of GalT interacting with the native Mabs. GalT had a recorded activity of 6.20 pmol/min/µg on native DP-12 IgG1 and 8.36 pmol/min/µg on native EG2-hFc, seen in **Figure 6.4**. A student ttest determined a p = 0.08 for these assays indicating that the difference may not have been significant. A caveat to these measurements is that the starting substrate in each Mab is not the same despite having molar equivalents of protein available; the GIs of the IgG1 and EG2-hFc are 0.310 and 0.660 respectively thereby having differing amounts of glycan substrate suitable for GalT activity. In order to ensure similar initial N-glycan structures as acceptors for GalT, purified IgG1 and EG2-hFc were exposed to galactosidase to cleave all attached galactose residues leaving only the core biantennary FG0 and G0 structures. The galactosidase treatment resulted in a minute amount of galactose residues remaining on either Mab as determined by HILIC-HPLC; IgG1 GI = 0.013

and EG2-hFc GI = 0.075. These modified Mabs were then exposed to GalT under the same conditions as the native Mabs. The modified IgG1 had a GalT activity of 8.68 pmol/min/µg while the modified EG2-hFc had an activity of 84.6 pmol/min/µg, see **Figure 6.5**. These are GalT specific activity increases of 40% in IgG1 and 912% in EG2-hFc. The increase in GalT activity in both cases is likely due to more substrate being available for galactosylation; a result of the galactosidase treatment. With a $p<0.02$, the much higher activity in EG2-hFc is significant with a root cause likely to be found in its size difference (80 vs 150 kDa) or in its amino acid makeup, see discussion.

Figure 6.3 Glycan profiles of IgG1 and EG2-hFc treated with GalT. Each of the protein A purified Mabs were placed in solution with GalT and UDP-gal with appropriate buffer containing Mn^{+2} overnight at 37°C. In-solution HILIC analysis was performed on each Mab.
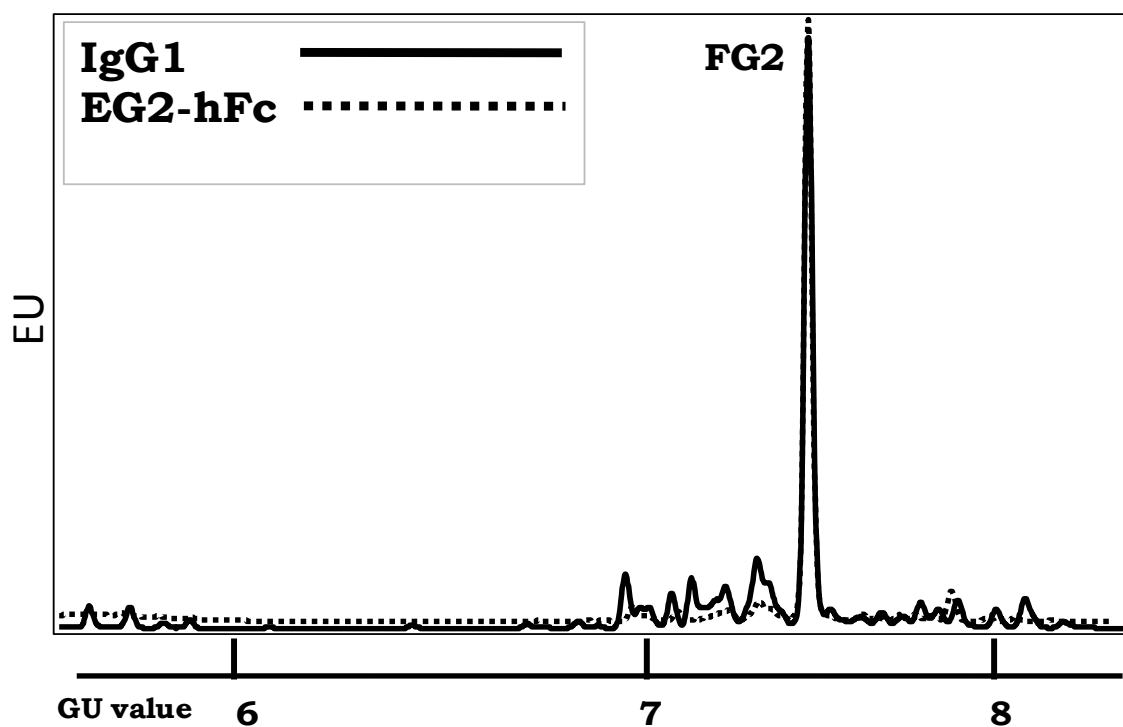
Figure 6.4 Specific activity of galactosyltransferase on native IgG1 and EG2-hFc Mabs with UDP-gal as donor. Using equivalent moles of each Mab in separate wells, GalT, UDP-gal and phosphatase were mixed in with appropriate buffer containing Mn^{+2} and incubated for 1 hour at 37°C. Wells were processed with Malachite green reagents to detect the released phosphates and read at 630 nm
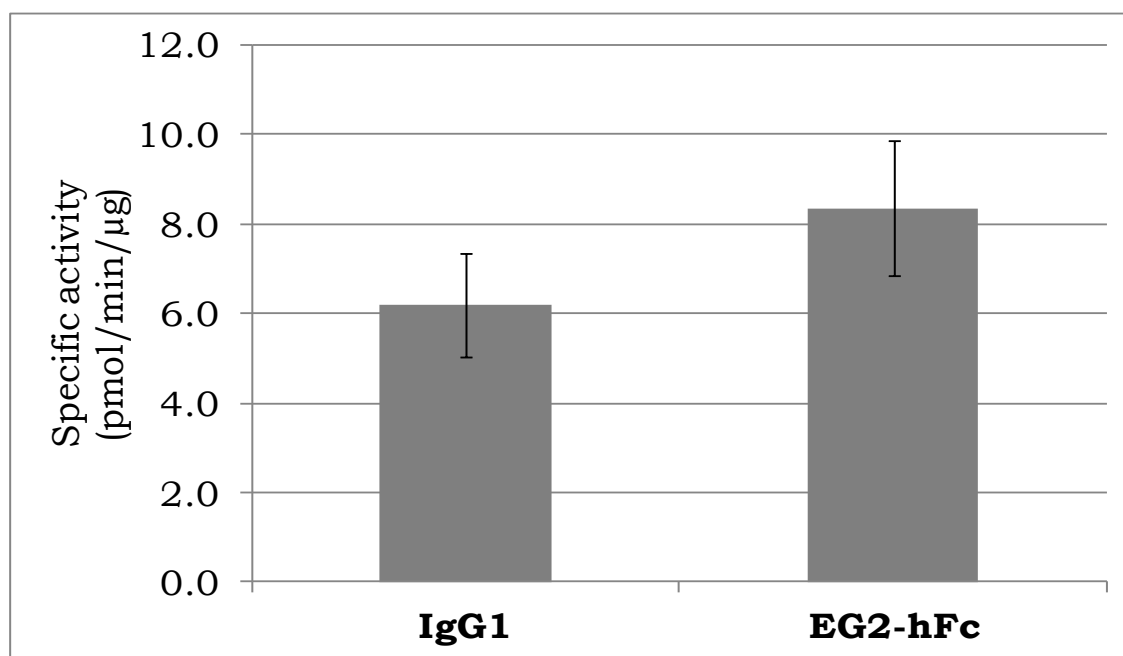
±SD, average of n=4

Figure 6.5 Specific activity of galactosyltransferase using galactosidase treated NS0 IgG1 and EG2-hFc Mabs with UDP-gal as donor. Each Mab was treated with β(1-4,6)-galactosidase and cleaned up with protein A prior to Nanodrop measurement of concentration. Equivalent moles of each Mab were placed in separate wells along with GalT, UDP-gal and phosphatase, mixed with appropriate buffer containing Mn^{+2}. Samples were incubated for 1 hour at 37°C and then processed with Malachite green reagents to detect the released phosphates; wells were read at 630 nm
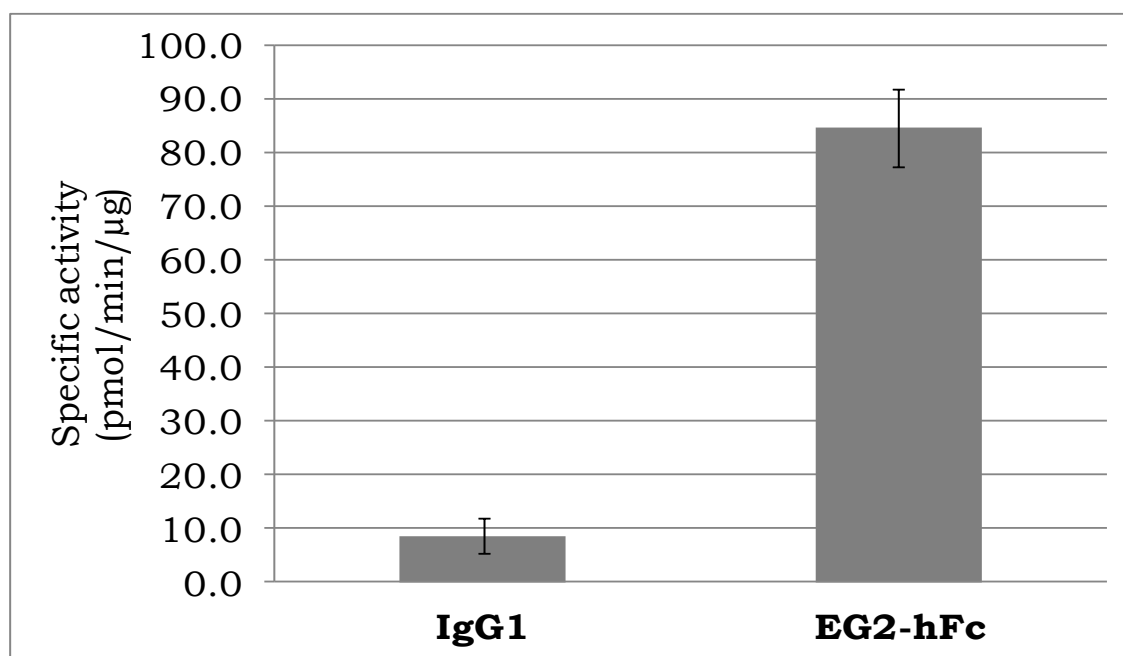
±SD, average of n=4

6.4. Discussion

6.4.1.   GalT activity in the presence of a reducing agent

Initial data with NS0 cell culture confirmed previous findings (Kunkel et al. 1998) that lower redox potentials would shift the GI of IgG1 towards a more agalactosylated state. Chapter 4 suggested several hypotheses to explain the mechanism of action including the idea that the GalT itself was being affected by the DTT in the media. DTT is membrane permeable and therefore may gain access to the Golgi and disrupt any disulfide bonds it encounters. An *in vitro* assay was designed to test for the vulnerability of GalT to reduction in the unlikely event that the entire DTT amount localized itself to the trans-Golgi. The findings clearly indicate that the levels of DTT used in any of the cell culture trials were not sufficient to cause direct interference of the soluble GalT. This non-disruption in soluble GalT activity *in vitro* makes it even more unlikely that the transmembrane version *in vivo* would respond to such low levels of reducing agent. This does not preclude that the DTT had an effect on the internal redox regulatory systems such as glutathione or thioredoxin in some or all intracellular compartments (Banach-Latapy et al. 2013). The potential remains that any perturbance to culture redox potential may cause a response from redox pathways internally, unfortunately the methods to measure such internal changes are not simple and still under development (Pouvreau 2014).

6.4.2.   Partial reduction of IgG1 and treatment with GalT

Previous findings that IgG1 was reduced through the initial loss of LCs followed by reduced HC disulfide bonds (Hong et al. 2009) was confirmed with the partial reduction of IgG1 by DTT. Using a non-reducing SDS-PAGE gel confirmed the expected structures even though an extra band was detected at approximately 125 kDa; this is an expected outcome when running non-denatured, non-linear samples. Related to this, a determination of the extent of reduced intrachain disulfide bonds cannot be made by SDS-PAGE. Due to the globular nature of fully folded antibodies, it is likely that the first disulfide bonds reduced are the more exposed interchain bonds. In Hutterer et al. (2013) the reduction of Mabs was shown to be specific for antibody class and LC type. The hypothesis here was that the temporary loss of LCs as the Mab traversed the Golgi created a new HC dimer that led to decreased access for galactosyltransferase. This was tested by using these partially reduced IgG1 fragments as substrates for GalT and analysing their glycans after treatment. The two incubation time points seen in **Table 6.1** would seem to indicate that there is a proclivity for GalT to act on Mabs with at least one LC attached to the HC dimer. The low GI of 50 and 100 kDa species in the 12 hour incubation trial, 0.348 and 0.389 respectively, shows a lack of galactosylation attributable directly to the substrates configuration. Likewise at the 24 hour incubation time, the two lowest GIs belonged to

the 50 and 100 kDa species at 0.692 and 0.786 respectively. This lends support to the hypothesis, most likely through a conformational shift in the HC thus limiting GalT access. GalT has been shown to be sterically hindered in other circumstances; for example when a bisecting GlcNAc is present, levels of galactosylation drop (Narasimhan et al. 1985; Pučić et al. 2011). Alternatively, cell lines can be designed to limit GalT expression thus leading to higher levels of bisecting GlcNAc (Hodoniczky et al. 2005; Umana et al. 1999). In any event, the lower level of galactosylation in low redox NS0 cultures but not in CHO cell products appears to indicate that this phenomenon is cell line specific, possibly due to different redox regulatory pathways in CHO cells.

6.4.3. IgG1 and EG2-hFc Mabs treated with GalT

When glycans of DP-12 anti-IL-8 and EG2-hFc were initially compared, the HILIC profiles were different with a typical low GI for IgG1 (≈0.300) and a very high GI for EG2-hFc (≈0.700). Both contained the typical biantennary structure but to different degrees of galactosylation and sialylation. Preliminary assumptions were that EG2-hFc was smaller and therefore allowed more access for glycosyltransferases to galactosylate. Other options such as variable GalT expression and UDP-gal pool levels were dismissed due to the fact that both Mabs were produced in CHO cells of similar lineage and grown in the same media under the same conditions. When GalT was assayed with both native

Mabs, the GalT activity levels were measured at 8.36 and 6.20 pmol/min/µg for EG2-hFc and IgG1 respectively. When the Mabs were agalactosylated, the values increased to 84.6 and 8.68 pmol/min/µg for EG2-hFc and IgG1 respectively. The almost 10x higher activity with EG2-hFc clearly indicates that GalT is able to better service these N-glycans. Two possible explanations for increased activity include: 1) the 80 kDa size of the Mab makes for increased accessibility and 2) point mutations in the Fc region of the Mab have caused greater accessibility.

With respect to size, in addition to lacking light chains, EG2-hFc also lacks the CH1 domain in the Fc region. The CH1 domain in IgG1 is responsible for interacting with the light chains and is associated with CH2 via the hinge region (Sheriff et al. 1996). The absence of CH1 in EG2-hFc would alter the conventional hinge region thus making for different access to glycosyltransferases (Jefferis 2009). The other possibility with regard to GalT access is the structure of the Fc region at the amino acid level. Three point mutations were introduced while constructing the human Fc region of EG2-hFc. Two of the mutations are in close proximity to the N-glycan site, D270G and Y278H, which may play a role in GalT contact through altered shape and charge properties (Liu et al. 2014), the third mutation is located distal to the glycan site and therefore not expected to interfere with glycosylation. Previous reports have shown that mutations in the Fc region could lead to altered glycan profiles (Jassal et al. 2001; Rose et al.

2013) with variable levels of sialylation and galactosylation. Process improvements to increase galactosylation have been sought after for a while now including downstream operations where purified IgG1 can be galactosylated *in vitro* (Warnock et al. 2005). A better understanding of how EG2-hFc attains such a high GI will be key in exploiting this mechanism.

6.5. Conclusion

Galactosylation of recombinant proteins may play an important role in the efficacy of therapeutics and determining the factors which influence their probabilities is important to understand. Through a series of *in vitro* assays, galactosyltransferase was tested and determined to not be susceptible to mild reducing environments and that its activity was more pronounced on larger IgG1 fragments (125,150 kDa) than smaller ones (50,100 kDa). When these findings are coupled with the discovery that disulfide bonds between LC and HC in IgG1 are more susceptible to reduction, they support the hypothesis that lower culture redox potentials in NS0 cultures contributes to a temporary structural shift in IgG1 within the Golgi that leads to lower GI values. Assays were also performed to determine the interactions of GalT with IgG1 compared to the humanized camelid EG2-hFc Mab. It was clearly shown with both native and degalactosylated Mabs, the EG2-hFc exhibited greater GalT activity most likely due to its difference in mass or due to point mutations within the Fc

region. Further examination of these elements could lead to glycoengineering opportunities on future Mabs.

Chapter 7 – Conclusion

The multibillion dollar biologics area of Big Pharma is dominated by monoclonal antibodies. How to create more efficacious antibodies is still being investigated, especially in the area of glycosylation. Depending on the type of glycan structure present, Mabs may reveal changes in serum half-lives, ADCC and CDC activity, as well as immunogenicity. The first step to this development is having the correct analytics on hand for proper glycan identification. The development of a higher throughput HILIC method with greater resolution allowed for more precise identifications with multiple recombinant proteins, including tissue plasminogen activator, hemagglutinin antigen and monoclonal antibodies. With analytics in place the goal then shifted towards affecting change in the microheterogeneity of Mab glycans.

Past research had shown that glycan profiles could be altered by engineering at the genetic level; use of siRNA or transfection of glycosyltransferases, or by manipulating cell culture parameters; dissolved oxygen, pH, temp, or by altering the media composition; promotion through inclusion of co-factors and glycan precursors or repression through use of protease inhibitors. The work presented here represents a novel method for glycan modification by altering the culture redox potential. This was based on the previous finding that low dissolved

oxygen concentration could affect glycan heterogeneity towards agalacto species. Using dithiothreitol to lower CRP showed that, although not a universal phenomenon, dramatic effects could be demonstrated in some instances like with the NS0 cultures that exhibited a drop of 50% in the Galactosylation Index in lower CRP cultures, and sometimes the change was less striking but still relevant as with the change in fucosylation rates of DP-12 anti-IL-8. Recall that the overall growth and productivity profiles for all cultures remained equivalent regardless of the DTT concentration in the media and only when the glycan profiles were generated did the differences emerge with respect to product quality.

Glycan patterns on Mabs are defined as critical quality attributes by regulatory drug agencies meaning that even their heterogeneic nature must fall in line with expected values. When the redox levels of a culture shift wildly during the course of a run, there is a strong possibility that these profiles will fall outside the normal values and fail qualification. Add to this the fact that glycan analysis is generally not performed until after purification is complete, and a great deal of time, effort and funds may have been wasted. The experiments outlined here may serve as a cautionary tale that CRPs may need at the least to be monitored and perhaps at most controlled to produce desirable glycans.

Monitoring the redox potentials of cultures may be sufficient for already established cell processes that have entered the clinical stage

however the most practical reality of this research can be found in its use as a modifier for glycans. As mentioned earlier, there are multitudes of ways to affect change in glycan profiles of Mabs but no one variable can support a monoglycoform production line. The whole process of Quality by Design, as introduced by the FDA, is to design from the outset a Mab with a specific target and mode of action which includes a glycan profile. In order to meet these demands, combinations of factors will need to be used for desired glycans. For example the combination of low redox potential and low pH could ensure high agalactosylated glycan content in an NS0 Mab.

The other facet of this research, which was unexpected, was the discovery of an unusually high GI in the camelid Mab EG2-hFc. With a GI ≈ 0.7, it is more than 2 fold higher than with NS0 and CHO IgG1. The high GI may contribute to longer serum half-life and its smaller size (80kDa) may contribute to better tissue distribution. Although the definitive cause for the high GI has not been answered, its increased interaction with galactosyltransferase may be an avenue of exploitation for future Mabs of all types.

This research adds to the understanding of glycosylation events and how they may be influenced by culture redox potential. It also has the practical value of offering another method in which to manipulate glycan profiles to a desired outcome, potentially towards a monoglycan form when

used in conjunction with other factors. In addition, the discovery that the chimeric camelid antibody EG2-hFc has a high GI may lead to methods of glycan modification at the structural level instead of culture parameter shifts.

Chapter 8 - References

Aggarwal, S., 2014. What's fueling the biotech engine—2012 to 2013. *Nature Biotechnology*, 32(1), pp.32–39.

Agrawal, V. et al., 2012. Stable Expression of Chimeric Heavy Chain Antibodies in CHO Cells. In D. Saerens & S. Muyldermans, eds. *Single Domain Antibodies*. Methods in Molecular Biology. Humana Press, pp. 287–303.

Ahn, J. et al., 2010. Separation of 2-aminobenzamide labeled glycans using hydrophilic interaction chromatography columns packed with 1.7 μm sorbent. *Journal of Chromatography B*, 878(3-4), pp.403–408.

Al-Rubeai, M. 2011. *Antibody Expression and Production.* Cell Engineering 7. Springer Science & Business Media.

Allen, S. et al., 1995. Intracellular Folding of Tissue-type Plasminogen Activator. *J. Biol. Chem.*, 270(9), pp.4797–4804.

Anthony, R.M. et al., 2008. Recapitulation of IVIG Anti-Inflammatory Activity with a Recombinant IgG Fc. *Science*, 320(5874), pp.373–376.

Anthony, R.M. et al., 2010. A Novel Role for the IgG Fc Glycan: The Anti-inflammatory Activity of Sialylated IgG Fcs. *Journal of Clinical Immunology*, 30(1), pp.9–14.

Appenzeller-Herzog, C. et al., 2010. Disulphide production by Ero1α–PDI relay is rapid and effectively regulated. *The EMBO Journal*, 29(19), pp.3318–3329.

Baker, K.N. et al., 2001. Metabolic control of recombinant protein N-glycan processing in NS0 and CHO cells. *Biotechnology and Bioengineering*, 73(3), pp.188–202.

Banach-Latapy, A. et al., 2013. Redox-sensitive YFP sensors for monitoring dynamic compartment-specific glutathione redox state. *Free Radical Biology and Medicine*, 65, pp.436–445.

Beckman, R.A. et al., 2007. Antibody constructs in cancer therapy. *Cancer*, 109(2), pp.170–179.

Beckmann, T. et al., 2011. Proteomic and metabolomic characterization of CHO DP-12 cell lines with different high passage histories. *BMC Proceedings*, 5(Suppl 8), p.P92.

Bell, A. et al., 2010. Differential tumor-targeting abilities of three single-domain antibody formats. *Cancer Letters*, 289(1), pp.81–90.

Berg, E.A. et al., 2014. Drug allergens and food—the cetuxiMab and galactose-α-1,3-galactose story. *Annals of Allergy, Asthma & Immunology*, 112(2), pp.97–101.

Bergman, L.W. et al., 1979. Formation of intermolecular disulfide bonds on nascent immunoglobulin polypeptides. *The Journal of Biological Chemistry*, 254(13), pp.5690–4.

Bergman, L.W. et al., 1978. Temporal relationship of translation and glycosylation of immunoglobulin heavy and light chains. *Biochemistry*, 17(24), pp.5174–80.

Birk, J. et al., 2013. Endoplasmic reticulum: reduced and oxidized glutathione revisited. *Journal of Cell Science*, 126(Pt 7), pp.1604–1617.

Börjesson, P.K.E., et al. 2006. Performance of Immuno–Positron Emission Tomography with Zirconium-89-Labeled Chimeric Monoclonal Antibody U36 in the Detection of Lymph Node Metastases in Head and Neck Cancer Patients. *Clin. Cancer Res.* 12, 2133–2140.

Borys, M.C. et al., 1993. Culture pH affects expression rates and glycosylation of recombinant mouse placental lactogen proteins by Chinese hamster ovary (CHO) cells. *Bio/technology (Nature Publishing Company)*, 11(6), pp.720–724.

Bosques, C.J. et al., 2010. Chinese hamster ovary cells can produce galactose-α-1,3-galactose antigens on proteins. *Nature Biotechnology*, 28(11), pp.1153–1156.

Brekke, O.H. et al., 2003. Therapeutic antibodies for human diseases at the dawn of the twenty-first century. *Nat Rev Drug Discov*, 2(1), pp.52–62.

Brooks, S.A., 2004. Appropriate glycosylation of recombinant proteins for human use. *Molecular Biotechnology*, 28(3), pp.241–255.

Buss, N.A. et al., 2012. Monoclonal antibody therapeutics: history and future. *Current Opinion in Pharmacology*, 12(5), pp.615–622.

Butler, M. et al., 2012. Recent advances in technology supporting biopharmaceutical production from mammalian cells. *Applied Microbiology and Biotechnology*, 96(4), pp.885–894.

Campbell, M.P. et al., 2008. GlycoBase and autoGU: tools for HPLC-based glycan analysis. *Bioinformatics*, 24(9), pp.1214–1216.

Chakravarthi, S. et al., 2006. The role of glutathione in disulphide bond formation and endoplasmic-reticulum-generated oxidative stress. *EMBO Reports*, 7(3), pp.271–5.

Chames, P. et al., 2009. Therapeutic antibodies: successes, limitations and hopes for the future. *British Journal of Pharmacology*, 157(2), pp.220–233.

Chen, C.S. et al., 2000. Redox-dependent trafficking of 2,3,4,5, 6-pentafluorodihydrotetramethylrosamine, a novel fluorogenic indicator of cellular oxidative activity. *Free Radical Biology & Medicine*, 28(8), pp.1266–1278.

Chung, C.H. et al., 2008. Cetuximab-induced anaphylaxis and IgE specific for galactose-alpha-1,3-galactose. *The New England journal of medicine*, 358(11), pp.1109–1117.

Dall'Acqua, W.F. et al., 2006. Properties of human IgG1s engineered for enhanced binding to the neonatal Fc receptor (FcRn). *The Journal of Biological Chemistry*, 281(33), pp.23514–23524.

Dalziel, M. et al., 2014. Emerging Principles for the Therapeutic Exploitation of Glycosylation. *Science*, 343(6166), p.1235681.

Dechant, M. et al., 2007 Effector Mechanisms of Recombinant IgA Antibodies against Epidermal Growth Factor Receptor. *The Journal of Immunology,* 179.5, pp.2936–2943.

Dechant, M. et al., 2001 IgA Antibodies for Cancer Therapy. *Critical Reviews in Oncology/Hematology* 39.1-2, pp.69–77.

Del Val, I.J. et al., 2010. Towards the implementation of quality by design to the production of therapeutic monoclonal antibodies with

desired glycosylation patterns. *Biotechnology Progress*, 26(6), pp.1505–1527.

Dickinson, B.C. et al., 2008. A Targetable Fluorescent Probe for Imaging Hydrogen Peroxide in the Mitochondria of Living Cells. *Journal of the American Chemical Society*, 130(30), pp.9638–9639.

Doherty, M. et al., 2012. High-throughput quantitative N-glycan analysis of glycoproteins. *Methods in molecular biology (Clifton, N.J.)*, 899, pp.293–313.

Elkabetz, Y. et al., 2008. Alternative pathways of disulfide bond formation yield secretion-competent, stable and functional immunoglobulins. *Molecular Immunology*, 46(1), pp.97–105.

Ferrara, C. et al., 2011. Unique carbohydrate–carbohydrate interactions are required for high affinity binding between FcγRIII and antibodies lacking core fucose. *Proceedings of the National Academy of Sciences*, 108(31), pp.12669–12674.

Fukuta, K. et al., 2000. Control of Bisecting GlcNAc Addition to N-Linked Sugar Chains. *Journal of Biological Chemistry*, 275(31), pp.23456–23461.

Galili, U., 2013. Anti-Gal: an abundant human natural antibody of multiple pathogeneses and clinical benefits. *Immunology*, 140(1), pp.1–11.

Gilar, M. et al., 2011. Characterization of glycoprotein digests with hydrophilic interaction chromatography and mass spectrometry. *Analytical biochemistry*, 417(1), pp.80–88.

Goetze, A.M. et al., 2011. High-mannose glycans on the Fc region of therapeutic IgG antibodies increase serum clearance in humans. *Glycobiology,* 21(7), pp.949–959.

Goldstein, G., 1987. Monoclonal antibody specificity: Orthoclone OKT3 T-cell blocker. *Nephron* 46, pp.5–11.

Gramer, M.J. et al., 2011. Modulation of antibody galactosylation through feeding of uridine, manganese chloride, and galactose. *Biotechnology and Bioengineering,* 108(7), pp.1591–1602.

Guo, A. et al., 2008. Electrophoretic evidence for the presence of structural isoforms specific for the IgG2 isotype. *Electrophoresis,* 29(12), pp.2550–2556.

Hamers-Casterman, C. et al., 1993. Naturally occurring antibodies devoid of light chains. *Nature,* 363(6428), pp.446–448.

Hamm, M. et al., 2013. Characterization of N-Linked Glycosylation in a Monoclonal Antibody Produced in NS0 Cells Using Capillary Electrophoresis with Laser-Induced Fluorescence Detection. *Pharmaceuticals (Basel, Switzerland),* 6(3), pp.393–406.

Hartman, T.E. et al., 2007. Derivation and characterization of cholesterol-independent non-GS NS0 cell lines for production of recombinant antibodies. Biotechnology and Bioengineering, 96(2), pp.294–306.

Heinrich, C. et al., 2011. Growth characterization of CHO DP-12 cell lines with different high passage histories. *BMC Proceedings,* 5(Suppl 8), p.P29.

Hennet, T., 2002. The galactosyltransferase family. *Cellular and Molecular Life Sciences CMLS*, 59(7), pp.1081–1095.

Hills, A.E. et al., 2001. Metabolic control of recombinant monoclonal antibody N-glycosylation in GS-NS0 cells. *Biotechnology and bioengineering*, 75(2), pp.239–251.

Hodoniczky, J. et al., 2005. Control of Recombinant Monoclonal Antibody Effector Functions by Fc N-Glycan Remodeling in Vitro. *Biotechnology Progress*, 21(6), pp.1644–1652.

Holland, M. et al., 2006. Differential glycosylation of polyclonal IgG, IgG-Fc and IgG-Fab isolated from the sera of patients with ANCA-associated systemic vasculitis. *Biochimica et Biophysica Acta (BBA) - General Subjects*, 1760(4), pp.669–677.

Hong, J. et al., 2009. Structural characterization of immunoglobulin G using time-dependent disulfide bond reduction. *Analytical Biochemistry*, 384(2), pp.368–370.

Hossler, P., 2012. Protein Glycosylation Control in Mammalian Cell Culture: Past Precedents and Contemporary Prospects. In W. S. Hu & A.-P. Zeng, eds. Genomics and Systems Biology of Mammalian Cell Culture. Advances in Biochemical Engineering Biotechnology. Springer Berlin Heidelberg, pp. 187–219.

Hossler, P. et al., 2009. Optimal and consistent protein glycosylation in mammalian cell culture. *Glycobiology*, 19(9), pp.936–949.

Houde, D. et al., 2010. Post-translational Modifications Differentially Affect IgG1 Conformation and Receptor Binding. *Molecular & Cellular Proteomics*, 9(8), pp.1716–1728.

Hutterer, K.M. et al., 2013. Monoclonal antibody disulfide reduction during manufacturing: Untangling process effects from product effects. *Mabs*, 5(4), pp.608–613.

Hwang, C. et al., 1991. The role of oxidation-reduction potential in monitoring growth of cultured mammalian cells. *Spier RE, Griffiths,JB, Meigner,B (eds) Production of biologics from animal cells in culture*, pp.548–567.

Jain, M. et al., 2005. Penetratin Improves Tumor Retention of Single-Chain Antibodies: A Novel Step toward Optimization of Radioimmunotherapy of Solid Tumors. *Cancer Research*, 65(17), pp.7840–7846.

Jarvis, D.L. et al., 1998. Engineering N-glycosylation pathways in the baculovirus-insect cell system. *Current opinion in biotechnology*, 9(5), pp.528–533.

Jassal, R. et al., 2001. Sialylation of Human IgG-Fc Carbohydrate by Transfected Rat α2,6-Sialyltransferase. *Biochemical and Biophysical Research Communications*, 286(2), pp.243–249.

Jeddi, P.A. et al., 1996. Agalactosyl IgG and beta-1,4-galactosyltransferase gene expression in rheumatoid arthritis patients and in the arthritis-prone MRL lpr/lpr mouse. *Immunology*, 87(4), p.654.

Jefferis, R., 2009. Glycosylation as a strategy to improve antibody-based therapeutics. *Nat Rev Drug Discov*, 8(3), pp.226–234.

Jefferis, R., 2012. Isotype and glycoform selection for antibody therapeutics. *Archives of Biochemistry and Biophysics*, 526(2), pp.159–166.

Jenkins, N. et al., 1996. Getting the glycosylation right: implications for the biotechnology industry. *Nature biotechnology*, 14(8), pp.975–981.

Kanda, Y. et al., 2007. Comparison of biological activity among nonfucosylated therapeutic IgG1 antibodies with three different N-linked Fc oligosaccharides: the high-mannose, hybrid, and complex types. *Glycobiology*, 17(1), pp.104–118.

Kaneko, Y. et al., 2006. Anti-Inflammatory Activity of Immunoglobulin G Resulting from Fc Sialylation. *Science*, 313(5787), pp.670–673.

Kao, Y.-H. et al., 2010. Mechanism of antibody reduction in cell culture production processes. *Biotechnology and Bioengineering*, 107(4), pp.622–632.

Karlsson, G. et al., 2008. Combination of Two Hydrophilic Interaction Chromatography Methods That Facilitates Identification of 2-Aminobenzamide-Labeled Oligosaccharides. *Journal of Chromatographic Science*, 46(1), pp.68–73.

Karsten, C.M. et al., 2012. Anti-inflammatory activity of IgG1 mediated by Fc galactosylation and association of FcγRIIB and dectin-1. *Nature Medicine*, 18(9), pp.1401–1406.

Kaufman, R.J. et al., 1979. Amplified dihydrofolate reductase genes in unstably methotrexate-resistant cells are associated with double minute chromosomes. *PNAS of the United States of America*, 76(11), pp.5669–5673.

Kilgore, B.R. et al., 2008. Comparability and Monitoring Immunogenic N-linked Oligosaccharides from Recombinant Monoclonal Antibodies from Two Different Cell Lines using HPLC with Fluorescence

Detection and Mass Spectrometry. In C. Kannicht, ed. *Post-translational Modifications of Proteins*. Methods in Molecular Biology™. Humana Press, pp. 333–346.

Kim, D.Y. et al., 2013. Fed-batch CHO cell t-PA production and feed glutamine replacement to reduce ammonia production. *Biotechnology progress*, 29(1), pp.165–175.

Kohler, G. et al., 1975. Continuous cultures of fused cells secreting antibody of predefined specificity. *Nature*, 256(5517), pp.495–497.

Kubota, T. et al., 2009. Engineered therapeutic antibodies with improved effector functions. *Cancer Science*, 100(9), pp.1566–1572.

Kunkel, J.P. et al., 2000. Comparisons of the glycosylation of a monoclonal antibody produced under nominally identical cell culture conditions in two different bioreactors. *Biotechnology Progress*, 16(3), pp.462–70.

Kunkel, J.P. et al., 1998. Dissolved oxygen concentration in serum-free continuous culture affects N-linked glycosylation of a monoclonal antibody. *Journal of Biotechnology*, 62(1), pp.55–71.

Laemmli, U.K., 1970. Cleavage of structural proteins during the assembly of the head of bacteriophage T4. *Nature*, 227(5259), pp.680–685.

Lee, C.M., 2010. The distribution of the therapeutic monoclonal antibodies cetuxiMab and trastuzuMab within solid tumors. *BMC Cancer*, 10(1), p.255.

Leong, S.R. et al., 2001. Adapting pharmacokinetic properties of a humanized anti-interleukin-8 antibody for therapeutic applications using site-specific pegylation. *Cytokine*, 16(3), pp.106–119.

Li, F. et al., 2010. Cell culture processes for monoclonal antibody production. mAbs, 2(5), pp.466–477.

Lifely, M.R. et al., 1995. Glycosylation and biological activity of CAMPATH-1H expressed in different cell lines and grown under different culture conditions. *Glycobiology*, 5(8), pp.813–822.

Lin, S.-C. et al., 2013. Different Immunity Elicited by Recombinant H5N1 Hemagglutinin Proteins Containing Pauci-Mannose, High-Mannose, or Complex Type N-Glycans. *PLoS ONE*, 8(6), p.e66719.

Liu, B. et al., 2014. The availability of glucose to CHO cells affects the intracellular lipid-linked oligosaccharide distribution, site occupancy and the N-glycosylation profile of a monoclonal antibody. *Journal of Biotechnology*, 170, pp.17–27.

Liu, H. et al., 2010. Ranking the Susceptibility of Disulfide Bonds in Human IgG1 Antibodies by Reduction, Differential Alkylation, and LC−MS Analysis. *Analytical Chemistry*, 82(12), pp.5219–5226.

Liu, H. et al., 2012. Disulfide bond structures of IgG molecules: Structural variations, chemical modifications and possible impacts to stability and biological function. *Mabs*, 4, pp.17–23.

Liu, X. et al., 2012. Immunotoxins constructed with chimeric, short-lived anti-CD22 monoclonal antibodies induce less vascular leak without loss of cytotoxicity. *Mabs* 4, pp.57–68.

Lodish, H.F. et al., 1993. The secretory pathway is normal in dithiothreitol-treated cells, but disulfide-bonded proteins are reduced and reversibly retained in the endoplasmic reticulum. *The Journal of Biological Chemistry*, 268(27), pp.20598–605.

Lux, A. et al., 2011. Impact of Differential Glycosylation on IgG Activity. In B. Pulendran, P. D. Katsikis, & S. P. Schoenberger, eds. *Crossroads between Innate and Adaptive Immunity III*. Advances in Experimental Medicine and Biology. Springer New York, pp. 113–124.

Maggon, K., Top Ten Monoclonal Antibodies 2010 - a knol by Krishan Maggon. Available at: http://knol.google.com/k/krishan-maggon/top-ten-monoclonal-antibodies-2010/3fy5eowy8suq3/143#

McGinnes, L.W. et al., 1997. Disulfide bond formation is a determinant of glycosylation site usage in the hemagglutinin-neuraminidase glycoprotein of Newcastle disease virus. *Journal of Virology*, 71(4), pp.3083–3089.

Mendelsohn, J. et al., 2000. The EGF receptor family as targets for cancer therapy. *Oncogene*, 19(56), pp.6550–6565.

Meneses, A. et al., 2000. Feedback Control of Redox Potential in Hybridoma Cell Culture. In *Animal Cell Technology: Products from Cells, Cells as Products*. pp. 23–29.

Meneses-Acosta, A. et al., 2012. Control of redox potential in hybridoma cultures: effects on Mab production, metabolism, and apoptosis. *Journal of Industrial Microbiology & Biotechnology*, 39(8), pp.1189–1198.

Mesecke, N. et al., 2008. A Novel Group of Glutaredoxins in the Cis-Golgi Critical for Oxidative Stress Resistance. *Molecular Biology of the Cell*, 19(6), pp.2673–2680.

Meulenbroek, A., 2008. *Human IgG subclasses: Useful diagnostic markers for immunocompetance* 3rd ed., Netherlands: Sanquin.

Mian, B.M. et al., 2003. Fully human anti-interleukin 8 antibody inhibits tumor growth in orthotopic bladder cancer xenografts via down-regulation of matrix metalloproteases and nuclear factor-kappaB. *Clinical cancer research: an official journal of the American Association for Cancer Research*, 9(8), pp.3167–3175.

Miethe, S. et al., 2014. Development of neutralizing scFv-Fc against botulinum neurotoxin A light chain from a macaque immune library. *Mabs* 6, pp.446–459.

Misaghi, S. et al., 2013. Resilient immortals, characterizing and utilizing Bax/Bak deficient Chinese hamster ovary (CHO) cells for high titer antibody production. *Biotechnology Progress*, 29(3), pp.727–737.

Mizushima, T. et al., 2011. Structural basis for improved efficacy of therapeutic antibodies on defucosylation of their Fc glycans. *Genes to cells: devoted to molecular & cellular mechanisms*, 16(11), pp.1071–1080.

Mohan, C. et al., 2010. Effect of inducible co-overexpression of protein disulfide isomerase and endoplasmic reticulum oxidoreductase on the specific antibody productivity of recombinant Chinese hamster ovary cells. *Biotechnology and Bioengineering*, 107(2), pp.337–346.

Monnier, P.P. et al., 2013. In Vivo Applications of Single Chain Fv (Variable Domain) (scFv) Fragments. *Antibodies* 2, pp.193–208.

197

Müthing, J. et al., 2003. Effects of buffering conditions and culture pH on production rates and glycosylation of clinical phase I anti-melanoma mouse IgG3 monoclonal antibody R24. *Biotechnology and bioengineering*, 83(3), pp.321–334.

Narasimhan, S. et al., 1985. Control of glycoprotein synthesis. Bovine milk UDPgalactose:N-acetylglucosamine beta-4-galactosyltransferase catalyzes the preferential transfer of galactose to the GlcNAc beta 1,2Man alpha 1,3- branch of both bisected and nonbisected complex biantennary asparagine-linked oligosaccharides. *Biochemistry*, 24(7), pp.1694–1700.

O'Callaghan, P.M. et al., 2010. Cell line-specific control of recombinant monoclonal antibody production by CHO cells. *Biotechnology and Bioengineering*, 106(6), pp.938–951.

Pacis, E. et al., 2011. Effects of cell culture conditions on antibody N-linked glycosylation—what affects high mannose 5 glycoform. *Biotechnology and Bioengineering*, 108(10), pp.2348–2358.

Park, S. et al., 2013. Carbohydrate microarrays. *Chemical Society Reviews*, 42(10), pp.4310–4326.

Pavlou, A.K. et al., 2005. The therapeutic antibodies market to 2008. *European Journal of Pharmaceutics and Biopharmaceutics*, 59(3), pp.389–396.

Percy, J.R. et al., 1975. A theoretical model for the covalent assembly of immunoglobulins. Application to the assembly of human immunoglobulin G in vitro. *The Journal of Biological Chemistry*, 250(6), pp.2398–2400.

Pluschkell, S.B.et al., 1995. Improved methods for investigating the external redox potential in hybridoma cell culture. *Cytotechnology*, 19(1), pp.11–26.

Pouvreau, S., 2014. Genetically encoded reactive oxygen species (ROS) and redox indicators. *Biotechnology Journal*, 9(2), pp.282–293.

Presta, L.G., 2008. Molecular engineering and design of therapeutic antibodies. *Current Opinion in Immunology*, 20(4), pp.460–470.

Price, T.J. et al., 2014. Panitumumab versus cetuximab in patients with chemotherapy-refractory wild-type KRAS exon 2 metastatic colorectal cancer (ASPECCT): a randomised, multicentre, open-label, non-inferiority phase 3 study. *Lancet Oncology* 15, pp.569–579.

Pučić, M. et al., 2011. High Throughput Isolation and Glycosylation Analysis of IgG–Variability and Heritability of the IgG Glycome in Three Isolated Human Populations. *Molecular & Cellular Proteomics*, 10(10), p.M111.010090.

Qasba, P.K. et al., 2008. Structure and function of beta -1,4-galactosyltransferase. *Current drug targets*, 9(4), pp.292–309.

Raju, T.S. et al., 2001. Glycoengineering of Therapeutic Glycoproteins: In Vitro Galactosylation and Sialylation of Glycoproteins with Terminal N-Acetylglucosamine and Galactose Residues. *Biochemistry*, 40(30), pp.8868–8876.

Raju, T.S., 2008. Terminal sugars of Fc glycans influence antibody effector functions of IgGs. *Current Opinion in Immunology*, 20(4), pp.471–478.

Raju, T.S. et al., 2012. Galactosylation variations in marketed therapeutic antibodies. *Mabs*, 4(3), pp.385–391.

Reichert, J.M., 2012. Marketed therapeutic antibodies compendium. *Mabs* 4, pp.413–415.

Robinson, K.M. et al., 2006. Selective fluorescent imaging of superoxide in vivo using ethidium-based probes. *Proceedings of the National Academy of Sciences of the United States of America*, 103(41), pp.15038–15043.

Rose, R.J. et al., 2013. Mutation of Y407 in the CH3 domain dramatically alters glycosylation and structure of human IgG. *Mabs*, 5(2), pp.219–228.

Royle, L. et al., 2007. Detailed Structural Analysis of N -Glycans Released From Glycoproteins in SDS-PAGE Gel Bands Using HPLC Combined With Exoglycosidase Array Digestions. In *Glycobiology Protocols*. pp. 125–143.

Royle, L. et al., 2008. HPLC-based analysis of serum N-glycans on a 96-well plate platform with dedicated database software. *Analytical Biochemistry*, 376(1), pp.1–12.

Serrato, J.A. et al., 2004. Heterogeneous conditions in dissolved oxygen affect N-glycosylation but not productivity of a monoclonal antibody in hybridoma cultures. *Biotechnology and Bioengineering*, 88(2), pp.176–188.

Sheeley, D.M. et al., 1997. Characterization of monoclonal antibody glycosylation: comparison of expression systems and identification of terminal alpha-linked galactose. *Analytical biochemistry*, 247(1), pp.102–110.

Sheriff, S. et al., 1996. Comparison of CH1 Domains in Different Classes of Murine Antibodies. *Journal of Molecular Biology*, 263(3), pp.385–389.

Shinkawa, T. et al., 2003. The Absence of Fucose but Not the Presence of Galactose or Bisecting N-Acetylglucosamine of Human IgG1 Complex-type Oligosaccharides Shows the Critical Role of Enhancing Antibody-dependent Cellular Cytotoxicity. *Journal of Biological Chemistry*, 278(5), pp.3466–3473.

Sinclair, A.M. et al., 2005. Glycoengineering: The effect of glycosylation on the properties of therapeutic proteins. *Journal of Pharmaceutical Sciences*, 94(8), pp.1626–1635.

Snovida, S.I. et al., 2010. A simple cellulose column procedure for selective enrichment of glycopeptides and characterization by nano LC coupled with electron-transfer and high-energy collisional-dissociation tandem mass spectrometry. *Carbohydrate research*, 345(6), pp.792–801.

Spearman, M. et al., 2011. The Role of Glycosylation in Therapeutic Antibodies. In M. Al-Rubeai, ed. *Antibody Expression and Production.* Cell Engineering. Springer Netherlands, pp. 251–292.

Stanley, P. et al., 2009. N-Glycans. In A. Varki et al., eds. *Essentials of Glycobiology.* Cold Spring Harbor (NY): Cold Spring Harbor Laboratory Press.

Stillebroer, A.B. et al., 2013. Phase 1 Radioimmunotherapy Study with Lutetium 177–labeled Anti-Carbonic Anhydrase IX Monoclonal Antibody Girentuximab in Patients with Advanced Renal Cell Carcinoma. *European Urology* 64, pp.478–485.

Szabo, Z. et al., 2011. Rapid High-Resolution Characterization of Functionally Important Monoclonal Antibody N-Glycans by Capillary Electrophoresis. *Analytical Chemistry*, 83(13), pp.5329–5336.

Trexler-Schmidt, M. et al., 2010. Identification and prevention of antibody disulfide bond reduction during cell culture manufacturing. *Biotechnology and Bioengineering*, 106(3), pp.452–461.

Umana, P. et al., 1999. Engineered glycoforms of an antineuroblastoma IgG1 with optimized antibody-dependent cellular cytotoxic activity. *Nat Biotech*, 17(2), pp.176–180.

Van Lith, M. et al., 2011. Real-Time Monitoring of Redox Changes in the Mammalian Endoplasmic Reticulum. *Journal of Cell Science*, 124(14), pp.2349–2356.

Warnock, D. et al., 2005. In vitro galactosylation of human IgG at 1 kg scale using recombinant galactosyltransferase. *Biotechnology and Bioengineering*, 92(7), pp.831–842.

Werner, R.G. et al., 2007. Glycosylation of therapeutic proteins in different production systems. *Acta Pædiatrica*, 96(s455), pp.17–22.

Wesolowski, J. et al., 2009. Single domain antibodies: promising experimental and therapeutic tools in infection and immunity. *Medical microbiology and immunology*, 198(3), pp.157–174.

Wuhrer, M. et al., 2007. Glycosylation profiling of immunoglobulin G (IgG) subclasses from human serum. *Proteomics*, 7(22), pp.4070–4081.

Yang, M. et al., 2002. Effects of Ammonia and Glucosamine on the Heterogeneity of Erythropoietin Glycoforms. *Biotechnology Progress*, 18(1), pp.129–138.

Yen, T.-Y. et al., 2000. Characterization of cysteine residues and disulfide bonds in proteins by liquid chromatography/electrospray ionization tandem mass spectrometry. *Journal of Mass Spectrometry*, 35(8), pp.990–1002.

Yu, M. et al., 2012. Production, characterization, and pharmacokinetic properties of antibodies with N-linked mannose-5 glycans. *Mabs*, 4(4), pp.475–487.

Zhang, J., Liu, X., et al., 2009. Transient expression and purification of chimeric heavy chain antibodies. *Protein expression and purification*, 65(1), pp.77–82.

Zhang, J. et al., 2009. Production of Chimeric Heavy-Chain Antibodies. In A. S. Dimitrov, ed. *Therapeutic Antibodies*. Methods in Molecular Biology™. Humana Press, pp. 323–336.

Zhang, P. et al., 2010. A functional analysis of N-glycosylation-related genes on sialylation of recombinant erythropoietin in six commonly used mammalian cell lines. *Metabolic Engineering*, 12(6), pp.526–536.

Zheng, K. e al., 2011. The impact of glycosylation on monoclonal antibody conformation and stability. *Mabs*, 3(6), pp.568–576.

Zhu, A. et al., 2002. Anti-N-glycolylneuraminic acid antibodies identified in healthy human serum. *Xenotransplantation*, 9(6), pp.376–381.